BASSEM MEKHAEIL

MASTER OF SCIENCE THESIS

THE DIABETES DRUG CANAGLIFLOZIN ENHANCES THE RESPONSE OF PROSTATE CANCER TO RADIOTHERAPY

By BASSEM MEKHAEIL, B.Sc.

A Thesis Submitted to the School of Graduate Studies in Partial Fulfilment of the Requirements for the Degree Master of Health Sciences

McMaster University MASTER OF SCIENCE (2020) Hamilton, Ontario (Medical Sciences)

TITLE:	The Diabetes Drug Canagliflozin Enhances the Response of Prostate Cancer to Radiotherapy
AUTHOR:	Bassem Mekhaeil, B.Sc (McMaster University)
SUPERVISOR:	Dr. Theodoros Tsakiridis

NUMBER OF PAGES: xiv, 129

LAY ABSTRACT

Radiation therapy is a key therapy for prostate cancer. Although it is very effective at treating early stages of prostate cancer, prostate cancer cells develop resistance to radiation therapy rendering it less effective. One way to overcome this obstacle is by delivering higher doses of radiotherapy. However, this leads to increased side effects caused by radiation on normal tissues surrounding the prostate. An additional potential solution to this problem is administering a drug that can make cancer cells more sensitive to radiotherapy. This way we can deliver lower doses of radiation to avoid side effects while treating the disease. This study focuses on using a drug called Canagliflozin in combination with radiation in order to improve the outcomes of radiotherapy in prostate cancer.

ABSTRACT

Canagliflozin (CANA) is a sodium-glucose co-transporter 2 (SGLT2) inhibitor used for the treatment of type II diabetes. There is recent evidence suggesting that Canagliflozin has antiproliferative effects against malignant tumours. Canagliflozin is able to inhibit cell growth and cancer progression by inhibiting mitochondrial complex I leading to a reduction in cellular ATP levels. This alteration in the energy status of the cell leads to AMP-activated kinase (AMPK) activation, which in turn downregulates protein synthesis, lipogenesis and induces cell cycle arrest. The aim of this thesis is to explore whether Canagliflozin can be combined with radiation to enhance the outcome of radiation therapy in the treatment of prostate cancer and to further our knowledge on the cellular pathways impacted by Canagliflozin. Proliferation and clonogenic survival assays were used to establish the antiproliferative effect of Canagliflozin *in vitro* alone and when combined with radiation. Prostate cancer cell lines with different mutation profiles were used to assess the effectiveness of the drug under different radiation doses. A xenograft model was then used to test Canagliflozin's effects *in vivo.* PC-3 cells were injected in the flank of *balb/c* nude mice. Mice were treated with Canagliflozin, radiation or a combined treatment and tumour growth was monitored. Furthermore, a western blot analysis of cells treated with Canagliflozin and radiation was performed to deepen our understanding of the cellular pathways affected by Canagliflozin. Our results show that Canagliflozin has an additive effect when combined with radiation. Canagliflozin was able to effectively downregulate the mTOR pathway, blocking mitosis and leading to cell cycle arrest. These findings provide evidence that Canagliflozin could be used as an adjunct to radiation therapy in clinical settings.

Acknowledgment

First and foremost, I would like to thank God for helping and guiding me throughout this experience. “I will praise You, O Lord, with my whole heart; I will tell of all Your marvelous works.” (Psalm 9:1).

I wish to express my deepest gratitude to my supervisor and mentor Dr. Theodoros Tsakiridis. Thank you for giving me the opportunity to work under your supervision and for allowing me to contribute to the existing knowledge of radiation oncology and cancer metabolism. Thank you for introducing me to the world scientific research. Thank you for your support and patience and for always pushing me to be a better version of myself.

I would also like to recognize the invaluable assistance of my committee members: Dr. Paola Muti and Dr. Gregory Steinberg. Your knowledge and experience are unparalleled. Thank you for your help and guidance throughout the project.

My appreciation also extends everyone in the Steinberg lab and the Tsakiridis lab. This work would have not been possible without you. Thank you for always helping me, encouraging me, teaching and training me and always being there whenever I needed help. I am forever grateful for the friendships and for the good memories.

I wish to also acknowledge the support of my family. None of this would have been possible without your help and continuous support. I am blessed to have such a lovely and caring family. To me, family is everything.

Finally, I dedicate this thesis to my grandfather, Talaat Ayad. Thank you for your unconditional love and your endless support. I cannot wait to see you.

Table of Contents

List of Figures

List of Tables

List of Abbreviations

3D-CRT: Three-Dimensional Conformal Radiation Therapy
4E-BP1: Eukaryotic translation initiation factor 4E Binding Protein 1
ACC: Acetyl CoA Carboxylase
ACLY: ATP Citrate Lyase
ADT: Androgen Deprivation Therapy
AF1: Activation Function 1
AF2: Activation Function 2
Akt/PKB: Protein Kinase B
AMPK: AMP-activated Kinase
AP-1: Activator Protein 1
AR: Androgen Receptor
ARA70: Androgen Receptor-associated protein 70
AREs: Androgen Receptor Elements
ASAP: Atypical Small Acinar Proliferation
ATM: Ataxia Telangiectasia Mutated
ATR: Ataxia telangiectasia and Rad3 related
BCAA: Branched-Chain Amino Acids
BPH: Benign Prostate Hyperplasia
BRCA1: Breast Cancer 1
BRCA2: Breast Cancer 2
CAB: Combined Androgen Blockade
CANA: Canagliflozin
CHEK2: Checkpoint Kinase 2
CPA: Cyproterone Acetate
CPT1: Carnitine Palmitoyl Transferase 1
CRPC: Castration-Resistant Prostate Cancer
CRTC2: CREB Regulated Transcription Coactivator 2
DBD: DNA Binding Domain
DES: Diethylstilbestrol
DHEA-S: Dehydroepiandrosterone Sulfate
DHEA: Dehydroepiandrosterone
DHT: Dihydrotestosterone
DNA: Deoxyribonucleic Acid
DRE: Digital Rectal Exam
DSB: Double-strand Breaks
EBRT: External Beam Radiation Therapy
eEF2: eukaryotic Elongation Factor 2
eEF2K: eukaryotic Elongation Factor 2 Kinase
EGF Epidermal Growth Factor
EGFR: Epidermal Growth Factor Receptor
EMT: Epithelial-Mesenchymal Transition
ER: Endoplasmic Reticulum
ERK: Extracellular Signal-Regulated Kinase
FATPs: Fatty Acid Transport Proteins

FOXA1: Forkhead Box A1
FOXO: Forkhead Box Protein O
FOXP1: Forkhead Box P1
Fru-2,6-P2: Fructose-2,6-bisphosphate
G2: Growth 2
G6P: Glucose 6 Phosphate
GAB1: GRB2-Associated-Binding protein 1
GEF: Guanine nucleotide Exchange Factor
GFAT1: Glutamine Fructore-6-Phosphate Aminotransferase 1
GLUTs: Glucose Transporters
GnRH: Gonadotropin Releasing Hormone
GP: Glycogen Phosphorylase
GRB2: Growth Factor Receptor Binding Protein 2
H3: Histone 3
HDR: High Dose Brachytherapy
HIF-1α: Hypoxia Inducible Factor 1α
HMGR: 3-hydroxy-3-methylglutaryl coenzyme A reductase
HNF4: Hepatocyte Nuclear Factor 4
HOXB13: Homeobox Protein 13
HRE: Hypoxia Response Elements
IEGs: Immediate-Early Genes
IGF-1: Insulin Growth Factor-1
IGF: Insulin-like Growth Factor
IL-6: Interleukin-6
IMRT: Intensity Modulated Radiation Therapy
ISUP: International Society of Urologic Pathology
kDa: Kilo Dalton
LBD: Ligand binding domain
LDR: Low Dose Brachytherapy
LH: Luteinizing Hormone
LHRH: Luteinizing Hormone-Releasing Hormone
LKB1: Liver Kinase B1
MAPK: Ras-Raf-Mitogen Activated Protein Kinase
MDM2: Mouse Double Minute 2 Homolog
MLH1: MutL Homolog 1
MSH2: MutS Homolog 2
MSH6: MutS Homolog 6
MSK: Mitogen and Stress-activated protein Kinase
mTOR: mammalian Target of Rapamycin
NCoR1: Nuclear Receptor Co-repressor 1
NF-κB: Nuclear Factor kappa-Beta
Nrf2: Nuclear factor erythroid 2-related factor 2
NSCLC: Non-Small Cell Lung Cancer
NTD: N-terminal Domain
P70S6K: Ribosomal Protein S6 Kinase
PALB2: Partner and Localizer of BRCA2

PCa: Prostate Cancer
PCD: Pyruvate Dehydrogenase Complex
PDH: Pyruvate Dehydrogenase
PDK1: Pyruvate Dehydrogenase Kinase 1
PFK: Phosphofructokinase
PGK1: Phosphoglycerate Kinase 1
PI3K: Phosphoinositide 3-kinase
PIA: Proliferative Inflammatory Atrophy
PIN: Prostatic Intraepithelial Neoplasia
PKM2: Pyruvate Kinase M2
PLD1: Phospholipase D1
PMS2: PMS homolog 2
PSA: Prostate-Specific Antigen
PTEN: Phosphatase and Tensin Homolog
RAD51D: RAD51 paralog D
RAPTOR: Regulatory-Associated Protein of mTOR
RNaseL: Ribonuclease L
ROS: Reactive Oxygen Species
RT: Radiation Therapy
S1P: Site 1 Protease
S2P: Site 2 Protease
S6: Ribosomal Protein S6
SBRT: Stereotactic Body Radiation Therapy
SGLTs: Sodium-Glucose Co-Transporters
SHC: Src Homology and Collagen
SOS: Son Of Sevenless 1
SRC1: Steroid Receptor Coactivator-1
SRC2: Steroid Receptor Coactivator-2
SRC3: Steroid Receptor Coactivator-3
SREBPs: Sterol-Response Element Binding Proteins
STAT3: Signal Transducer and Activator of Transcription 3
TCF: Ternary Complex Factor
TGF-α: Transforming Growth Factor-α
TIF2: Transcriptional Intermediary Factor 2
TMPRSS2: Transmembrane Serine Protease 2
TNF: Tumour Necrosis Factor
TNM: Tumour, Node, Metastasis
TRAIL: TNF-related Apoptosis Inducing Ligand
TRAMP: Transgenic Adenocarcinoma Mouse Prostate
TRUS: Transrectal Ultrasound
TSC: Tuberous Sclerosis Complex
TURP: Transurethral Resection of the Prostate
TXNIP: Thioredoxin-Interacting Protein
VEGFR: Vascular Endothelial Growth Factor Receptor

Declaration of Academic Achievement

Contributions to concepts and design of research: Bassem Mekhaeil, Dr. Theos Tsakiridis, Dr. Gregory Steinberg and Dr. Paola Muti.

Contributions to data interpretation: Bassem Mekhaeil, Dr. Theos Tsakiridis, Dr. Gregory Steinberg, Dr. Paola Muti, Olia Biziotis.

CHAPTER I - INTRODUCTION

INTRODUCTION

1.1 The prostate gland

Prostate cancer (PCa) signifies uncontrolled growth of the cells of the prostate. The prostate is a walnut-sized gland present in the lower pelvis anterior to the rectum and inferior to the bladder. It is part of the male reproductive system. It produces prostatic fluid rich in proteins, minerals and enzymes with the purpose to nourish and protect sperm. This fluid is mixed with the sperm to make the seminal fluid. The prostate gland naturally grows in size in response to chronic stimulation by male androgens (testosterone) leading to benign prostatic hyperplasia (BPH). However, this frequently leads to development of pre-cancerous conditions such as prostatic intraepithelial neoplasia (PIN), atypical small acinar proliferation (ASAP) and proliferative inflammatory atrophy (PIA) (LeBlanc et al., 2019). On the other hand, the growth of prostatic cells might signify a malignant tumour. It often starts as an uncontrolled growth of the glandular cells of the prostate which is a type of cancer called adenocarcinoma. Tumours in epithelial cells of the prostate account for most cases of PCa (Oh et al., 2003). Those cells can grow into and destroy nearby tissue. They can also metastasize and invade distant organs throughout the body. There are also a few other rare types of PCa such as sarcoma and small-cell carcinoma. However, adenocarcinoma of the prostate accounts for approximately 95% of PCa (Alizadeh & Alizadeh, 2014). Tumours frequently are multifocal and grow in one or more sites of the prostatic gland.

1.2 Prostate cancer epidemiology

PCa remains the most commonly diagnosed cancer in Canadian men and accounts for approximately 48% of all cancers diagnosed in 2019. Approximately 1 in 8 males, are expected to be diagnosed with PCa during their lifetime (Smith et al., 2019). 99% of PCa cases are expected to be males over the age of 50 years, with very few incidents in males younger than 40 years of age. It is estimated that 1 in 29 males (4% approximately) will die from PCa. Approximately 84% of those deaths are expected to occur for males older than 70 years of age. Although the incidence rate of PCa is high, the mortality rate remains relatively low with only 9.5% chance of dying from the disease if you have it. The mortality rate has been increasing between 1984 and 1994. However, it has been declining since, due to improved treatments and screening tests (Smith et al., 2019). The Canadian cancer society estimates that in 2020, 23300 men will be diagnosed with PCa, which is approximately 20% of new cancer cases in men. Furthermore, an estimate of 4200 men will die from PCa in 2020 (*Prostate Cancer Statistics - Canadian Cancer Society*, n.d.). Globally, PCa remains the fourth commonly diagnosed cancer. It accounted for approximately 7.1% of newly diagnosed cases and 3.8% of deaths in 2018 (*Age Standardized (World) Incidence Rates, Prostate, All Ages*, 2018).

1.3 Prostate cancer etiology and risk factors

There are a few risk factors associated with PCa. The first and most common risk factor is age. Race and ethnicity are other risk factors that have been linked to PCa. PCa is more prevalent among black men compared to white and Asian males. The reason behind these differences remains unknown. Geography is another common risk factor for PCa. PCa is more common in northwest Europe, North America, Australia and on the Caribbean islands than

Africa, Asia, Central America and South America (Leitzmann & Rohrmann, 2012). Although the reasons are not known, intensive screening and advancement in diagnostic tests might be the reason why PCa is more prevalent in developed countries as opposed to developing countries. Changes in diets and lifestyles may also explain these differences. In addition, Family history suggests that genetic factors might play a role in the development of PCa. However, most men who are diagnosed with PCa do not have a family history of it (A. R. Patel & Klein, 2009). There are a few inherited mutations that have been linked to PCa. Mutations in the tumour suppressor genes Breast Cancer 1 (BRCA1) and Breast Cancer 2 (BRCA2) have been linked to PCa. Those proteins are involved in DNA repair. Another gene that might contribute to the development of PCa, especially at a younger age, is Homeobox protein Hox-B13 (HOXB13) (Pilie et al., 2016). HOXB13 is able to suppress AR activity, however, the G84E mutant variant is associated with overgrowth of the prostate (Fitzgerald et al., 2017; Jung et al., 2004). Another tumour suppressor gene that is usually mutated is Ribonuclease L (RNaseL). RNaseL is normally involved in apoptosis of abnormal prostate cells. However, when it is mutated, cells do not undergo programmed cell death, which can lead to an increased risk of PCa. DNA damage response genes are also mutated in hereditary PCa. This includes checkpoint kinase 2 (CHEK2), ataxia telangiectasia mutated (ATM), partner and localizer of BRCA2 (PALB2) and RAD51D. In addition, genes who are responsible for DNA mismatch repair such as MutS homolog 2 (MSH2), MutS homolog 6 (MSH6), MutL homolog 1 (MLH1) and PMS2 might also be mutated. Men with Lynch syndrome (hereditary non-polyposis colorectal cancer) have increased risk for developing PCa throughout their life (Cooney, 2017; Dong, 2006). Finally, social, diet and environmental factors increase the risk for PCa. Obesity, smoking, inflammation of the prostate,

sexually transmitted infections and vasectomy have also been considered risk factors. However, the link between them and PCa remains unclear (Leitzmann & Rohrmann, 2012).

1.4 Diagnosis and grading

Digital rectal examination (DRE) for the prostate for lumps and evaluation of patient blood levels of the Prostate Specific Antigen (PSA) are standard early diagnostic tests for PCa. PSA is a protease, a normal enzyme synthesized by the prostatic gland and is an essential component of normal semen. There is currently a scientific debate on what the normal level of PSA is. Normal PSA levels differ amongst individuals based on age, race and more importantly individual biology. Circulating PSA levels increase with age. Although the PSA test is a very sensitive, it is not a very specific marker of PCa, especially in the range between 4 ng/mL and 10 ng/mL (Roddam et al., 2005) and can lead to a large number of false positive case identifications, therefore prostate biopsies are required (Adhyam & Kumar Gupta, 2012).

Furthermore, Transrectal ultrasound (TRUS) is used to measure the size of the gland while looking for abnormalities. It is used to guide needle biopsies. Biopsy is used as the ultimate diagnostic test where a hollow needle is inserted in the prostate in order to collect tissue samples (10-12 samples) (Harvey et al., 2012).

1.5 Prostate cancer stages

There are clinical and histological grading systems for PCa. The clinical system is referred to as tumour, node, metastasis system (TNM) while the histological system is referred to as the Gleason score. The TNM requires a DRE while the Gleason score requires a pathologist to examine a specimen or a biopsy. Table 1.1 shows the TNM grading system. Pathologists assign a Gleason score with the sum of a primary and a secondary morphologic patterns of the tumour.

The Gleason scheme was introduced in the 1960s-1970s. It has been evolving ever since. The Gleason grading system that is used today has been modified in 2014 by the International Society of Urologic Pathology (ISUP). The Gleason score is a sum of two numbers. The primary pattern refers to the predominant pattern while the secondary pattern is the second most common pattern. A pattern can have a number of 1-5 in order to describe the tumour. Pattern 1 is characterized by distinct, well-differentiated, rounded individual glands. Pattern 2 describes cells that are not well defined as pattern 1 with increased tumour-stromal boundaries and irregularities at the periphery of the nodule. Pattern 3 is the most common pattern and is characterized by moderately differentiated cells with cribriform structures. Pattern 4 describes poorly differentiated tumours with fused glands and cribriform patterns. Pattern 5 describes the most poorly differentiated cells with necrotic tissue. Based on the score, which ranges from 2 to 10, a grade is given (Chen & Zhou, 2016; Cheng et al., 2012; Humphrey, 2004). ISUP recommended a five-tier grading classification, with grades 1 to 5 being based on Gleason scores (Egevad et al., 2016). Grade groups (I-V) represent the level of prognosis with grade I having the most favorable prognosis and Grade V having the poorest prognosis (Table 1.2 shows this grading system) (Chen & Zhou, 2016; Cheng et al., 2012; Humphrey, 2004). In clinical practice, prostate cancer is broadly divided into localized and metastatic. Localized disease is separated into three risk categories; low risk, intermediate risk and high risk, defined by a combination of T score, Gleason score and PSA value using risk stratification schemes such as that proposed by D'Amico (Table 1.3) (D'Amico et al., 1998;).

Table 1.1: TNM Grading system

Clinical Stage (TNM)	Description
Tx	Tumour cannot be assessed
T0	No evidence of primary tumour
T1	Tumour not visible by imaging nor palpable
T1a	Tumour incidental histological finding ($\leq 5\%$ of tissue resected)
T1b	Tumour incidental histological finding ($> 5\%$ of tissue resected)
T1c	Tumour identified by needle biopsy
T2	Tumour confined within the prostate
T2a	Tumour $\leq 50\%$ of one lobe
T2b	Tumour $> 50\%$ of one lobe (not both lobes)
T2c	Tumour present in both lobes
T3	Tumour extends through the prostate capsule
T3a	Extracapsular extension (unilateral or bilateral)
T3b	Tumour invades seminal vesicle
T4	Tumour invades adjacent structures other than the seminal vesicles
Nx	Lymph nodes were not assessed
N0	No metastasis in regional lymph nodes
N1	Metastasis in regional lymph nodes
M1	Existence of distant metastasis
M1a	Non-regional lymph nodes metastasis
M1b	Bone metastasis
M1c	Other sites with or without bone disease

Table 1.2: Gleason Score

Grade	Gleason Score
I	≤6
II	3+4=7
III	4+3=7
IV	8
V	9-10

Table 1.3 D'Amico Risk Classification

Risk Category	PSA value	Gleason Score	Clinical T stage
Low (must have all criteria)	$\leq 10\ ng/mL$	≤6	T1-T2a
Intermediate (must have all criteria if not low risk)	$\leq 20\ ng/mL$	7	T1/T2
High (one is sufficient)	$\geq 20\ ng/mL$	8-10	T3a-T4

1.6 Prostate cancer treatments

There are currently multiple approaches to manage PCa. Every patient will have his own treatment plan depending on a few factors such as the PSA, Gleason score, stage and type of the tumour, the side effect profile of each treatment as well as personal preference. Active surveillance is a widely used option for patients with early disease. This involves a program of close monitoring of tumour progression through serial DREs, PSA measurements, three to four times a year and annual re-biopsies. Active treatment will begin if there is evidence that the tumour is progressing (Kinsella et al., 2018).

1.6.1 Surgery

1.6.1.1 Radical prostatectomy

Radical prostatectomy involves the removal of the prostate gland. This is an appropriate treatment for fit younger patients, with low surgical risks and early localized PCa (Sooriakumaran et al., 2014). Since low risk patients are now frequently managed with surveillance and surgery in high risk PCa does not have an established role, prostatectomy is mainly utilized in intermediate risk patients. There are a few types of radical prostatectomy. Retropubic radical prostatectomy involves the removal of the prostate gland as well as lymph nodes while perineal radical prostatectomy does not involve the removal of lymph nodes and is therefore a shorter and less painful procedure (Lepor, 2005). Furthermore, radical prostatectomy could also be performed with the assistance of a robotic system, rendering the procedure less invasive with fewer complications (Finkelstein et al., 2010; Wroński, 2012).

1.6.1.2 Surgery side effects

There are numerous side effects related to this treatment. These include but are not limited to damage to nearby organs, reactions to anaesthesia, bleeding from surgery, urinary incontinence as well as erectile dysfunction. In regard to erectile dysfunction, surgeons try to spare the nerves responsible for erections through an approach called nerve-sparing approach. Frequently, prostate tumours are larger than expected and nerve sparing cannot be achieved without compromising cancer control (Lepor, 2005).

1.6.2 Radiation therapy

Radiation therapy controls cancer through induction of DNA damage, which is proportionally greater in cancer cells compared to normal cells, and leads to inhibition of tumor cell growth, cell cycle arrest and induction of cancer cell death (see section 1.12 for cellular effects of ionizing radiation).

1.6.2.1 External beam radiation therapy (EBRT)

EBRT uses a linear accelerator to deliver radiotherapy in the form of high energy photons from outside the patient to internal organ targets such as the prostate. Modern accelerators modulate EBRT in terms of photon energy, shape and timing of photon beams in order to achieve optimal tumour targeting and eventual control. This is attained when cancer cells receive radiation with minimal or negligible radiation dose to surrounding healthy tissues. Three-dimensional models as well as other techniques are used to accomplish this (Zaorsky, Harrison, et al., 2013).

1.6.2.2 Three-dimensional conformal radiation therapy (3D-CRT)

3D-CRT utilizes technological advancements in order to map the tumour and deliver radiation doses directly to the prostate. Different beams are aimed from different angles to the prostate which decreases scattering and reduces the damage to nearby organs (Dal Pra & Souhami, 2016).

Intensity Modulated Radiation Therapy (IMRT) and Volumetric Arc Therapy (VMAT): IMRT is one of the most commonly used forms of RT for the treatment of prostate cancer. It ensures the conformity of the radiation dose to the target volume (Taylor & Powell, 2004). To accomplish that, linear accelerators deliver multiple modulated radiation beams from optimized fixed angles with the aim of sparing normal tissues and concentrating high dose radiotherapy on the tumour (Zaorsky, Harrison, et al., 2013). This technique is typically used to deliver conventional fractionation or hypo-fractionated radiotherapy (1.8-3 Gy per fraction) (Taylor & Powell, 2004). VMAT consists an evolution of IMRT where modulated beams of RT are delivered continuously around the patient (target) in Arcs. The technique is progressively taking over IMRT since it improves greatly conformality of treatment and speed of treatment delivery.

Stereotactic Body Radiation Therapy (SBRT): SBRT uses patient immobilization, image-guidance techniques and high precision accelerators to deliver higher doses of radiation to a specific site with significantly improved dose drop off into normal tissues. Since it can deliver high precision radiotherapy, doses per fraction are significantly increased safely (up to 20 Gy per fraction) resulting in shorter time of treatment delivery and frequently, lower overall radiotherapy dose (Zaorsky, Harrison, et al., 2013).

Proton Beam Radiation Therapy: This type of radiation uses the energy of charged protons instead of X-ray (photon) beams. X-ray beams release energy before and after they hit their

target. On the other hand, protons deposit their energy with higher precision to the target. Proton beam radiation therapy also uses 3D approaches in order to optimize tumour control while limiting the damage to healthy organs. Proton therapy may offer high degree of conformality of radiotherapy dose delivery, but the equipment required for this treatment are significantly more costly and require increased use of resources making this treatment challenging to implement. (S. Patel et al., 2014).

1.6.2.3 Conventional fractionation – Dose escalated radiotherapy (RT)

Standard treatment of PCa with RT is delivered over many fractions. Conventional fractionation consists of fractions of 1.8-2 Gy of RT delivered 39 to 40 times for a total of 78-80 Gy over a period of 8 weeks (5 daily fractions per week) (Zaorsky, Ohri, et al., 2013). This treatment was developed due to the resistance of PCa to RT and was established with clinical trials which showed that dose escalated RT is required for improved PCa local control (Morgan et al., 2018).

1.6.2.4 Hypofractionation

Radiobiological models suggest that delivery of lower overall dose of RT delivered in larger daily fractions over a shorter period of time can result in similar tumor control as prolonged courses of radiotherapy of higher overall dose (Morgan et al., 2018). Studies in the last 2 decades showed that PCa RT can be safely and effectively delivered in larger fraction sizes (up to 3.1 Gy per fraction) and fewer fractions overall; an approach to RT delivery called hypofractionation. This is based on the PCa radiobiology which involves a high degree of

radiation resistance, a slow PCa cell cycle and relatively higher sensitivity to larger doses of RT per fractions (Desideri et al., 2014).

In order to understand the relevance of hypofractionation, it is important to understand the a/b ratio. Cells with a low a/b ratio are late-responding cells while cells with high a/b ratio are early-responding cells. Cells with low a/b ratio have the capacity to repair DNA damage between fractions rendering radiation therapy less effective. Interestingly, PCa has a significantly low a/b ratio which makes hypofractionation more favourable than conventional fractionation (Desideri et al., 2014).

Several clinical studies compared different radiation schedules for PCa in order to explore the advantages and disadvantages of different models. The CHHiP trial included patients with intermediate risk PCa. Patients were randomly assigned into two groups; conventionally fractionated radiation therapy or hypofractionated radiation therapy. The conventional schedule consisted of 74 Gy in total, split over 37 fractions; meaning 2 Gy per session. On the other hand, patients assigned to the hypofractionation group received a total of 60 Gy over 20 fractions (3Gy per fraction) or 57 Gy over 19 fractions and three to six months of androgen deprivation therapy (ADT) (see section 1.6.3 for ADT). Results show that the group that received 60 Gy of radiation was non-inferior to the group that received conventional treatment in terms of biochemical or clinical failure free survival at five years. However, they could not claim that the group that received only 57 Gy was non-inferior to the group that received conventional radiation. There was no difference in the side effects seen in all three groups (Dearnaley et al., 2016).

Another study that compared conventional treatment to hypofractionation was the Ontario Clinical Oncology Group PROFIT study. Patients with intermediate risk localized prostate cancer were assigned into one of two groups; the conventional radiation group which

received 78 Gy of radiation over 39 fractions or the hypofractionation group that received 60 Gy of radiation over 20 fractions. Results have shown that the group that received 60 Gy was non-inferior to the other group in terms of biochemical or clinical disease-free survival (Lausch et al., 2017).

Stereotactic body radiotherapy (SBRT)

Furthermore, the development of SBRT in recent years allowed investigation of Ultra-hypofractionated radiotherapy for PCa that utilized treatments delivered in just five fractions of radiotherapy for a significantly lower total dose of 35-40Gy. Non-randomized clinical trials showed that this treatment is well tolerated and provides excellent local controls in early stage PCa while early data of randomized trial (PACE) verify that SBRT is indeed as well tolerated by patients as hypofractionated RT and may be the preferred RT treatment approach in the near future (Brand et al., 2019).

1.6.2.5 Brachytherapy

Brachytherapy is another technique used to deliver radiation. It requires the insertion of a radioactive isotope in the prostate. This technique allows for the transfer of energy caused by the decay of the isotope. It uses lower energy RT that does not travel long distances into tissues and has therefore the advantage of not delivering high dose of RT to surrounding normal organs (Skowronek, 2017). There are two types of brachytherapy; low dose brachytherapy (LDR) and high dose brachytherapy (HDR). In regard to LDR, radioactive implants are inserted in order to deliver a low dose of radiation over a long period of time (weeks/months). The most commonly used radioactive substances are Iodine-125 or palladium-103. LDR is used to treat early stage PCa that is growing slowly and has a low risk of recurrence. On the other hand, HDR uses

temporary radioactive implants (typically 10 minutes per session) that deliver a high dose of radiation. Treatments typically last one to two days. The most commonly used radioactive substance for HDR are Iridium-192 and cesium-137. This type of radiation is used to treat low risk PCa or as a RT boost treatment in high risk PCa in combination with EBRT (Skowronek, 2013). Brachytherapy is an invasive technique and it falls out of favor as high precision RT treatments such as SBRT with a very favourable toxicity profile are being developed (Cihan, 2018).

1.6.2.6 Radiation therapy side effects

Bowel or bladder toxicity, fatigue and erectile dysfunction are some of the key side effects of PCa RT. Radiation toxicity of the bowel, known as radiation proctitis, causes damage and inflammation to the lower part of the rectum. This condition might lead to rectal leakage and blood in the stool and diarrhea. Usually these issues resolve after radiation but can persist. Radiation can also cause inflammation of the bladder, a condition referred to as radiation cystitis. This condition leads to hematuria and dysuria. Chronic side effects of radiation include urinary frequency and erectile dysfunction. However, improved precision of RT delivery limit bladder side effects and could improve urination and erectile dysfunction is more frequently in the older age groups and develops develop over time (Michaelson et al., 2008).

1.6.3 Androgen deprivation therapy (ADT)

Another type of treatment for PCa is ADT. In 1941, Huggins and colleagues first introduced the treatment of metastatic prostate cancer with ADT. They found that castration before puberty prevents normal development of the prostatic gland into a mature organ while

castration after puberty leads to the regression of the prostate gland. They tested their hypothesis by achieving castration through orchiectomy (the surgical procedure of removing both testicles) and they monitored tumour progression after orchiectomy. They reported that the prostate underwent obvious regression in most cases. The prostate decreased in size by 50% just four months after orchiectomy and the gland became softer. In 1967, Huggins and Hodges were awarded the Nobel prize for their ground-breaking research (Huggins, 1941). Nowadays, ADT remains the common treatment for advanced and metastatic prostate cancer. However, there are multiple ways to achieve androgen deprivation besides surgical castration (Perlmutter & Lepor, 2007). This is primarily due to the side effects of surgical castration which include but are not limited to metabolic problems, body mass loss, erectile dysfunction, irreversibility as well as negative psychological effects. This is why biochemical castration is favored over surgical castration (Schröder et al., 2012).

1.6.3.1Androgen receptor (AR) structure and function

The AR gene is located on the X chromosome and it has a 2575 nucleotides coding region. The resulting protein is a 110- kDa protein consisting of three major functional domains. The first domain is called the N-terminal domain (NTD), the second domain is called the DNA binding domain (DBD) and the third domain is called the C-terminal ligand binding domain (LBD) (Tan et al., 2015). The AR acts as a transcription factor. In the nucleus, dimerization of ARs occur to allow them to bind to androgen response elements (AREs) in promoter regions of target genes to promote their transcription. Target genes include PSA, transmembrane serine protease 2 (TMPRSS2) and other genes responsible for prostate cell growth and survival (Green et al., 2012). The DBD domain allows the binding of the AR to promoter and enhancer regions

of the target genes. This allows the NTD and LBD to carry out their activation functions and promote the transcription of those genes. The NTD consists of two sites: Activation function 1 (AF1) and activation function 2 (AF2). It is worth noting that AF1 is constitutively active while AF2 activation requires the binding of a ligand (see section 1.7.1 below for the intracellular mechanism of action of the AR) (Tan et al., 2015).

1.6.3.2 Castration-resistant prostate cancer (CRPC)

A large fraction of PCa patients may develop resistance to castration after several years rendering the disease castrate resistant (Feng & He, 2019). There are a few suggested mechanisms that can explain the development of CRPC. The first mechanism involves the overexpression of ARs. This is explained through different mechanisms such as increased transcription rates, amplification of the AR locus and stabilization of the AR's mRNA or protein. Another plausible explanation for this phenomenon is AR mutations. Some mutations cause AR activation without the need of a ligand or through ligands other than androgens such as weak adrenal androgens and other steroid hormones, including dehydroepiandrosterone (DHEA), estrogens, progesterone, and cortisol (Green et al., 2012). Splice variants that bypass the ligand requirement for AR activation is another suggested mechanism. Another mechanism is the recruitment of cofactors. AR activity is induced by several cofactors and inhibited by suppressors. In CRPC and recurrent PCa, various cofactors are enhanced such as transcriptional intermediary factor 2 (TIF2), steroid receptor coactivators 1-3 (SRC1-3) and androgen receptor-associated protein 70 (ARA70). On the other hand, the depletion of corepressors such as nuclear receptor co-repressor 1 (NCoR1) and prohibitin are linked to recurrent PCa. Several signal transduction pathways might also contribute to AR activation without the need of androgens.

Those pathways include epidermal growth factor (EGF), insulin-like growth factor 1(IGF1), Ras-Raf-mitogen activated protein kinase (MAPK), signal transducer and activator of transcription 3 (STAT3) as well as phosphoinositide-3 kinase (PI3K) and protein kinase B (Akt) (Green et al., 2012).

1.6.3.3 Classification of ADT

Luteinizing hormone-releasing hormone (LHRH) agonists

LHRH is a hormone released by the hypothalamus that causes the release of luteinizing hormone (LH) from the pituitary gland. Subsequently, LH causes the release of testosterone from the testicles. LHRH agonist (also called gonadotropin releasing hormone (GnRH) agonists) act by continuously stimulating the hypothalamus to produce and secrete LH. This results in hypothalamic insensitivity to LHRH, which leads to a reduction in testosterone levels and production. LHRH *eventually* achieves hypogonadism as effective as orchiectomy (Polotti et al., 2017). The most currently used LHRH in Canada are Leuprolide (Lupron), Goserelin (Zoladex), Triptorelin (Trelstar) and Histrelin (Vantas).

LHRH antagonists

LHRH antagonists (also called GnRH antagonists) achieve tumour control by reducing the levels of LH produced and secreted by the pituitary gland. LHRH antagonists achieve that through competing with endogenous GnRH to bind to their receptors. This leads to the inhibition of LH secretion and consequent reduction in testosterone levels (Polotti et al., 2017). The most commonly used drug in this category is called Degarelix (Firmagon) and is given as a monthly injection (Clinton et al., 2017).

Antiandrogens

Antiandrogens are a class of drugs that compete with androgens to bind ARs and hinder their function to promote cell growth and proliferation. There are two types of antiandrogens: steroidal antiandrogens and non-steroidal antiandrogens. Cyproterone acetate (CPA) is a steroidal antiandrogen that acts through two different pathways. The first pathway is the apparent inhibition of AR activity and the second mechanism involves the inhibition of testosterone production through the blockade of gonadotropin secretion. On the other hand, there are various drugs classified as non-steroidal antiandrogens such as Flutamide (Euflex), Bicalutamide (Casodex), nilutamide (Anandron) and Enzalutamide (Xtandi) (Polotti et al., 2017). The first three are considered first generation antiandrogen while Enzalutamide is considered second generation antiandrogen. In other words, Enzalutamide is more effective at blocking the AR pathway and translocation because it binds with higher affinity than the former three. The treatment with non-steroidal antiandrogens may cause an increase in the production of testosterone as opposed to steroidal antiandrogens. It is worth noting that antiandrogens might be used in combination with LHRH in order to avoid the surge in testosterone levels that causes a tumour flare reaction when LHRH therapy is first started. This is called combined androgen blockade (CAB) (Polotti et al., 2017).

1.6.3.4 ADT adverse effects

Similar to other treatments, ADT has multiple side effects. Side effects include but are not limited to weight gain, physical weakness and loss of muscle mass, bone thinning, fatigue, depression, breast tenderness and growth (gynecomastia) as well as sexual problems including erectile dysfunction, shrinkage of the testicles and penis and low sex drive (Nguyen et al., 2015).

1.6.4 Chemotherapy

In the late 1900's chemotherapy was primarily used as a palliative therapy for prostate cancer. It was not until 2004 that chemotherapy was shown to have an effect on overall survival (Nader et al., 2018). Nowadays, chemotherapy is used to treat metastatic PCa, CRPC as well as to relieve the symptoms of advanced and late stage PCa. A few chemotherapy agents are used alone or in combination with other drugs to achieve tumour control. Docetaxel, which is a taxane derivative is the first-line chemotherapy that is able to improve overall survival. Docetaxel achieves tumour control by binding microtubule and preventing AR nuclear translocation. It also leads the cell to undergo apoptosis by inducing B-cell lymphoma-2 (Bcl-2) phosphorylation. After failure of docetaxel to achieve tumour control newer taxanes are being used. Cabazitaxel is another semi-synthetic derivative of taxane. It is a tubulin binding drug that is used after the failure of docetaxel to achieve tumour control. Similar to previous drugs, Cabazitaxel can be used alone and in combination with prednisone. Since it has apparent adverse effects and it shows similar efficacy to docetaxel, it is not recommended as a first-line treatment for chemotherapy-naïve tumours (Nader et al., 2018). Other chemotherapy drugs used less frequently in PCa are paclitaxel, mitoxantrone, estramustine, doxorubicin, epirubicin and vinorelbine (Nader et al., 2018).

1.6.4.1 Chemotherapy Adverse Effects

Since this is a systemic treatment, there are multiple side effects associated with it. Side effects vary from patient to patient and depend on the drug that is being administered. They can be experienced during the treatment period or after. Adverse effects include but are not limited to

fatigue, hair loss, loss of appetite, nausea, diarrhea, vomiting as well as low blood cell counts (McQuade et al., 2016).

1.6.4.2 Mechanism of PCa cell growth, survival and resistance to cytotoxic therapy

PCa cells develop resistance to cytotoxic therapy due to numerous reasons. Continuous activation of ARs achieved through gain of function mutations, gene amplification of ARs as well as upregulation of coregulators causes radiotherapy and chemotherapy resistance. Overexpression of ARs leads to cancer progression and apoptosis inhibition. Likewise, the expression of other proteins involved in apoptosis may also be altered. In addition, activation of key metabolism and growth stimulating signaling pathways such as PI3K and Akt and mammalian target of rapamycin complex 1 (mTORC1) leads to chemotherapy resistance. The activation of hypoxia inducible factor -1α (HIF-1α) downstream of mTORC1 allows the cell to survive in hypoxic environment and promotes angiogenesis, cell survival and metastasis. Similarly, loss of function mutations of tumour suppressor gene Tp53 and phosphatase and tensin homolog (PTEN) as well as overexpression of growth factors and cytokines such as interleukin-6 (IL-6) and nuclear factor-κB (NF-κB) lead to chemotherapy resistance. Functional and structural alterations to microtubules affecting docetaxel binding to β-tubulin as well as upregulation of β-tubulin also cause resistance (Lohiya et al., 2016).

1.7 Cellular mechanism stimulating cancer cell growth

1.7.1 *Androgens and androgen receptor signaling*

Growth of normal prostate cells and PCa is stimulated by combined effects of the AR and growth factor receptors such as the Epidermal Growth Factor Receptor (EGFR). ARs are crucial

for the growth of the prostate gland. They function as transcription factors, influencing the transcription of several genes responsible for cell growth a cell cycle progression. Testosterone diffuses through the cell and is subsequently converted into dihydrotestosterone (DHT) (Figure 1.1). DHT binds very tightly to AR which is present in the cytoplasm and leads to its nuclear translocation where it affects gene transcription. In the nucleus, AR binds to various coactivators such as ARA70 and the P160 family of coactivators. Coactivators have histone acetylation and chromatin remodelling activities. ARs also interact with various transcription factors in order to regulate gene expression. FOXA1 is the main transcription factor interacting with ARs. Other transcription factors include GATA2 and Oct1 which modulate ARs activity and gene expression (Takayama & Inoue, 2013).

ARs function is also regulated by growth factors. EGF signaling pathway directly promote ARs activity. Src, a tyrosine kinase involved in EGFR activation, directly phosphorylates ARs at tyrosine 534. This leads to the nuclear translocation of ARs and enhancement of its transcriptional activity. In addition, extracellular signal-regulated kinases 1/2 (ERK1/2), another key factor in the mitogen-activated protein kinase (MAPK) pathways is believed to promote AR activity (Takayama & Inoue, 2013).

Amyloid precursor protein (APP) is one of the genes that have been identified as a main AR target. It promotes PCa cell growth in an AR dependent manner. Forkhead Box P1 (FOXP1) and other forkhead family members are another set of genes regulated by ARs. However, studies have shown that FOXP1 negatively regulate ARs activity in PCa cells. Other genes regulated by ARs include ADP-ribosylation factor GTPase-activating protein 3 (ARFGAP3), Calcium/calmodulin-dependent protein kinase kinase 2 (CaMKK2) and the 14-3-3 family of

genes which promote cell proliferation and cancer progression (Freeman & Morrison, 2011; Lin et al., 2015; Obinata et al., 2012; Takayama & Inoue, 2013).

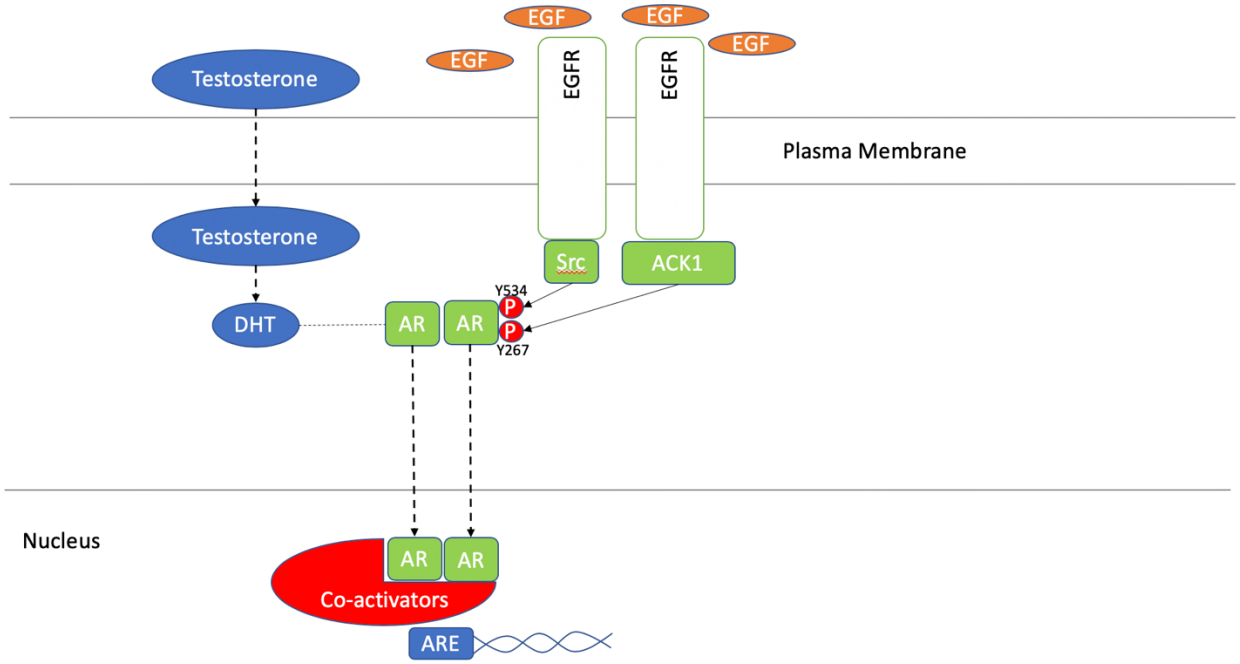

Figure 1.1: Androgens and AR signaling

Cytoplasmic AR is activated by binding directly to DHT or by phosphorylation by Src or ACK1. Once activated, it translocates to the nucleus where it dimerizes and binds to co-activators. ARs then act as transcription factors by binding to AREs in the promoter region of target genes.

1.7.2 EGFR and other growth factors:

1.7.2.1 RAS-RAF-MAPK-ERK pathway

The EGFR pathway is one of the pathways that is commonly upregulated in multiple cancers including prostate cancer. Upregulation of this pathway leads to an array of events including cell cycle progression, cell differentiation and migration as well as apoptosis inhibition. EGFR is activated by binding to growth factors such as EGF, transforming growth factor-α (TGF-α) and amphiregulin. Once EGFR is bound to its ligand, it undergoes dimerization which leads to transphosphorylation of tyrosine residues of the intracellular C-terminus. After

phosphorylation, growth factor receptor binding protein 2 (GRB2) directly binds to Y1068 and Y1086 residues of the C-terminal tail of EGFR. In addition, Src homology and collagen (SHC) binds to Y1148 and Y1173 residues which leads to its phosphorylation at Y317. This phosphorylation site becomes a binding site for GRB2. The adaptor molecule GRB2 then recruits son of sevenless 1 (SOS) which is a guanine nucleotide exchange factor (GEF) for the RAS protein. SOS facilitates the conversion of GDP to GTP of the RAS protein which causes a conformational change in RAS leading to its binding with RAF-1. Although RAS does not directly activate RAF-1, it does however initiate its translocation to the plasma membrane where it is phosphorylated at S338 and Y341 and hence activated. Activated RAF-1 is then able to phosphorylate MEK1/2 at S217 and S221 which in turn phosphorylates ERK1/2 at T202 and Y204. ERK1/2 has an array of downstream targets responsible for regulating the cell cycle. ERK1/2 phosphorylates RSK1 at T573 which can then be translocated in the nucleus and activate proto-oncogene c-fos and SRF. ERK1/2 itself can also be translocated to the nucleus where it activates ternary complex factor (TCF) which in turn promotes the transcription of immediate early genes (IEGs) such as c-myc and c-fos which are involved in cell proliferation and survival. Similarly, it activates ETS, ELK-1 c-JUN and SP-1 which mediate cellular differentiation and tumorigenesis (Wee & Wang, 2017).

1.7.2.2 PI3K-Akt-mTOR

EGFR also regulates the PI3K-Akt-mTOR pathway (Figure 1.2). PI3K is comprised of two subunits; the regulatory subunit P85 and the catalytic subunit P110. After the binding of GRB2 to the intracellular C-terminus of EGFR, GRB2-associated-binding protein 1 (GAB1), an adaptor protein binds to it and is therefore phosphorylated at Y446, Y472, and Y589. Those

phosphorylation sites are the binding sites for the P85 subunit of PI3K. The catalytic subunit can then convert PIP2 to PIP3 by phosphorylating the former. PIP3 binds the pleckstrin homology (PH) domain of Akt causing its translocation to the plasma membrane. This is where it gets phosphorylated. Akt is phosphorylated at two sites T308 and S473. Although T308 phosphorylation is sufficient for Akt activation, maximal activation requires the phosphorylation of S473. Pyruvate Dehydrogenase Kinase 1 (PDK1) phosphorylates Akt at T308 while mTORC2 phosphorylates S473. Activated Akt is then able to directly phosphorylate Tuberous Sclerosis Complex 2 (TSC2) at five sites S939, S981, S1130, S1132 and T1462. This inhibitory phosphorylation leads to the inactivation of mTORC1 and therefore the suppression of protein synthesis. In cancer cells, Akt has been involved with increasing glucose uptake by upregulating glucose transporters. This promotes aerobic glycolysis and causes the Warburg effect (Wee & Wang, 2017).

1.7.2.3 EGFR regulation of the cell cycle

EGFR is able to activate CDK4/6-cyclin D complex to help the cell progress through the G1 phase. ERK1/2 phosphorylation of c-FOS and c-JUN and hence the activation of Activator protein 1 (AP-1) complex promote cyclin D expression (Figure 1.2). Likewise, the PI3K-Akt pathway also upregulates cyclin D activity through the transcription of c-FOS. In addition, activity of ERK1/2 has been associated with the downregulation of $p27^{kip1}$, a CDK4/6 inhibitor. Furthermore, Akt is able to inhibit the CDK inhibitors $p21^{CIP1/WAF1}$ by phosphorylating T145, and $p27^{kip1}$ by phosphorylating T157 and T198. Akt can also inhibit FOXO1 which promotes the transcription of $p27^{kip1}$ and $p21^{WAF1}$(Wee & Wang, 2017).

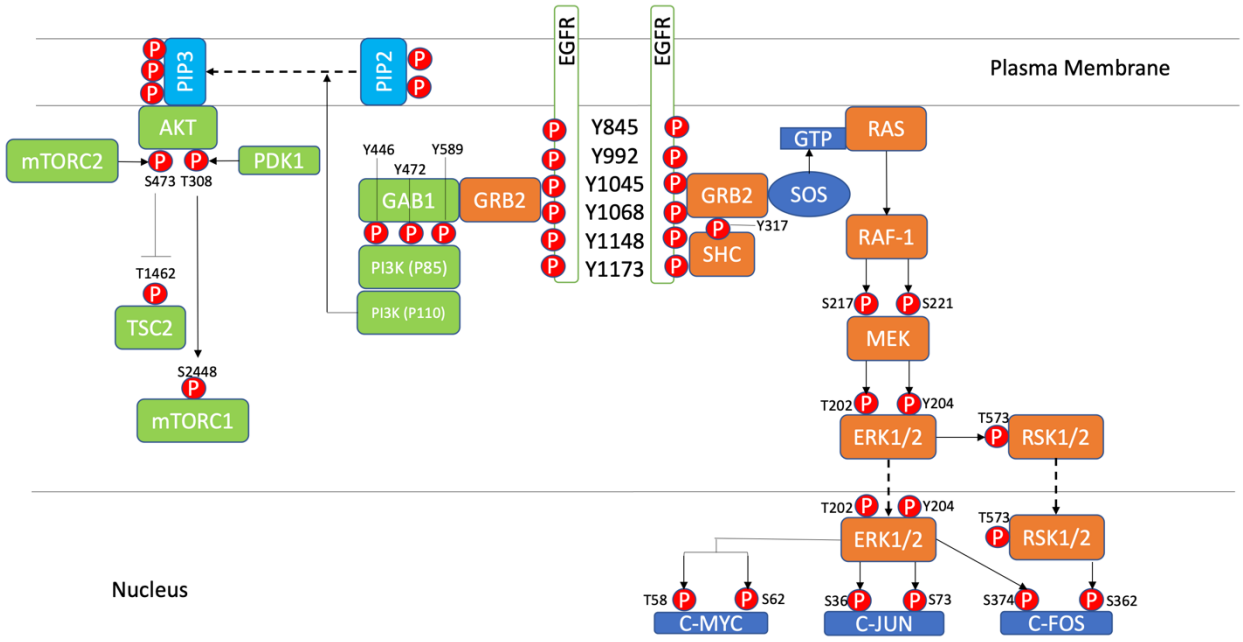

Figure 1.2: EGFR signaling pathways.

Upon binding to growth factors, EGFR undergoes transphosphorylation which leads to the recruitment of GRB2 and SHC. GRB2 then recruits SOS which facilitates the conversion of GDP to GTP on RAS. The latter then activates RAF-1 which phosphorylates and activates MEK. Subsequently, ERK1/2 is activated which leads to the activation of RSK1/2. RSK1/2 translocates to the nucleus and phosphorylates c-fos. ERK1/2 can also undergo nuclear translocation and phosphorylate c-JUN, c-myc and c-fos. On the other hand, GRB2 can recruit GAB1 which leads to the activation of PI3K. PI3K in turn converts PIP2 to PIP3 allowing for the recruitment and activation of Akt. Phosphorylated Akt, through mTORC2 or PDK1 can then activate mTORC1 through its phosphorylation or through the inhibitory phosphorylation of TSC2.

1.7.3 *PI3K/ PDK/ PTEN /Akt/ mTOR*

PI3K is a protein serine and lipid (inositol) kinase that is a key effector of many growth factor cell surface receptors including EGFR and HER2. It is activated in many cancers due to EGFR and RAS mutations (Yuan & Cantley, 2008). PI3K allows for the conversion of PIP2 to PIP3. PTEN is a tumour suppressor protein that dephosphorylates PIP3 and therefore, inhibits downstream signaling including activation of Akt and mTORC1. However, PTEN mutations are

common in many cancers including prostate cancer which leads to constant activation of the PI3K-Akt-mTOR pathway (Yuan & Cantley, 2008).

1.7.4 The mTOR pathway

The mTOR pathway regulates protein synthesis and cell proliferation and therefore is essential for cell survival and proliferation. There are two mTOR complexes; mTORC1 and mTORC2. mTORC1 is primarily responsible for protein synthesis and translation while mTORC2 is a regulator of the actin cytoskeleton (Saxton & Sabatini, 2017a). The mTORC1 consists of several proteins including mTOR, regulatory-associated protein of mTOR (RAPTOR) and mLST8 subunit. Similarly, mTORC2 consists of mTOR, mLST8 and rapamycin-insensitive companion of mTOR (RICTOR) instead of RAPTOR. mTORC1 has many positive and negative regulators. Negative regulators include tuberous sclerosis complex (TSC) 1 (hamartin) and TSC2 (tuberin) as well as PTEN which is a negative regulator of the PI3K/Akt pathway. On the other hand, positive regulators include several growth factors such as insulin-like growth factor-1 (IGF-1) and its cognate receptor IGFR-1 as well as vascular endothelial growth factor receptors (VEGFRs) (Porta et al., 2014). mTORC1 has various downstream targets through which protein synthesis is regulated. mTORC1 directly phosphorylates and activates p70S6K on T389 which, in turn, leads to ribosomal protein S6 phosphorylation on S240 and therefore its activation (Ferraril & Thomas2, 1994; Hong et al., 2014). Furthermore, mTORC1 directly phosphorylates Eukaryotic translation initiation factor 4E Binding Protein 1 (4E-BP1) on S65 (Qin et al., 2016). This phosphorylation leads to its dissociation from eIF-4E which enables 5′cap-dependent mRNA translation to take place (Saxton & Sabatini, 2017a).

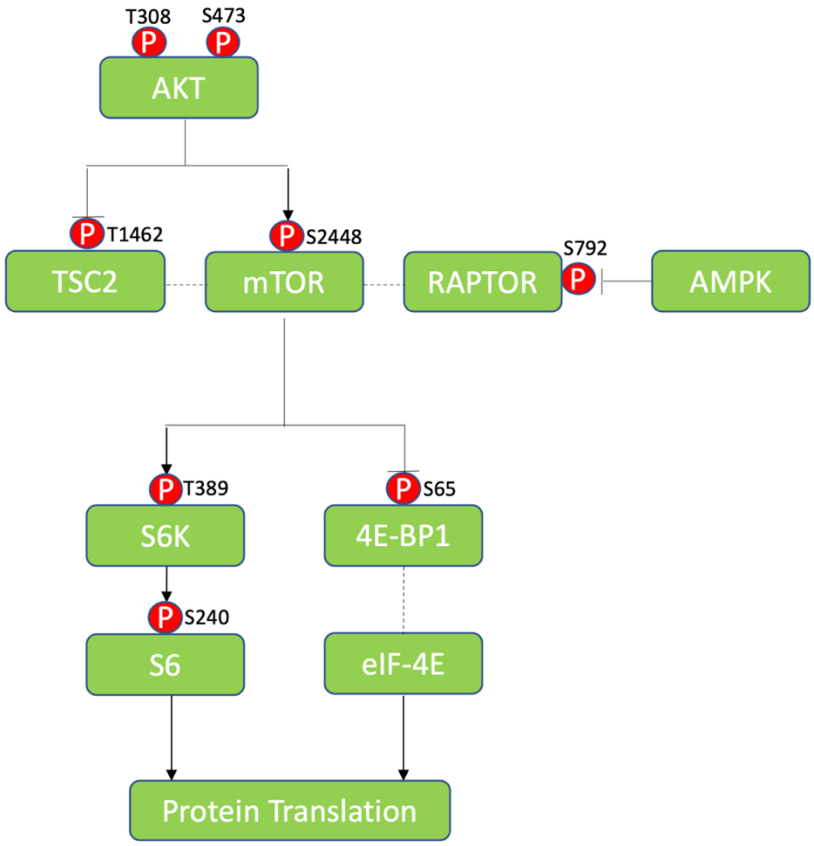

Figure 1.3: The mTOR pathway

Phosphorylated Akt activates mTOR by directly phosphorylating it or by inhibiting TSC2 which leads to the activation of mTORC1. AMPK can also activate mTORC1 through the phosphorylation of RAPTOR which causes its dissociation from mTOR. Activation of mTORC1 results in the phosphorylation of S6K which in turn phosphorylates the ribosomal protein S6. In addition, the inhibitory phosphorylation of 4E-BP1 by mTORC1 leads to its dissociation from eIF-4E which promotes 5′cap-dependent mRNA translation. Activation of the mTOR pathway leads to protein synthesis and cell proliferation.

1.7.5 HIF-1α

HIF-1α is a transcription factor that mediates multiple cellular pathways in response to low oxygen levels. Typically, solid tumours experience hypoxia due to the obstruction and compression of blood vessels surrounding them. As a result, HIF-1α is activated in order to allow the cell to progress through the cell cycle (Masoud & Li, 2015). Heterodimerization of

HIF-1α with HIF-1β is essential to mediate the action of HIF-1α. However, HIF-1β is constitutively expressed in the cell. Dimerization of both subunits allows for the binding to hypoxia response elements (HRE)-DNA sequence on target genes (Masoud & Li, 2015).

HIF-1α expression is regulated by several upstream pathways. The PI3K-Akt-mTOR pathway is one of the main pathways involved in the regulation of HIF-1α. Phosphorylation of 4E-BP1 by mTOR results in the enhanced cap-dependent translation of HIF-1α. Likewise, phosphorylation of S6 allows for the ribosomal translation of HIF-1α. Furthermore, the RAS-RAF-MAPK-ERK pathway is also involved in the translation and activation of HIF-1α. ERK1/2 directly phosphorylates 4E-BP1 and S6K which leads to HIF-1α translation. In addition, ERK1/2 phosphorylates CBP/p300 which are coactivators enhancing HIF-1α activity. This allows for the formation of HIF-1α /p300 complex which induces the transcription of target genes. On the other hand, p53 has been associated with HIF-1α degradation. Under normoxia, p53 binds to HIF-1α and allows for mouse double minute 2 homolog (MDM2) mediated ribosomal degradation of HIF-1α. This explains the reason why HIF-1α expression is upregulated in many types of cancers (Masoud & Li, 2015).

HIF-1α mediates the transcription of an array of genes responsible for tumour metastasis, angiogenesis, energy metabolism, cell differentiation and apoptosis. Under hypoxic environments, HIF-1α upregulates the transcription of GLUT1 and GLUT4 in an attempt to increase glucose uptake by the cell. The transcription of other glycolytic enzymes such as Fructose-2,6-bisphosphate (Fru-2,6-P2), namely phosphoglycerate kinase 1 (PGK1) and pyruvate kinase M2 (PKM2) is also regulated by HIF-1α (W. Liu et al., 2012). This allows the cell to transition to aerobic glycolysis (Lum et al., 2007) which leads to decreased oxidative phosphorylation and increased lactate production. Moreover, HIF-1α activates the gene encoding

PDK1 which leads to an increase of the inhibitory phosphorylation of pyruvate dehydrogenase (PDH). This cascade of events stops the conversion of pyruvate to acetyl-CoA and hence its entry and utilization in the Krebs cycle (W. Liu et al., 2012).

Another key transcription factor regulated by HIF-1α is TWIST. TWIST is crucial in mediating epithelial-mesenchymal transition (EMT) and metastasis. In addition, HIF-1α regulates the expression of different adhesion molecules such as α5β3, $\alpha 5\beta 5$, and β1 intergrins. It also downregulates transcription factor 3 (TCF3), ZFHX1A, ZFHX1B resulting in downregulation of E-cadherin gene transcription (W. Liu et al., 2012). Furthermore, studies on cardiac and renal fibroblasts showed the implication of HIF-1α in increasing type I procollagen α1 mRNA. Other studies on peripheral lung parenchyma and pulmonary artery of rats have showed that type I, II and IV procollagen mRNA were increased as a result of hypoxia. However, cancer studies are still required to confirm these in the hypoxic tumour environment (Gilkes et al., 2014). Another key regulator of angiogenesis and a downstream target of HIF-1α is vascular endothelial growth factor (VEGF) (W. Liu et al., 2012).

1.7.6 DNA replication: Modulation of histone function by MAPKs

Histones are a family of nuclear proteins that allow DNA packaging. Histones are highly modified post-translationally through phosphorylation, acetylation as well as methylation. Modifications to histones are linked several biological processes such as DNA repair, chromatin condensation, chromosome segregation and cell cycle progression. Histone 3 (H3) phosphorylation at S10 is a marker for cells undergoing mitosis. More specifically, it is believed that H3 phosphorylation occurs at the G2 phase in order to initiate DNA condensation. This is required for chromosome segregation and hence the progression through the cell cycle (Healy et

al., 2012). Some studies suggest that H3 phosphorylation facilitates acetylation which makes the DNA more accessible (Edmondson et al., 2002). Healy and colleagues were able to summarize the pathway leading to H3 phosphorylation. They claim that EGFR, upon binding to EGF, leads to a cascade of events resulting in H3 phosphorylation (Figure 1.4). Activated ERK1/2 and p38 MAPK translocate to the nucleus, which results in the activation of transcription of target genes such as the immediate-early genes (IEG). Further studies showed that activation of mitogen and stress-activated protein kinase (MSK1/2), which is a target of ERK1/2 and p38 MAPK, directly phosphorylates H3 at serine 10 and 28. This phosphorylation allows for cell cycle progression and IEG transcription (Healy et al., 2012).

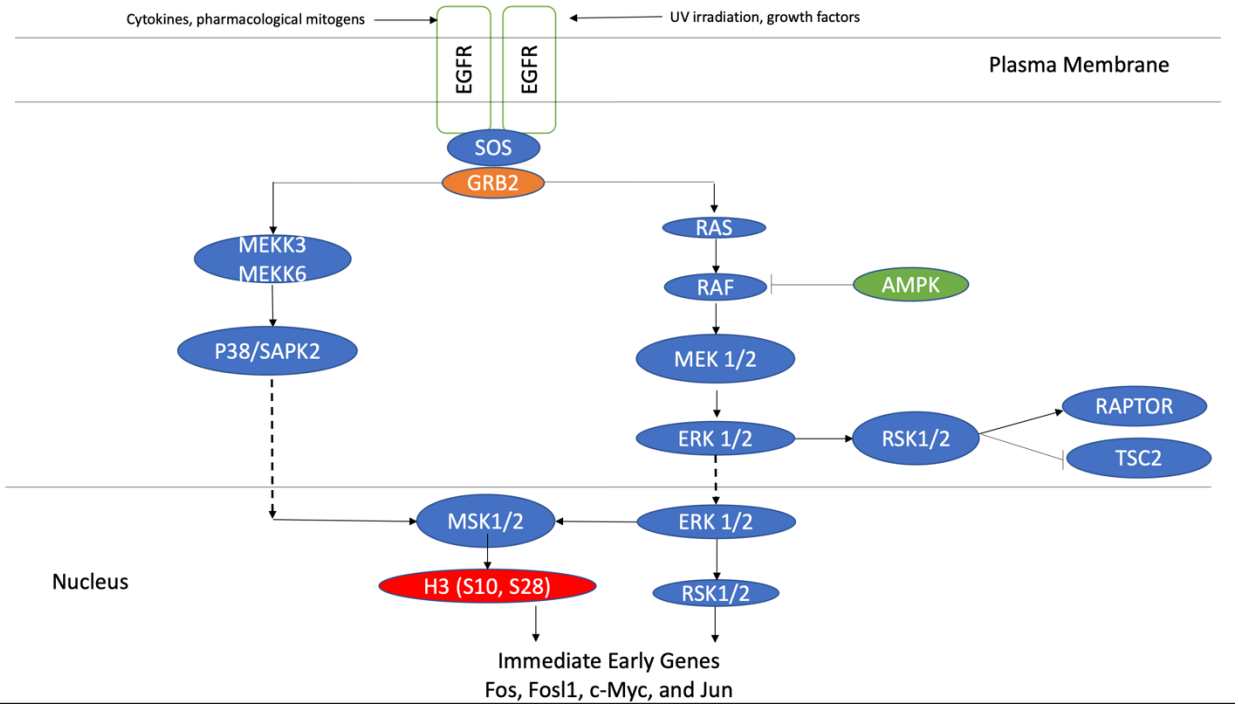

Figure 1.4: Pathways leading to H3 phosphorylation

Activated EGFR recruits SOS and GRB2 allowing for the activation of RAS. RAS, a small GTPase molecule then activates RAF which in turn phosphorylates MEK1/2. The latter then activates ERK1/2 which is able to activates RSK1/2 in the cytoplasm but also undergoes nuclear translocation and activate RSK1/2 as well as MSK1/2. Cytoplasmic RSK1/2 is able to phosphorylate RAPTOR as well as TSC2. It is worth noting that AMPK is able to inhibit the

activity of RAF. In addition, GRB2 can also activated MEKK3/6 which activate p38 MAPK. The latter is able to translocate in the nucleus causing the activation of MASK1/2 which in turn phosphorylates H3 at S10 and S28.

1.8 Molecular signaling in prostate cancer

1.8.1 P53

P53 is a tumour suppressor protein that is mutated in many malignancies including PCa. It is involved in a number of cellular processes such as cell-cycle checkpoints, senescence, autophagy and apoptosis. Activation of AMP-activated kinase (AMPK) as well as other kinases such as ATM, CHK1, ataxia telangiectasia and Rad3-related protein (ATR) and CHK2 are involved in p53 activation (Park et al., 2002). ATM and ATR phosphorylate p53 at S15 which leads to its stabilization and ultimately executing its DNA-damage response (Park et al., 2002). Upon activation, p53 is able to induce G1 cell cycle arrest by primarily activating the cyclin-dependent kinase inhibitor $P21^{waf1/cip1}$. In addition, p53 is able to disrupt the function of the cyclin B1/CDC2 complex which leads to G2/M cell cycle arrest. p53 can also induce apoptosis through several mechanisms. In response to IR, p53 can translocate to the mitochondria and alter their outer membrane permeability. This leads to the release of pre-apoptotic factors. In addition, p53 can also interact with p53-up-regulated modulator of apoptosis (PUMA) in order to induce apoptosis (Park et al., 2002).

1.8.2 $P27^{kip1}$

$P27^{kip1}$ is a CDK inhibitor involved in G1/S cell cycle arrest. Unphosphorylated $p27^{kip1}$ serves as a CDK inhibitor, however, upon phosphorylation, several events may occur. $P27^{kip1}$ binds and physically block the catalytic site of the CDK as well as ATP binding. $P27^{kip1}$ is highly

modified post-translationally. Phosphorylation on T187 by cyclin E/CDK2 leads to its ubiquitination and degradation (J. Lee & Kim, 2009) while phosphorylation on T157 and T198 by Akt leads to its cytoplasmic retention. This leads to $p27^{kip1}$ inactivation and thus successful progression through the cell cycle (Viglietto et al., 2002). It is worth noting that $p27^{kip1}$ downregulation and inactivation is observed in many cancers especially when Akt and SRC activity is upregulated (J. Lee & Kim, 2009).

1.9 Sensors of Metabolic stress

1.9.1 AMP-activated Kinase (AMPK) as an Energy Stress Sensor

AMPK senses the energy state of the cell and regulates various cellular processes to maintain energy homeostasis. AMPK is composed of three different subunits (Steinberg & Carling, 2019). The α subunit is the catalytic subunit while the β and γ subunits are regulatory subunits. Once the cell is in a low energy state, and the AMP to ATP ratio is high, AMPK is activated. AMP is able to bind the γ subunit, which induces a conformational change that allows for the phosphorylation of Threonine 172 in the α subunit. This conformational change not only allows for the phosphorylation but also protect against the dephosphorylation of the catalytic subunit. The main upstream kinase that phosphorylates threonine 172 is called liver kinase B1 (LKB1) (Shackelford & Shaw, 2009). This phosphorylation is needed for ultimate AMPK activation. AMPK activity can then be increased by up to 100-fold leading to alterations of an array of metabolic pathways which include carbohydrates, fatty acid, cholesterol and amino acid metabolism, mitochondrial biogenesis and cell growth (Steinberg & Carling, 2019).

1.9.2 AMPK Regulation of Fatty Acids and Cholesterol Synthesis

Energy stress leads to an increase in the ratio of AMP to ATP in the cell which mediates an AMPK-dependent suppression of fatty acid and cholesterol synthesis resulting in reduction of lipid stores and promotion of fatty acid oxidation to help recover intracellular ATP levels. Synthesis of cholesterol as well as fatty acids involves the same intracellular metabolite, acetyl-CoA (Steinberg & Carling, 2019). In the cholesterol synthesis pathway, AMPK inhibits 3-hydroxy-3-methylglutaryl coenzyme A reductase (HMGR) by phosphorylating serine 872, which is the rate-limiting enzyme in the mevalonate pathway. This leads to a lower serum and liver cholesterol (Loh et al., 2019). Furthermore, with respect to fatty acid synthesis, acetyl CoA is converted to malonyl-CoA through Acetyl CoA Carboxylase (ACC). There are two known isoforms of ACC; ACC1 and ACC2. The former is found in lipogenic tissues such as adipose tissue while the latter exists predominantly in heart and skeletal muscles. AMPK is known to phosphorylate ACC1 and ACC2 at Ser79 and Ser212 respectively, thus, inhibiting the conversion of acetyl-CoA to malonyl-CoA, which is the first step in fatty acid synthesis (Fullerton et al., 2013). For a more prolonged response, AMPK may inhibit this pathway by altering transcription factors called sterol-response element binding proteins (SREBPs). SREBP 1a and SREBP 1c regulate the transcription of genes involved in the synthesis of fatty acids, while SREBP 2 regulate the transcription of genes involved in cholesterol synthesis (Eberlé et al., 2004). Precursor SREBPs molecules are retained in the endoplasmic reticulum (ER) membranes through a tight association with SREBP cleavage activating protein. In order to be activated, SREBPs are released from the ER into the Golgi apparatus where two functionally distinct proteases, site 1 protease (S1P) and site 2 protease (S2P), sequentially cleave the precursor protein. S1P cleaves within the hydrophilic luminal loop of the SREBP precursor while

S2P cleaves the protein within the first transmembrane fragment. The functional protein then undergoes a nuclear translocation where it binds to its target genes. It should be mentioned that all of the studies on SREBP process mechanism and control by sterols have been performed *in vitro*, but these mechanisms have not been established in vivo yet (Steinberg & Carling, 2019). AMPK accomplishes the inhibition of SREBP1c and SREBP2 by phosphorylating Ser372 and Ser374 respectively which in turn attenuates the activation process and inhibits proteolytic cleavage in the Golgi apparatus (Steinberg & Carling, 2019).

1.9.3 AMPK Regulation of Carbohydrate Metabolism

AMPK regulates carbohydrate metabolism through multiple pathways ranging from glucose uptake to glucose storage. It promotes glucose uptake by translocating glucose transporter type 4 (GLUT4) and Glucose transporter type 1 (GLUT1) from an intracellular location to the plasma membrane. This step is achieved by several pathways (Kurth-Kraczek et al., 1999). One pathway involves the inhibitory phosphorylation of the RAB GTPase-activating protein (GAP) GTPase TBC1D1 by AMPK. This prevents the sequestering of GLUT4 to the Golgi apparatus (Steinberg & Carling, 2019). In addition, AMPK phosphorylates 1-phosphatidylinositol 3-phosphate 5-kinase, (PIKfyve), at Ser307. This promotes its translocation to endosomes to facilitate GLUT4 translocation (Y. Liu et al., 2013). Similarly, phospholipase D1 (PLD1) activation by AMPK activates ERK which in turn causes GLUT4 translocation (J. H. Kim et al., 2010). For a more prolonged response, AMPK phosphorylates histone deacetylase 4 (HDAC4) which increases myocyte enhancer factor and GLUT4 expression (Steinberg & Carling, 2019).

In cells that express mostly GLUT1, AMPK is reported to increase activation and cell surface expression of GLUT1 (Fryer et al., 2002). In addition, AMPK directly phosphorylates thioredoxin-interacting protein (TXNIP) which leads to its degradation. TXNIP suppresses glucose uptake directly, through two main mechanisms. The first mechanism involves the direct binding of TXNIP to the glucose transporter GLUT1 which induces GLUT1 internalization through clathrin-coated pits. The second mechanism involves a reduction in the level of GLUT1 messenger RNA (mRNA). As a results, TXNIP degradation increases GLUT1 plasma membrane localization and mRNA expression (Steinberg & Carling, 2019; N. Wu et al., 2013). In the cytoplasm, glucose is converted to Glucose 6 phosphate (G6P) by hexokinase. This indicates the first key step in glycolysis because it causes glucose trapping within cells (Teslaa & Teitell, 2014). AMPK can then elevate the rates of glycolysis by directly phosphorylating phosphofructokinase 2 (PFK2). This leads to the synthesis of fructose-2,6-bisphosphate, an allosteric activator of phosphofructokinase 1 (PFK1), which in turn catalyzes the irreversible conversion of fructose-6-phosphate into fructose-1,6-bisphosphate (Sciacovelli et al., 2014). PFK2 exists in multiple isoforms, and only the cardiac and the inducible isoforms (present in tumour cells and haemopoietic cells) are regulated by AMPK (Steinberg & Carling, 2019). AMPK does not only promote glycolysis in order to increase the concentration of ATP in the cell, but it also decreases the rate of glycogen synthesis to make glucose more readily available for glycolysis. This is achieved through the inhibitory phosphorylation of glycogen synthase at S7 (Jeon, 2016). However, it was found that this inhibition is not consistent. Subsequent studies have shown that more prolonged activation of AMPK can indirectly increase glycogen synthesis by increasing glucose uptake and G6P production (Aschenbach et al., 2002). Furthermore, to ensure that G6P is not consumed in the hexosamine biosynthesis, AMPK phosphorylates

Glutamine fructose-6-phosphate aminotransferase 1 (GFAT1) at S243 to inhibit its activity. By inhibiting GFAT1, the rate limiting enzyme of the hexosamine biosynthesis, AMPK ensures that G6P is directed towards glycolysis rather than glycogen synthesis (Steinberg & Carling, 2019). Additionally, AMPK promotes glycogenolysis by activating glycogen phosphorylase (GP) (Jeon, 2016).

In the liver, AMPK inhibits gluconeogenesis by inhibiting different transcription factors such as CREB regulated transcription coactivator 2 (CRTC2) and hepatocyte nuclear factor 4 (HNF4).

Those transcription factors promote the expression of enzymes involved in gluconeogenesis such as phosphoenolpyruvate carboxykinase and glucose-6-phosphatase. AMPK can also achieve gluconeogenesis inhibition through the phosphorylation of class IIa histone deacetylases. This causes their nuclear exclusion. Subsequently, the transcription factor FOXO in the nucleus is not activated, which leads to the suppression of gluconeogenic enzymes (Mihaylova et al., 2011).

1.9.4 AMPK Regulation of Protein Synthesis

An alternative way of conserving cellular ATP levels is inhibiting protein synthesis which a high energy process. More specifically, AMPK suppresses protein synthesis by inhibiting the mTORC1 which includes the catalytic subunit mTOR. This is achieved through the direct inhibitory phosphorylation of Tuberous Sclerosis Complex 2 (TSC2) and Regulatory-associated protein of mTOR (RAPTOR) at S1345 and S792 respectively (Gwinn et al., 2008a; Inoki et al., 2003). This inhibitory phosphorylation causes the disassembly of TORC1 and therefore its inactivation (Hughes Hallett et al., 2015; Jeon, 2016). For a more prolonged response, AMPK downregulates ribosomal RNA synthesis by phosphorylating transcription

initiation factor 1A. Additionally, it directly inhibits translational elongation by activating eukaryotic elongation factor 2 kinase (eEF2K) which in turn causes the inhibitory phosphorylation of eukaryotic elongation factor 2 (eEF2) (Jeon, 2016).

1.9.5 AMPK regulation of mitochondria

The mitochondria, being the powerhouses of the cell, coordinates metabolic pathways in order to generate enough energy for the cell. In the mitochondria, pyruvate dehydrogenase complex (PDC) converts pyruvate to acetyl CoA so it can be processed further by enzymes in the Krebs cycle. In addition, pyruvate carboxylase allows for the conversion of pyruvate to oxaloacetate which is another substrate for the Krebs cycle. Mitochondria are able to alter the Krebs cycle in case of low glucose availability to utilize other substrates to feed the Krebs cycle for generation of electron carriers that produce ATP. Glutamine, the most abundant amino acid in plasma, is converted to α-ketoglutarate, which can then be injected in the Krebs cycle to generate NADH and FADH2. First, glutaminase converts glutamine into glutamate. This reaction is followed by the conversion of glutamate to α-ketoglutarate which can be utilized as a substrate for the Krebs cycle. This process is called glutamine anaplerosis, which describes the use of glutamine to produce intermediates that can be used in the Krebs cycle. Furthermore, branched-chain amino acids (BCAA) could also be used in the Krebs cycle. Amino acids such as leucine, valine and isoleucine can be used to generate acetyl CoA and succinyl CoA which is a Krebs cycle intermediate. In regard to fatty acid metabolism, the carnitine palmitoyl transferase 1 (CPT1) enzyme allows for the translocation of long chain fatty acids in the mitochondrion. This is achieved by converting fatty acyl CoAs into acyl-carnitines. Inside the mitochondria, CPT2 reverses this reaction and liberate fatty acids from carnitine. It is important to mention the

association between CPT1 and Malonyl CoA. Malonyl CoA, which is generated by ACC, is able to inhibit the import of acyl-carnitine by repressing CPT1. This is because the presence of Malonyl CoA represents the first metabolite in the fatty acid synthesis pathway. However, during low energy states, AMPK inhibits the activity of ACC which in turn reduces the amount of Malonyl CoA. As a result, CPT1 is activated and Fatty acid oxidation takes place in the mitochondria. Subsequently, acetyl CoA molecules can be used in the Krebs cycle to generate energy (Spinelli & Haigis, 2018).

Through the Krebs cycle, the mitochondria produce NADH and FADH2 which can then be utilized to generate ATP through the electron transport chain. Electrons are deposited in the inner mitochondrial membrane where their energy is utilized to pump protons into the intermembrane space. This movement allows ATP synthase to generate ATP (Spinelli & Haigis, 2018).

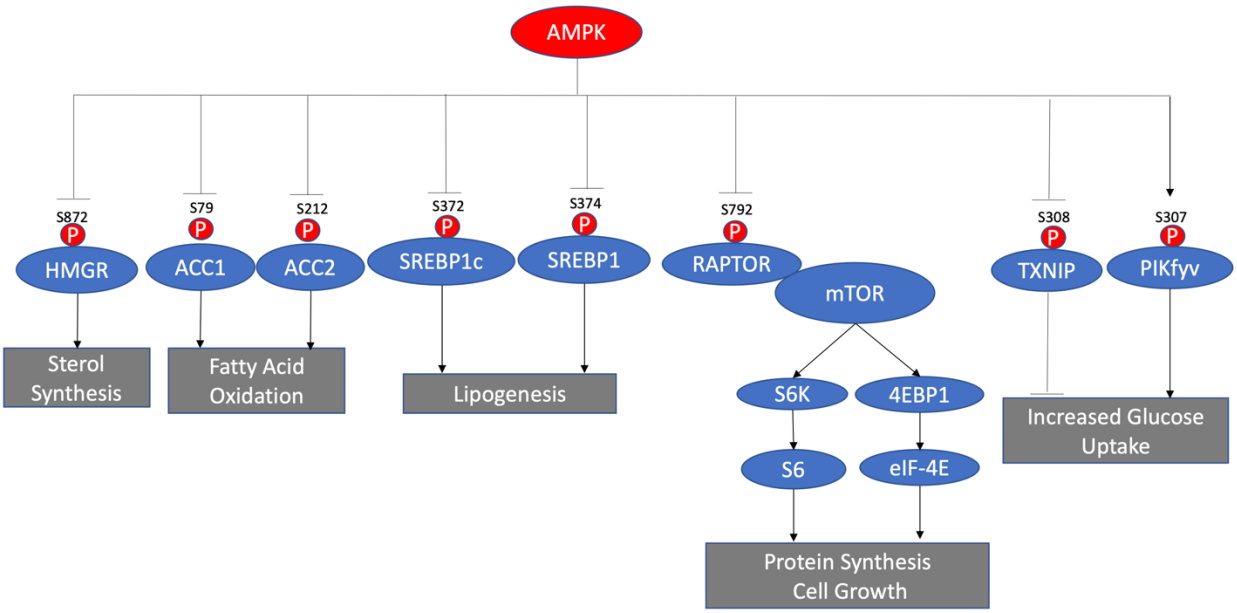

Figure 1.5: AMPK regulation of cellular processes

AMPK responds to low energy levels by regulating several cellular and metabolic pathways. It inhibits HMGR which in turn reduce sterol synthesis. AMPK also decrease fatty acid oxidation by directly inhibiting ACC. In addition, AMPK suppresses lipogenesis through the inhibitory phosphorylation of SREBP1. In regard to protein synthesis, AMPK directly phosphorylates

RAPTOR which leads to its dissociation from mTORC1 which in turn suppresses protein synthesis. AMPK is also able to increase glucose uptake by inhibiting TXNIP and activating PIKfyv.

The mitochondria are also involved in the biosynthesis of amino acids, fatty acid and cholesterol in the presence of excess energy. During high-energy levels, citrate, a Krebs cycle intermediate might be used for anabolic reactions such as fatty acid and cholesterol synthesis. Mitochondrial citrate is exported to the cytosol through the malate-citrate antiporter, SLC25A1 where it can be converted to acetyl CoA by ATP citrate lyase (ACLY) to support de novo lipogenesis. Glutamine and glucose synthesis can also be initiated in mitochondria. Mitochondria glutamine synthase can convert glutamate into glutamine. Finally, gluconeogenesis can also be initiated in the mitochondria. Although it is predominantly a cytosolic process, the first step occurs in the mitochondria. Following the conversion of oxaloacetate to malate, malate is exported from the mitochondria where it undergoes further steps of the gluconeogenesis pathway (Spinelli & Haigis, 2018).

1.10 Cancer Metabolsim

1.10.1 Carbohydrates metabolism

Glucose Transport in cells.

Glucose is the main source of energy in the majority of healthy cells. It is processed through a series of catabolic reactions in order to produce ATP which allows the cell to maintain its biological function, grow and proliferate (Dashty, 2013). There are two types of transporters that allow glucose to enter into the cell. The first type is called sodium–glucose co-transporters (SGLTs) and the second type is called facilitated diffusion glucose transporters (GLUTs). In humans, there are six types of SGLTs. SGLTs transport sodium ions and glucose in the same

direction of the membrane, hence, they are called symporters. They are ATP independent, which means that they do not actively transport sodium against its concentration gradient. However, they rather depend on the concentration gradient as a source of chemical potential. Those transporters are present at different organs throughout the body. For instance, SGLT2 transporters are mainly present in the kidney, more specifically in the proximal convoluted tubule of the nephron where they help in the reabsorption of glucose from the glomerular filtrate. On the other hand, SGLT1 transporters are present on the apical membranes of the small intestine to help with glucose absorption. SGLTs have different affinity for glucose and different capacities. On the other hand, there are 14 GLUTs types present in humans. GLUTs transport glucose across the plasma membrane by means of facilitated diffusion. Therefore, they do not require a source of energy to transport glucose. Different transporters have different affinities to glucose and are located in different organs. In addition, some of them are hormone regulated. For instance, GLUT4 is insulin-responsive such that insulin can result in a 10 to 20 fold increase in the amount of glucose transported (Navale & Paranjape, 2016).

Glucose Metabolism

Once inside the cell, glucose undergoes a series of steps that result in the generation of ATP which is the main source of energy for most biological processes. Glycolysis is the first step where the six-carbon glucose molecule is broken down into two three-carbon pyruvates. This step takes place in the cytoplasm of the cell and does not require oxygen. Anaerobic glycolysis yields 2 ATP and two lactic acid molecules. On the other hand, aerobic glycolysis yields 2 ATP, two pyruvate molecules and two $NADH_2$ molecules which can then be used to generate ATP. Once pyruvate is obtained from glycolysis, it undergoes decarboxylation in the mitochondria through an oxidative carboxylation reaction catalyzed by PDC. The products of this reaction are

one molecule of acetyl-CoA and one $NADH_2$. This step is a transition step between glycolysis which occurs in the cytosol and the Krebs cycle which takes place in the mitochondria. During the Krebs cycle, the two pyruvate molecules are degraded to release their energy. The Krebs cycle yields 3 $NADH_2$, 4 CO_2, 1 $FADH_2$, 2 CoA and 2 GTP per one pyruvate molecule. The coenzymes $NADH_2$ and $FADH_2$ are then used in the oxidative reaction (Dashty, 2013). They utilize the energy provided by the hydrogen ions to synthesize ATP from ATP and P_i (Bonora et al., 2012).

1.10.2 Lipid metabolism

Mammalian cells receive fatty acids and cholesterol from their environment but also synthesize their own (de novo synthesis). Fatty acids acids are transported into the cell through fatty acid transport proteins (FATPs). There are six types of FATPs which are present in cells utilizing fatty acids. FATPs are able to transport long chain as well as very long chain fatty acids into the cell. In order for fatty acid oxidation to occur, fatty acids must translocate into the mitochondria where they can undergo β-oxidation. Since the mitochondrial membrane is impermeable to acyl-CoAs, a carnitine shuttle present at the mitochondrial outer membrane allow for the import of long chain acyl-CoAs (Houten & Wanders, 2010). Once inside the mitochondria, long chain acyl-CoAs undergo several steps in order to generate energy. The first step is accomplished by an enzyme called acyl-CoA dehydrogenase which forms a trans double bond between the alpha and the beta carbon of the acyl-CoA chain. Enoyl CoA hydratase accomplishes the second step which involves a hydration of the double bond. The third step requires beta-hydroxyl acyl CoA dehydrogenase which dehydrogenates the fatty acid chain. Finally, the bond between the alpha and beta carbons is cleaved and the result is a two-carbon

shorter fatty acid chain and one molecule of acetyl CoA. The previous steps might be repeated until the entirety of the long fatty acid chain is converted to acetyl CoA. This process results in the production of a number of electron carriers NADH and $FADH_2$ which can then be used to generate ATP (Talley & Mohiuddin, 2020).

1.10.3 De novo lipogenesis

De novo lipogenesis is the process by which the cell converts carbohydrates to fatty acids which can then be esterified to triglycerides for storage. The first step in this process is accomplished by ACLY. This enzyme allows for the conversion of citrate to acetyl-CoA which is then converted to malonyl-CoA by ACC a key rate limiting step of de novo lipogenesis. Fatty acid synthase (FASN) can then convert malonyl-CoA to palmitate which can then be used to form complex fatty acids (Ameer et al., 2014). Synthesis of FA allows for the building of the cell membrane. They can be esterified to form phospholipids which are the building blocks of the plasma membrane. This supports the high proliferative rate of cancer cells by facilitating the formation of microdomains for signal transduction, intracellular trafficking as well as invasion and migration. FA synthesis can also be used to store energy which can then be used to fuel the cell in response to low glucose levels. Furthermore, lipids can mediate several post-translational modifications to promote several processes involved in cell survival and proliferation (Zadra et al., 2013). For instance, the attachment of the myristoyl group to the N-terminal of Akt results in its activation. In addition, prenylation and palmitoylation of RAS small GTPase family members allows for their translocation to the cell membrane (Mor & Philips, 2006).

Cholesterol synthesis is another process that is upregulated in a number of cancers including prostate cancer. HMGR allows for the conversion of HMG-CoA to mevlonate. This is

the rate limiting step of cholesterol synthesis. Cholesterol can then be used to regulate the fluidity of the plasma membrane and mediate signal transduction pathways such as the PI3K-Akt pathway. Furthermore, intermediates of the cholesterol pathways such as geranylgeranyl pyrophosphate, and farnesyl pyrophosphate to prenylated proteins such as RAS family members which are implicated indifferent processes including metastasis and invasion. In addition, sterols are essential for the synthesis of steroid hormones and androgen which are crucial for PCa cells growth and survival (Zadra et al., 2013).

1.11 Deregulation of tumor cell metabolism.

1.11.1 Warburg effects

The concept of the Warburg effect was first introduced by Otto Warburg and colleagues in the 1920s (Otto Warburg et al., 1927). Their observation was that tumour cells take up large amounts of glucose compared to healthy cells. A large fraction of the glucose entering the cell was used to produce lactate despite the presence of oxygen, a process named "aerobic glycolysis". This generates increased levels of lactate and lower amounts of ATP, compared to oxidative phosphorylation. Ever since this discovery, researchers tried to find explanations as to why the Warburg effect occurs in tumour cells and why tumour cells preferentially use aerobic glycolysis to generate ATP. There are different theories that might explain this phenomenon. One of the plausible explanations is that aerobic glycolysis is a rapid generation ATP. When compared to mitochondrial respiration, aerobic glycolysis yields lower amounts of ATP. However, the rate of glucose metabolism through aerobic glycolysis is much faster than oxidative phosphorylation. As a result, over a certain period, the total amounts of ATP produced are comparable between aerobic glycolysis and oxidative phosphorylation. Considering the difference in kinetics between

both methods, it is apparent that a cell that is dependent on aerobic glycolysis would have an advantage when competing for energy resources since it has a higher rate of glucose utilization. Since the tumour microenvironment includes many cell types such as immune cells, it would be advantageous for tumour cells to adapt such mechanism in order to compete for the scarce source of energy, namely glucose. Another plausible explanation for the Warburg effect is the use of glucose to support the biosynthesis requirements of the proliferating cell. Glucose provides a source of carbon that can be used for the generation of lipids, proteins and nucleotides. Similarly, the Warburg effect leads to the regeneration of NAD^+ from NADH. This constant supply of NAD^+ will allow the cell to maintain its energy levels. A third explanation highlights the involvement of aerobic glycolysis to produce a favourable microenvironment for the tumour. As previously highlighted, aerobic glycolysis produces a large amount of lactate that is able to make the microenvironment relatively acidic. Lowering the pH of the tumour environment is beneficial for the tumour for multiple reasons. Acidification of the microenvironment allows for enhanced invasiveness of the tumour and cell motility. It can also lead to extracellular matrix degradation and intercellular signaling modifications. In addition, depleting the energy resources from the tumour environment hinder the ability of tumour infiltrating lymphocytes to exhibit their effector functions. Finally, the Warburg effect can influence cell signaling by generating reactive oxygen species (ROS). Alteration in the levels of ROS levels can lead to different events such as cell membrane damages, inactivating PTEN etc. (Liberti & Locasale, 2016). Under hypoxic conditions represented by the tumour microenvironment, HIF-1α expression is upregulated which promotes the Warburg effect. HIF-1α induces the transcription of glucose transporters leading to an increase of glucose uptake. Similarly, glycolytic enzymes' expression is upregulated which allows the cell to utilize aerobic glycolysis as means of energy production

instead of oxidative phosphorylation (W. Liu et al., 2012). Faubert and colleagues have shown that AMPK is a negative regulator of aerobic glycolysis. Their results suggest that AMPK knockdown can cooperate with the Myc genes to promote tumour growth and progression. AMPK silencing also caused increased glucose uptake and extracellular acidification. Finally, silencing HIF-1α reversed the effect of silencing AMPK which indicates that AMPK's negative regulation of aerobic glycolysis is dependent on HIF-1α (Faubert et al., 2013). While the Warburg effect is common in most tumours, prostate cancer, especially at early stages, depends on different pathways to generate energy. Generally, Glucose uptake is not increased in prostate cancer tumours since lipids are more commonly used to produce energy. However, there is mounting evidence that late stage PCa cells utilize aerobic glycolysis since their glucose uptake is relatively high (Eidelman et al., 2017).

1.12 Cellular effects of cancer therapy: Ionizing radiation.

Ionizing radiation (IR) is a common treatment for many types of cancers due to its ability to disrupt the integrity of the genome and induce cellular damage that ultimately leads to cell death. First and foremost, IR is used to cause DNA damage which elicits different responses within the cell. DNA damage include single strand breaks, double strand breaks, DNA crosslink and DNA-protein crosslinks. It can also cause DNA damage by reactive oxygen species (ROS) (Wang et al., 2018). Immediately after DNA damage occurs, ATM and ATR are activated in order to initiate DNA repair mechanisms in the cell. Histone H2AX phosphorylation at S139 by ATM allows for the assembly of DNA repair proteins in the site of DNA damage. ATM also phosphorylates BRCA1, p53-binding protein 1 (53BP1), Mediator of DNA Damage Checkpoint

1 (MDC1) in addition to checkpoint proteins CHK1 and CHK2. As a result, progression through the cell cycle is arrested (Podhorecka et al., 2010).

Two main pathways are involved in DNA damage repair; homologous recombination (HR) and non-homologous end joining (NHEJ). NHEJ allows the ligation of DNA overhangs where the break occurs. However, when the DNA needs processing before ligation, this may lead to inaccuracies and the deletion of genetic information. On the other hand, HR does not involve inaccuracies, and this is due to the use of a homologous sequence. Therefore, HR can only occur during the S or G2 phase where undamaged sister chromatids are present (Maier et al., 2016). However, if the damage is not repairable, the cell will undergo apoptosis or senescence (Wang et al., 2018).

Furthermore, IR damages different organelles within the cell. The endoplasmic reticulum (ER) is one of the organelles damaged by IR. Endoplasmic reticulum stress leads to autophagy and apoptosis. IR also damages the mitochondria by altering the permeability of its membranes. The integrity of the plasma membrane is also disrupted by IR which leads to alterations in its permeability and mobility. Other organelles such as lysosomes and ribosomes are also affected by IR (Wang et al., 2018).

IR can also alter the behaviour of cancer cells. It can promote EMT and facilitate invasion and metastasis. In addition, it can also promote angiogenesis by activating the PI3K-Akt -mTOR pathway which in turn leads to the activation of HIF-1α. HIF-1α mediates the activation of angiogenesis markers such as VEGF while allowing the cell to survive in hypoxic environment (Wang et al., 2018).

1.13 Mechanisms of Cell Death: Effects of RT

Radiation therapy uses typically photon beams to cause cellular DNA damage and cancer cell death. There are different types of cell deaths that the cell might undergo.

Apoptosis (programmed cell death): This mechanism is characterized by the shrinkage of the cell and the formation of apoptotic bodies. Apoptosis is achieved through two main pathways; the intrinsic apoptotic pathway and the extrinsic apoptotic pathway. The intrinsic pathway involves the release of cytochrome c from the mitochondria. This is achieved through multiple mechanisms such as the accumulation of p53 in the nucleus which leads to the expression of pro-apoptotic genes including BCL2, PUMA, NOXA and BAX. In the extrinsic pathway, death receptors and tumor necrosis factor (TNF) receptor gene superfamily are responsible for initiating the apoptosis signaling pathway. These receptors have a cytoplasmic "death domain" which causes the transduction of the signal from the cell membrane to intracellular pathways. The endpoint of both the intrinsic and extrinsic pathways is called the execution phase which involves activation of the proteolytic caspase pathway (Maier et al., 2016). Caspase-3 is the main effector of this step. It is cleaved and thus activated by caspase-8 and caspase-9 (P. F. Liu et al., 2017). Cleaved caspase-3 can then activate the endonuclease CAD which can then degrade chromosomal DNA. In addition, cleaved caspase-3 induces cytoskeletal reorganization and disintegration of the cell into apoptotic bodies (Elmore, 2007).

Mitotic Catastrophe: This mechanism of cell death is caused by mis-segregation during mitosis (Elmore, 2007). Mutations to p53 as well as loss or impairments of key checkpoint proteins may cause the cell to enter mitosis prematurely. This may result in the production of cells with mitotic abnormalities, multiple nuclei and with abnormal morphology due to unrepaired DNA damage. Centrosomes might also be over-duplicated due to these events. Cumulatively, those events

result in cell death by caspase dependent or caspase independent pathways (Elmore, 2007). Cell death caused by radiation is predominantly through mitotic catastrophe (Baskar et al., 2012).

Necrosis: Unlike programmed cell death, this mechanism is generally passive. It takes places without the need of protein synthesis or homeostatic mechanisms (Syntichaki & Tavernarakis, 2002). Necrosis occurs due to genetic insults or extreme environments such as hypoxia, hypoglycemia or high levels of ROS. As a result, several events take place such as DNA degradation. In addition, swelling of the cell and rupture of the cell membrane occur after exposure to radiation. The nucleus changes its shape due to vacuolization and non-condensed chromatin while the mitochondria and the endoplasmic reticulum dilate. This type of cell death is seen less frequently than the previous types (Baskar et al., 2012).

Senescence: Senescent cells are viable cells however; these cells are not able to replicate and undergo mitosis typically in response to severe environmental stress. The phenotype expressed by those cells is called stress-induced premature senescence. The activation of $p53/p21^{cip1}$ is crucial for the maintenance of this phenotype. Senescent cells are metabolically active, and they can secrete growth factors to impact the survival and growth of neighbouring cells. However, unlike quiescent cells, they are not responsive to growth factor or mitogenic stimuli (Baskar et al., 2012). They are unable to synthesize DNA or undergo mitosis. After a period of time they flatten and enlarge, show increased granularity and *eventually* undergo apoptosis (Maier et al., 2016).

Autophagy: Autophagy by definition denotes “self-eating”. During this process the cell digests itself through autophagic and lysosomal compartments. This mechanism allows degradation and recycling of cellular components (Baskar et al., 2012). There are three main mechanism of autophagy. Macro-autophagy is described by the delivery of cargo by double membrane bound

vesicles to the lysosome for its degradation. Micro-autophagy involves the invagination of lysosomes to engulf cytosolic components. Finally, chaperone-mediated autophagy allows proteins to be recognized by lysosomal-associated membrane proteins and transported across the lysosomal membrane (Glick et al., 2010).

1.14 Cellular sensitivity of PCa cells to RT

PCa, especially high risk PCa, develops radiation resistance. Although the mechanism is not fully understood, molecular pathways leading to DNA damage repair and cell survival are well-described. This is primarily due to a low α/β ratio which characterizes late responding cells. As a result, PCa cells are able to repair DNA damage caused by radiation between radiation fraction rendering RT less effective. It is important to note that late responding cells are more sensitive to higher RT dose per fraction than higher overall RT dose with low fraction doses. Another phenomenon that alters the response of cells to radiation is the phase of cell cycle. For instance, cells in the late phase *S*, in the early G_1, and in the quiescence phase G_0 are more resistant to radiation than cells in other phases. For instance, quiescent cells are not proliferating regularly and therefore have the opportunity to repair any damage caused by radiation before dividing (Desideri et al., 2014).

Radio-resistance can also be explained by the activity of growth factor pathways involved in PCa growth and progression. The EGFR pathway and the downstream PI3K-Akt -mTOR pathway allow irradiated cells to progress through the cell cycle. Likewise, the RAS-RAF-MAPK-ERK pathway serves a similar role by inducing the transcription of key regulators of the cell cycle. In addition, loss of function mutations to the tumour suppressor protein p53 results in the development of radio-resistance. p53 regulates the expression of different genes responsible for

cell cycle and apoptosis. Likewise, prostate cancer stem cells (PCSCs) play a crucial role in maintaining the radioresistant phenotype of PCa. By being in a quiescent state, PCSCs ensure the integrity of their genome by repairing damage caused by radiation (Alberti, 2014).

1.15 DNA damage repair and radiation resistance

DNA damage is rapidly sensed in cells by ATM and ATR (Chaiswing et al.,2018). ATM responds to DNA double-strand breaks (DSB) within minutes and is activated by S1981 phosphorylation to cause cell cycle arrest through different pathways. ATM causes G1/S cell cycle arrest through the ATM-p53-p21/ATM-Chk2-CDC25A pathways, while it causes cell cycle arrest at G2/M phase through the ATM-p53-p21/ATM-p53-CDC2-cyclin B1 pathways (Jin and Oh, 2019). In that way, ATM can stop cell cycle progression and allow cells to repair their DNA before replicating. Radio-resistant cells show overexpression and increased activity of ATM (Chaiswing et al.,2018).

Another mechanism by which cells can develop radio-resistance is through alterations in cellular dynamics namely the activation of Akt. Akt is activated by radiation downstream of ATM, which in turn, enhances glycolysis and activates the mTOR pathway (Chaiswing et al.,2018). Other studies suggested that oxidative stress caused by radiation could contribute to a radio-resistant phenotype in those tumour cells. Oxidative stress regulates different nuclear factors such as p53, erythroid-derived 2-related factor 2 (Nrf2) and NF-κB which causes DNA repair leading to cell survival and tumour progression (Chaiswing et al.,2018).

1.16 Pre-clinical models for the study of prostate cancer

1.16.1 In Vitro

There are various cell-lines with different mutation profiles used for pre-clinical studies. There are androgen-responsive PCa cell lines such as LNCaP and 22Rv1 and androgen-irresponsive cell lines such as DU145 and PC-3. 22Rv1 is the only cell line derived from a localized PCa while the other three cell lines are derived from metastatic tumours. 22Rv1 cells were derived from a xenograft of the parental cell line CWR22 (Sramokoski et al., 1999). DU145 cells were harvested from a brain metastasis of a 69-years old male, while PC-3 cell lines were derived from bone metastasis of 62 years old Caucasian male. Finally, LNCap cells were harvested from a supraclavicular lymph node metastasis of a 50-years old male in 1977.

Every cell line has a slightly different mutation profile allowing us to study different characteristics of PCa. PC-3 cells do not express p53, DU145 and 22Rv1 have a mutant variant of Tp53 while LNCaP cells have wild type Tp53 (Dinnen, et al., 2007). PC-3 and LNCaP cells do not express PTEN while DU145 and 22Rv1 express wild type PTEN (Lotan et al., 2011). Table 1.3 includes a summary of the mutations found in each cell line (Artimo et al., 2012; Barretina et al., 2012; Rouillard et al., 2016; Tate et al., 2019).

Table 1.4: PCa cell lines Mutation Profiles

Cell Line	Gene	Mutation Type	Protein Change	Zygosity
PC-3	Tp53	Frameshift deletion	A138fs	Homozygous
	PTEN	Whole gene deletion		Homozygous
DU145	Tp53	Missense mutation	V274F, P223L	Heterozygous
	MLH1	Splice site	N/A	Unknown
		Missense mutation	A586V	Unknown
	TSC1	Missense mutation	G1034C	Unknown
	WT1	Missense mutation	Q120E	Unknown
		Missense mutation	S204R	Unknown
	NF1	Missense mutation	P2472H	Unknown
	BRCA1	Missense mutation	S2284L	Unknown
	KDR	Missense mutation	C466F	Unknown

	CTNNB1	Missense mutation	A305G	Unknown
	ZFHX3	Missense mutation	P2385L	Unknown
			P643H	Unknown
	STK11	Frameshift deletion	KP178fs	Unknown
	RB1	Nonsense mutation	K715*	Homozygous
	CDKN2A	Missense mutation	D84Y	Homozygous
				Homozygous
22Rv-1	Tp53	Splice site	Q331R	Heterozygous
	AR	Missense mutation	H875Y	Homozygous
	TGFBR2	Frameshift deletion	K153Sfs*35	Homozygous
	ZFHX3	Frameshift deletion	G1926fs	Heterozygous
	PIK3CA	Missense mutation	Q546R	Unknown
	PIK3C2A	Frameshift deletion	T114fs	Unknown
LNCaP	PTEN	Frameshift deletion	K6fs	Unknown
	APC	Missense mutation	R2714C	Unknown
	CDK4	Missense mutation	P110L	Unknown
	CDH1	Missense mutation	P94T	Unknown
	FLT4	Missense mutation	Y1091C	Unknown
	EP300	Missense mutation	G1778W	Unknown
	PAX8	Missense mutation	R64K	Unknown
	ERBB3	Missense mutation	K177N	Unknown
	MEN1	Nonsense mutation	Y318*	Heterozygous
	AR	Missense mutation	T878A	Homozygous
	PRKAR1A	Missense mutation	R16Q	Unknown
	NCOR2	Missense mutation	L167P	Unknown
	ABL2	Missense mutation	R135Q	Unknown
	PIK3R1	Nonsense mutation	R639*	Heterozygous

1.16.2 In Vivo models of PCa

Xenografts

The most widely used PCa model is mouse xenograft, where human prostate cancer cells (PC-3, DU145, 22Rv1 and LNCaP) are injected subcutaneously or orthotopically. The advantages of using a subcutaneous injection include easy accessibility limited need for technical expertise. One of the limitations of this model is that measuring tumours using a caliper might lead to inconsistencies due to human errors and changes in the mouse weight and hydration status. On the other hand, orthotopic models allow the introduction of the tumour cells into the prostate. One of the advantages of this model is the interaction between the implanted tumour

and the organ of interest. This also allows to study the tumorigenic and metastatic potential of the cells. The main disadvantage for this model is the complexity of the procedure and the limited number of cells that can be introduced in the prostate (Cunnungham and You, 2015).

Syngeneic

Syngeneic models can also be used to study PCa in vivo. This model uses cell lines that are extracted or derived from the same strain of mice we are using in the experiment. This is particularly useful to study immunotherapeutic approaches for the treatment of PCa. For instance, TRAMP cells were extracted from a 32-week tumor of the transgenic adenocarcinoma mouse prostate (TRAMP) model developing in C57BL/6 mice. Three cell lines were established; TRAMP-C1, TRAMP-C2 and TRAMP-C3. They represent different stages of cancer progression. TRAMP-C3 cells are not capable of forming tumours in vivo while the other two cell lines can (Foster et al., 1997).

Genetic

PTEN Knockout Mice

Loss of function of PTEN is associated with the development of PCa. Mice who lack functional PTEN develop invasive carcinoma and metastasis in only 12 weeks. This model is useful because it represents a range of conditions seen in human patients (Cunningham & You, 2015).

P53 Mutant Mice

Elgavish and colleagues were able to generate mice with p53 mutations. A Rat probastin promoter (rPB) and a mutant Tp53 fragment were used to obtain this model. This led to PIN grade III and IV of 52-week old mice (Elgavish et al., 2004; X. Wu et al., 2013).

Patient-derived xenograft (PDX)

PDX models use cells that are extracted from patients. After the surgical extraction of the tumour, cells are injected directly into immuno-suppressed mice without any handling or passaging in vitro. Consequently, cells retain their genetic, molecular and histological characteristics, their heterogeneity and response to treatments (Del Vecchio et al., 2016).

1.17 Targetting Cancer Metabolism as Cancer Therapy

1.17.1 Metformin's Anticancer Effects

Metformin is the most commonly used drug for the treatment of type II diabetes. The use of metformin has been associated with decreased risk of several cancers including liver cancer and colon cancer (He et al., 2015). Its mechanism of action in the treatment of type II diabetes consists of lowering blood glucose by decreasing hepatic glucose production and reducing intestinal glucose absorption (Dumitrescu et al., 2015). This is achieved through the inhibition of mitochondrial complex I in the liver. This leads to a significant increase in the ratio of AMP to ATP in the cell which results in subsequent AMPK activation. AMPK is activated through several mechanisms. The binding of AMP to the AMPKγ subunit is sufficient to increase AMPK activity by 1000-fold. In addition, several upstream kinases are also able to phosphorylate and activate AMPK. Once activated, AMPK modulates numerous cellular pathways, described above, resulting in an increase of glucose uptake in the liver (Kasznicki et al., 2014a). In addition, metformin is able to decrease glucose uptake in the intestines by increasing anaerobic glucose metabolism in enterocytes (Rena et al., 2017).

Many studies were conducted to illustrate the antiproliferative effects of metformin. There are different mechanisms that describe the effects of metformin on cancer cells. Metformin

is found to inhibit cell growth and cell division by reducing the levels of insulin and IGF-1 in the circulation. Those systemic hormones are involved in the activation of several cellular pathways such as the PI3K/Akt pathway that leads to the activation of the mTOR pathway. Another pathway that is activated by IGF-1 is the Ras/Raf/ERK pathway which results in cell growth and proliferation. Therefore, reduction in the levels of these hormones will hinder the cell's ability to proliferate. Metformin blocks the mTOR pathway by activating AMPK, leading to activation of TSC2 which causes the inhibition of mTOR with protein biosynthesis. Other studies have shown that metformin is able to cause cell cycle arrest at G1 phase by increasing the activity of p53 (Kasznicki et al., 2014b). Metformin is shown to repress EMT hence, reducing the metastatic potential of cancer cells (Zaidi et al., 2019). The mounting evidence of Metformin's mechanism of action in controlling tumour progression from pre-clinical studies has led to numerous clinical trials investigating protective role of metformin against cancer. Several older retrospective series and newer randomized trials studies looked at the effect of metformin on different cancers including prostate cancer. Meta-analysis of two randomized controlled trials and eight observational studies of PCa show that the use of metformin has no significant effect on the risk of PCa (Franciosi et al., 2013). Similar results were observed in other forms of cancers such as ovarian cancer. Home and colleagues showed that metformin offers no protection against malignancies (Home et al., 2010). However, several meta-analyses investigating observational studies highlight the protective effects of metformin against malignancies. This could be due to different types of time related biases as argued by Suissa and Azoulay (Suissa & Azoulay, 2012). On the other hand, Metformin's tolerability remains an obstacle. Metformin results in GI adverse effects in 20-30% of patients which may lead to metformin discontinuation (Rena et al., 2017). Complications may include myocardial infraction as well as lactic acidosis. Furthermore, renal

impairment, congestive heart failure and coronary artery disease has been associated with metformin especially with elderly patients. Side effects also include vomiting, diarrhea, stomach upset and nausea (Nasri & Rafieian-Kopaei, 2014).

1.17.2 Sodium-glucose co-transporter 2 inhibitors

Similar to metformin, sodium-glucose co-transporter 2 (SGLT2) inhibitors such as canagliflozin (CANA), dapagliflozin and empagliflozin are used for the treatment of diabetes. However, the mechanism of action is different. SGLT2 are responsible for approximately 90% of glucose absorption in the renal proximal tubules. By inhibiting those transporters, SGLT2 inhibitors are able to increase glucose secretion and ultimately reduce blood glucose levels (Jakher et al., 2019). SGLT2 inhibitors have been investigated for their anti-proliferative effects. Although they all serve a similar role in the regulation of blood glucose, only Canagliflozin has shown antiproliferative effects similar to metformin (Villani et al., 2016).

1.17.3 Canagliflozin

In 2013, the diabetes drug Canagliflozin (trade name Invokana), branded by Janssen Pharmaceuticals, became FDA approved for the treatment of type II diabetes. Canagliflozin is an SGLT2 inhibitor. SGLT-2 are glucose transporters found in the proximal tubules of the kidneys and are responsible for the reabsorption of 90% of glucose from the filtrate back to the blood. By inhibiting this transporter, Canagliflozin can reduce the amount of blood glucose while increasing the concentration of glucose in the urine. Canagliflozin is commonly used at doses of 100 mg or 300 mg per day (Prasanna Kumar et al., 2017). It has a 65% oral bioavailability with a half-life of 10-13 hours depending on the dose with a peak concentration of approximately 4.7 ug/mL in the serum (Devineni et al., 2013a; Sarnoski-Brocavich & Hilas, 2013).

Our group investigated the effects of Canagliflozin on prostate cancer and non-small cell lung cancer (NSCLC) models. We found that Canagliflozin was able to inhibit mitochondrial complex I-supported respiration, which in turn leads to a reduction in the levels of ATP. This leads to the activation of AMPK which results in inhibition of mTOR and acetyl-CoA carboxylase (Villani et al., 2016). In a different paper by Li and colleagues, researchers suggested that Canagliflozin inhibited the kinase activity of T790M EGFR in cell-free assay. The T790M EGFR mutation blocks tyrosine kinase inhibitors, hence, EGFR inhibitors. They also proposed that Canagliflozin induces apoptosis by inhibiting the autophosphorylation of EGFR and its downstream pathways in non-small-cell lung carcinoma (NSCLC) cells (Li et al., 2017). Hung and colleagues reported that Canagliflozin suppresses growth of hepatocellular carcinoma (HCC) cells in vitro and in vivo. They argue that this effect is independent of SGLT2 inhibition. Furthermore, Canagliflozin treatment lead to β-catenin inhibition (Hung et al., 2019). Kaji and colleagues, highlighted the ability of Canagliflozin to induce G2/M cell cycle arrest and apoptosis in Huh7 and HepG2 cells.

Canagliflozin does not induce hypoglycemia in non-diabetic patients (Roy, 2019). And is described to have cardioprotective properties. The Canagliflozin cardiovascular assessment study (CANVAS) shows that patients treated with Canagliflozin had lower incidents of death from cardiovascular causes, nonfatal myocardial infarction and nonfatal stroke compared to patients in the placebo group (Neal et al., 2017).

1.18 Rationale and Aims of this Research

The work described in this thesis focuses on understanding the interaction between Canagliflozin and radiation. This is crucial for several reasons. Using Canagliflozin in combination with radiation for the treatment of prostate cancer could allow us to improve the outcome of radiation and reduce the dose of radiation patients are exposed to, while maintaining a consistent or rather a stronger anti-proliferative effect. Understanding the mechanism of action will allow us to better comprehend the role of metabolism on cancer development. Canagliflozin presents an economical and approved therapy, which if it is proven to be beneficial, can be readily available for cancer patients. Understanding Canagliflozin mechanism of action in cancer cells and animal models of PCa will help define the potential of this drug to improve the therapeutic ratio of radiotherapy and the promise for further clinical investigation in PCa patients.

Based on our previous observations we hypothesized that Canagliflozin may sensitize prostate cancer cells to radiation and enhance its anti-tumour activity.

To test this hypothesis, the following aims were proposed:

1. to establish the radio-sensitizing effect of Canagliflozin in vitro;
2. to understand the mechanism by which Canagliflozin sensitizes cells to radiation And
3. to investigate the radio-sensitizing effects of Canagliflozin in vivo.

CHAPTER II - METHODOLOGY

METHODOLOGY

2.1 Materials

Canagliflozin ($C_{24}H_{25}FO_5S$) powder (purchased from MedChemExpress (MCE) Monmouth Junction, NJ) was used for all *in vitro* experiments after dilution in DMSO. For *in vivo* experiments, animals were fed Canagliflozin chow diet generated by Envigo (Indianapolis, IN) from clinical grade Canagliflozin (Invokana 300 mg tablets, Jansen Inc.) at 416.7 ppm. Based on the average daily consumption of chow diet, Canagliflozin diet was designed to deliver a dose of 50 mg/Kg.

Primary and secondary antibodies used immunoblotting were purchased from Cell Signaling Technology (CST). Table 2.1 includes the catalog number for each antibody as well as the dilution used.

All standard chemicals were purchase from Fisher Scientific (Toronto, ON), Sigma Aldrich (Oakville, ON), Bio Rad (Mississauga, ON) and Bioshop (Burlington, ON).

Table 2.1: Antibodies used for Immunoblotting

1° Antibody	Catalog Number	Dilution	2° Antibody	Catalog Number	Dilution
P-AMPK (T172)	#2532S	1:1000	Anti-Rabbit IgG, HRP-linked Antibody	#7074S	1:10000
P-RAPTOR (S792)	#2083S				
P-Akt (S473)	#4058S				
P-Akt (T308)	#9275S				
Akt	#9272S				
P-mTOR (S2448)	#2971S				
mTOR	#2983S				
p70S6K	#9202S				
P-P70S6K (T389)	#9205S				
S6	#2217S				
P-S6 (S240/244)	#2215S				
4E-BP1	#9644S				
P-4E-BP1 (S65)	#9451S				
HIF-1α	#36169S				
$P27^{kip1}$	#3688S				

H3	#4499S				
P-H3 (S10)	#53348S				
P38 MAPK	#8690S				
P-P38 (T180/Y182)	#4511S				
ERK	#4695S				
P-ERK (T202/Y204)	#4370S				
GAPDH (14C10)	#5174S	1:5000			
B-actin (13E5)	#5125S				

2.2 Mammalian Cell lines and Cell Culture

Human prostate cancer cell lines (PC-3) cells were purchased from ATCC. DU145, 22Rv1 as well as radioresistant DU145 (Ghiam et al., 2017) and 22Rv1 cells were received as a gift from Dr. Stanley Liu. The DU145 and 22Rv1 radioresistant cells were developed by delivering 2 Gy of radiation per day for multiple days (5 days per week) to generate conventionally fractionated radioresistant cells (CFRT). DU145 received 59 fractions of radiation while 22Rv1 received a total of 45 fractions.

DU145 cells were cultured in DMEM media (purchased from Gibco: Burlington, ON or Wisent Bioproducts: St-Bruno, Québec). The media was supplemented with 10% (v/v) fetal bovine serum (FBS) (purchased from Gibco: Burlington, ON or Wisent Bioproducts) and 1% (v/v) Antibiotic-Antimycotic (purchased from Gibcoor Wisent Bioproducts). Radioresistant DU145 were cultured in DMEM media. The media was supplemented with 10% (v/v) FBS and penicillin (100 U/mL) – streptomycin (100 μg/mL) (purchased from Gibcoor Wisent Bioproducts). PC-3 and 22Rv1 cells were cultured in RPMI-1640 (ATCC modified) media (purchased from Gibco or Wisent Bioproducts). The media was supplemented with 10% (v/v) FBS and 1% (v/v) Antibiotic-Antimycotic. Radioresistant 22Rv1 cells were cultured in RPMI-1640 (ATCC modified) media. The media was supplemented with 10% (v/v) FBS and penicillin

(100 U/mL) – streptomycin (100 µg/mL). All cells were cultured in a $37°C$ incubator with 5% CO_2. Cells were passaged using standard protocols.

2.3 Proliferation Assays

Cells were seeded in 96 well plates with a seeding density of 500 cell/well. They were then incubated overnight at $37°C$ and 5% CO_2 in order for the cells to adhere. The following day, the cells were treated with different concentrations of Canagliflozin ranging from 0 μM to 60 μM. After at least four hours, different doses of radiation ranging from 0 Gy to 16 Gy were delivered to the cells through external beam radiation (Varian clinical linear accelerators). Plates were placed on the patients' treatment couch with a 1 cm superflab bolus on top of them. The distance between the source of radiation and the bolus was 100 cm, and the gantry was placed vertically at 0°. After radiation, the cells were then incubated at $37°C$ and 5% CO_2 for 5-7 days. The experiment was stopped once the control wells reach 75% confluence. Cells were then fixed with 100 $\mu L/well$ of 10% formalin for 10 minutes. Once the cells were fixed, they were stained with 100 $\mu L/well$ of 0.5% crystal violet for 10 minutes. The wells were then being washed with water to remove residual crystal violet and were left to dry in room temperature overnight. Once the plates were dry, wells were treated with 100 $\mu L/well$ of 0.05 M NaH_2PO_4 for 10 minutes at room temperature in order for the stain to solubilize. Finally, absorbance was measured with a plate reader at 570 nm.

2.4 Clonogenic Survival Assays

Cells were seeded in 12 well plates with different seeding densities ranging from 500 $\mu L/well$ to 6000 cell/well based on the radiation dose delivered to the plate. The cells were

incubated overnight at $37°C$ and 5% CO_2 in order to adhere to the plate. The following day, the cells were treated with different concentrations of Canagliflozin (0 μM – 30 μM) in the morning. After at least 4 hours, different doses of radiation ranging from 0 Gy to 8 Gy were delivered to the cells through external beam radiation as described above. The plates were then being incubated at $37°C$ and 5% CO_2 until colonies of 50 or more cells were found in the control wells. Once the colonies were formed, the experiment was stopped, and the cells were then fixed with 1 mL/well of 10% formalin for 10 minutes. Once the cells were fixed, they were stained with 500 $\mu L/well$ of 0.5% crystal violet for 10 minutes. The wells were then being washed with water to remove residual crystal violet and are left to dry at room temperature overnight. Once the plates were dry, the number of colonies were counted under the microscope.

2.5 Immunoblotting

2.5.1 Lysates preparation

Cells were seeded in 6 well plates at a density of $2 \times 10^5 - 3 \times 10^5$ per well. They were then incubated overnight at $37°C$ and 5% CO_2 in order to adhere to the plate. Cells were treated the following day with Canagliflozin alone or Canagliflozin and radiation. For the first experiment, where cells were treated with Canagliflozin alone for different periods of time, cells were treated at different times and the experiment was stopped 24 hours after the first treatment. For the second experiment, where the effects of Canagliflozin and radiation were examined, cells were treated with different concentrations of Canagliflozin (0-30 μM) in the morning. At least four hours later, different radiation doses ranging from 0 Gy to 8 Gy were delivered and the cells were then incubated at $37°C$ for 48 hours.

The cells were then washed with PBS and lysed using an SBJ cell lysis buffer containing 50 mM HEPES, 150 mM NaCl, 100 mM NaF, 10 mM Na-pyrophosphate, 5 mM EDTA and 250

mM of sucrose. 1mM Dithiothreitol (DTT), 1% Triton-X, 1mM Na-orthovanadate and 1% complete protease inhibitor was added to the previous mixture immediately before lysing the cells. Samples were then frozen at $-80°C$.

2.5.2 Sample Preparation

Samples were then thawed, then rotated at 14000 rpm at 4°C. The supernatant was isolated, and a BCA protein assay protocol was performed. Samples were prepared with 4x SDS sample buffer (40% glycerol, 240 mM Tris-HCl pH 6.8, 8% SDS, 0.04% bromophenol blue, 5% β-mercaptoethanol), to a final concentration of 1 μg/μL. Samples were then denatured by being exposed to $95°C$ for 5 minutes. Subsequently, a western blot analysis is performed on cell lysates.

2.5.3 SDS-PAGE and Western Blotting

Samples were loaded onto different percentage gels depending on the molecular weight of the proteins of interest. 10 μL of each sample was loaded into a separate lane. Gels were run at 120 V for approximately 90 minutes for protein separation to occur. Proteins were then electrically transferred from the polyacrylamide gel onto a PVDF membrane using a wet transfer apparatus. Transfers were performed using a 10% methanol transfer buffer. It was conducted at 90 V for 90 minutes. Membranes were blocked immediately after transfer with a 5% bovine serum albumin (BSA) in 1X Tris buffered saline-Tween-20 (TBST) (containing 50 mM Tris, 150 mM NaCl, 1M HCl, pH7.4, 0.1% Tween-20) blocking buffer for one hour.

2.5.4 Antibody Incubation, Immunodetection and Densitometry

Membranes were probed with primary antibodies and left on a rocker overnight in a $4°C$ room. The following day, primary antibodies were removed, and the membranes were washed with TSBT for 30 minutes (3 X 10 minutes). Membranes were then probed with secondary rabbit or mouse antibodies, depending on the protein of interest, for one hour. Membranes were then washed again with TBST for 30 minutes (3 X 10 minutes). For detection, membranes were probed with Enhanced Chemiluminescence (ECL) substrate or super signal substrate then visualized using a chemiluminescence imager. Blots were then processed using the image J software.

2.6 Animal Experiments

All Experiments were approved by the McMaster Animal Ethics Committee and conducted following the guidelines of animal research (AUP # 16-12-41). Homozygous nu/nu male Balb/c nude mice were purchased from Charles River (28-42 days old) and were housed in a clean room for at least two weeks prior to the beginning of the experiments. Mice were kept in groups of four mice per cage in a room with a 12-hour light/dark cycle. All mice were fed standard chow diet (17 % kcal fat: Diet 8640, Harlan Teklad, Madison, WI) and were drinking sterile water (Baxter LOT W9J01Q0) *ad libitum* before the beginning of the experiments. $1x10^6$ cells of PC-3 cells were injected subcutaneously in the right flank of mice. Tumours were measured using a caliper. Once tumours reach 50 mm^3 they were assigned to one of three treatment group or a control group (5 mice per group except for the RT group which had 4 mice). Mice were fed a regular chow diet in the control group. Mice in the Canagliflozin group were fed a Canagliflozin diet. Mice in the radiation group were radiated 5 days after being assigned to

their treatment group while being fed a regular chow diet. Finally, mice who were treated with Canagliflozin and radiation were fed Canagliflozin diet throughout the experiment and were radiated 5 days post assignment.

2.6.1 Mice Radiation

Mice were placed in a plexiglass induction chamber then they were anesthetized with isoflurane (CAF SOP GEN 727 Rodent Anesthetic Machine). Once they were anesthetized, they were placed in a HEPA filter ventilated plexiglass restrainer tube. Anesthetized mice in the restrainer tube were taken to a clinical LINAC (Varian Linear Accelerator capable of delivering 6 MV X-rays) unit where they received radiation. The restraint tube was placed on the patients' treatment couch and the radiation field was narrowed to $2\ cm \times\ 2\ cm$. Optical lasers were used to manually target the isocenter to the tumour. A wax mold cap was placed on the tube. The LINAC was being operated by qualified personnel of the radiotherapy department in order to deliver 5 Gy of radiation (6 MV X-rays 554 mu) with the gantry placed at $90^{\circ} and\ 270^{\circ}$. After delivering radiation, the anesthesia machine was turned off and the mice were taken back to their room. The mice were place in their cages and are attended until they were fully awake. The cages of irradiated mice were then being placed on a heating pad.

2.6.2 Tumour Growth and monitoring

Tumour volumes were monitored throughout the study using a caliper. Tumour volumes were measured using the following equation; $L \times W^2 \times 0.5236$. Mice were sacrificed 60 days after their assignment. Tumours were collected and sectioned vertically through the center. Half

of the tumour was fixed in 10% formalin for 48 hours then transferred to 70% ethanol solution. The other half of the tumour was frozen.

2.7 Statistical Analysis

Values are reported as means with bars indicating the standard error of means (SEM) using GraphPad Prism 8. Several tests were used to test significant differences between groups such as independent t-test as well analysis of variance (One-Way ANOVA and Two-Way ANOVA) with Tukey HSD and Bonferroni *post-hoc* tests depending on the experiment. IC50 values were obtained using a non-linear regression for the inhibitory effect of the drug. Combination index analyses was obtained using CompuSyn software. The software uses the Chou-Talalay method to determine additivity, synergism or antagonism (Chou, 2010).

CHAPTER III - RESULTS

RESULTS

3.1 Effect of Canagliflozin and radiation alone on the proliferation and colony formation ability of prostate cancer cell lines

Proliferation assays were used to examine the ability of cells to proliferate and replicate their DNA. Cells were left to grow for approximately 5 days post treatment where they undergo multiple cell cycles. The results obtained from proliferation assays reflect total DNA content in each condition. Results in treatment groups are expressed relative to the control group. On the other hand, clonogenic assays serve a different role. They examine the cell's oncogenic capacity, its ability to form surviving colonies (>50 cells) from a single cell. Previously, our group demonstrated the anti-proliferative effect of Canagliflozin on different cell lines including two PCa cell lines namely PC-3 and 22Rv1 (Villani et al., 2016). The first set of experiments aimed to confirm the previously reported findings as well as document the sensitivity of PCa cell lines to Canagliflozin and radiation in cell lines not tested before.

Figure 3.1 highlights the sensitivity of PCa cell lines to Canagliflozin and radiation detected in proliferation and clonogenic survival assays. Figure 3.1A shows the responsiveness of PC-3, DU145, and 22Rv1 cells to Canagliflozin alone. It is evident that PC-3 cell lines were the most sensitive to Canagliflozin while DU145 cell lines were the most resistant to Canagliflozin with IC50 values of 20.41μM and 40.85 μM respectively (Table 3.1). Furthermore, Figure 3.1B shows that cell lines have differential sensitivity to radiation. DU145 cell lines are the most resistant to radiation with a half maximal dose of 6.636 Gy while 22Rv1 cell lines are the most sensitive to radiation with a half maximal dose of 1.224 Gy (Table 3.2). On the other hand, figure 3.1C illustrates the effect of Canagliflozin alone on DU145 and PC-3 cells for clonogenic survival. Similar to proliferation assays, DU145 cell lines were more resistant to

Canagliflozin when compared to PC-3 cell lines with IC50 values of 18.69 μM and 16.82 μM, respectively (Table 3.3). Finally, figure 3.1D shows that PC-3 and DU145 cell lines' ability to form colonies is hindered by radiation with PC-3 cell lines being slightly more sensitive to radiation especially at 4 and 6 Gy.

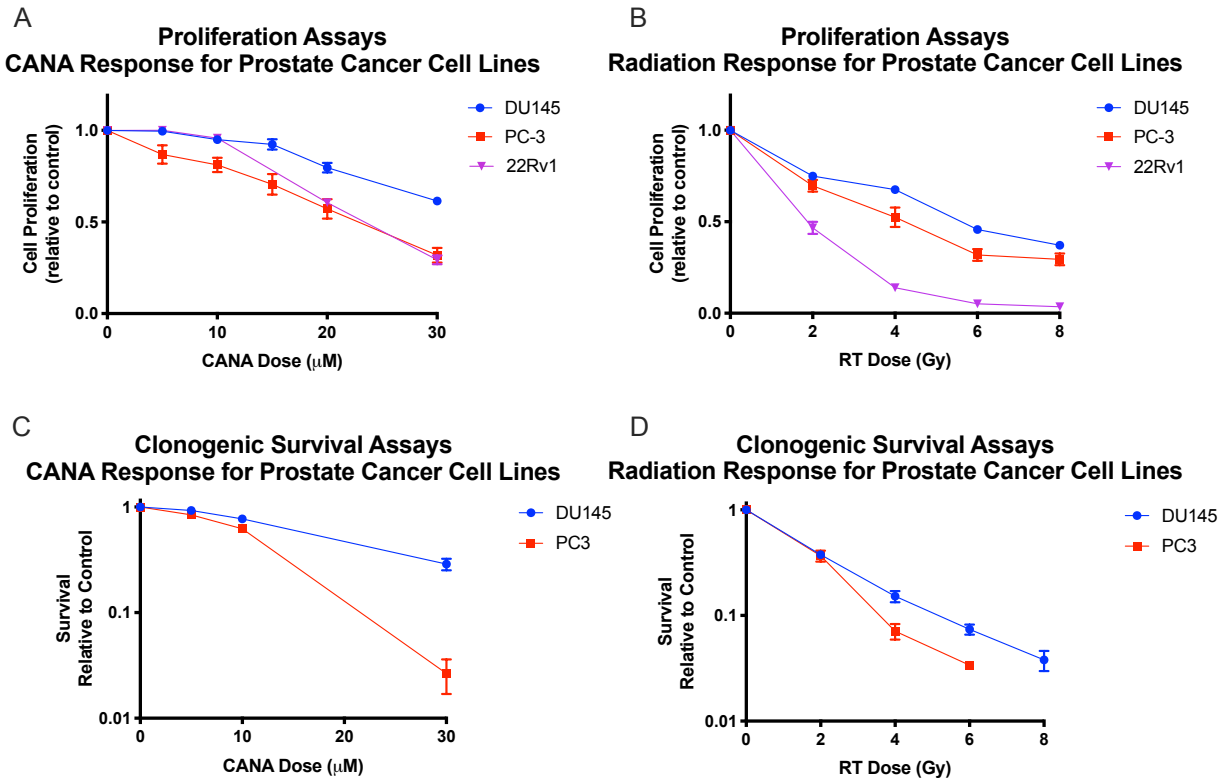

Figure 3.1: The response of prostate cancer cell lines to Canagliflozin and radiation. Proliferation and clonogenic assays were performed on different prostate cancer cell lines to determine their sensitivity to Canagliflozin and radiation. Cells were treated with different concentrations of Canagliflozin ranging from 0 to 30 uM or different doses of radiation ranging from 0 to 8 Gy. **A)** The effect of Canagliflozin on the proliferation of PCa cells lines. **B)** The effect of radiation on the proliferation of PCa cell lines. **C)** The effect of Canagliflozin on the colony formation ability of PCa cell lines (Log scale). **D)** The effect of radiation on the colony formation ability of PCa cell lines (Log scale). The results are expressed as the mean with the bars indicating the standard error mean (SEM). Three separate experiments were performed to obtain the results, n=3.

Table 3.1: The half-maximal inhibitory concentration (IC50) of Canagliflozin on the proliferation of prostate cancer cell lines.

Cell Line	Radiation Dose (Gy)	IC50 (uM)
22Rv1	0	21.18
	2	26.36
	4	23.36
PC-3	0	20.41
	2	21.04
	4	21.98
DU145	0	40.85
	2	42.50
	4	47.13

Table 3.2: The half-maximal dose of radiation on the proliferation of prostate cancer cell lines.

Cell Line	Half Maximum Effective Dose (Gy)
22Rv1	1.224
PC-3	4.382
DU145	6.445

3.2 Effect of the combined treatment of Canagliflozin and radiation on the proliferation of prostate cancer cell lines

Next experiments were performed with combined Canagliflozin and radiation treatment in order to better understand the interaction between these treatments. These experiments were performed to determine the effect of combined Canagliflozin and radiation treatment on the proliferative capacity of different PCa cell lines with differential mutation profiles. Figure 3.2 A-C shows the responsiveness of PCa cell lines to the combined treatment. In all cell lines (PC-3, DU145 and 22Rv1) Canagliflozin's antiproliferative capacity is optimal in lower radiation doses

(2-4 Gy) and diminishes with higher radiation doses. Furthermore, the IC50 values for PC-3 cell lines as well as 22Rv1 cell lines are less than $30uM$, which is clinically achievable. For 22Rv1 cells the IC50 values were 21.18 uM and 26.36 uM for 0 and 2 Gy respectively, while the IC50 values for PC-3 cells were 20.41 uM and 21.04 uM for 0 and 2 Gy respectively (Table 3.1). However, DU145 demonstrated resistance to Canagliflozin which is explained by higher IC50 values of 40.85 uM and 42.50 uM for 0 and 2 Gy, respectively (Table 3.1). To better interpret the results, a combination index analysis was performed in order to understand whether the effect of Canagliflozin is synergistic, additive or antagonistic to radiation. The combination index plots in figure 3.2 D-F show an additive effect of Canagliflozin when combined to that of radiation, which suggest that Canagliflozin may in fact be used as an adjunct to radiotherapy.

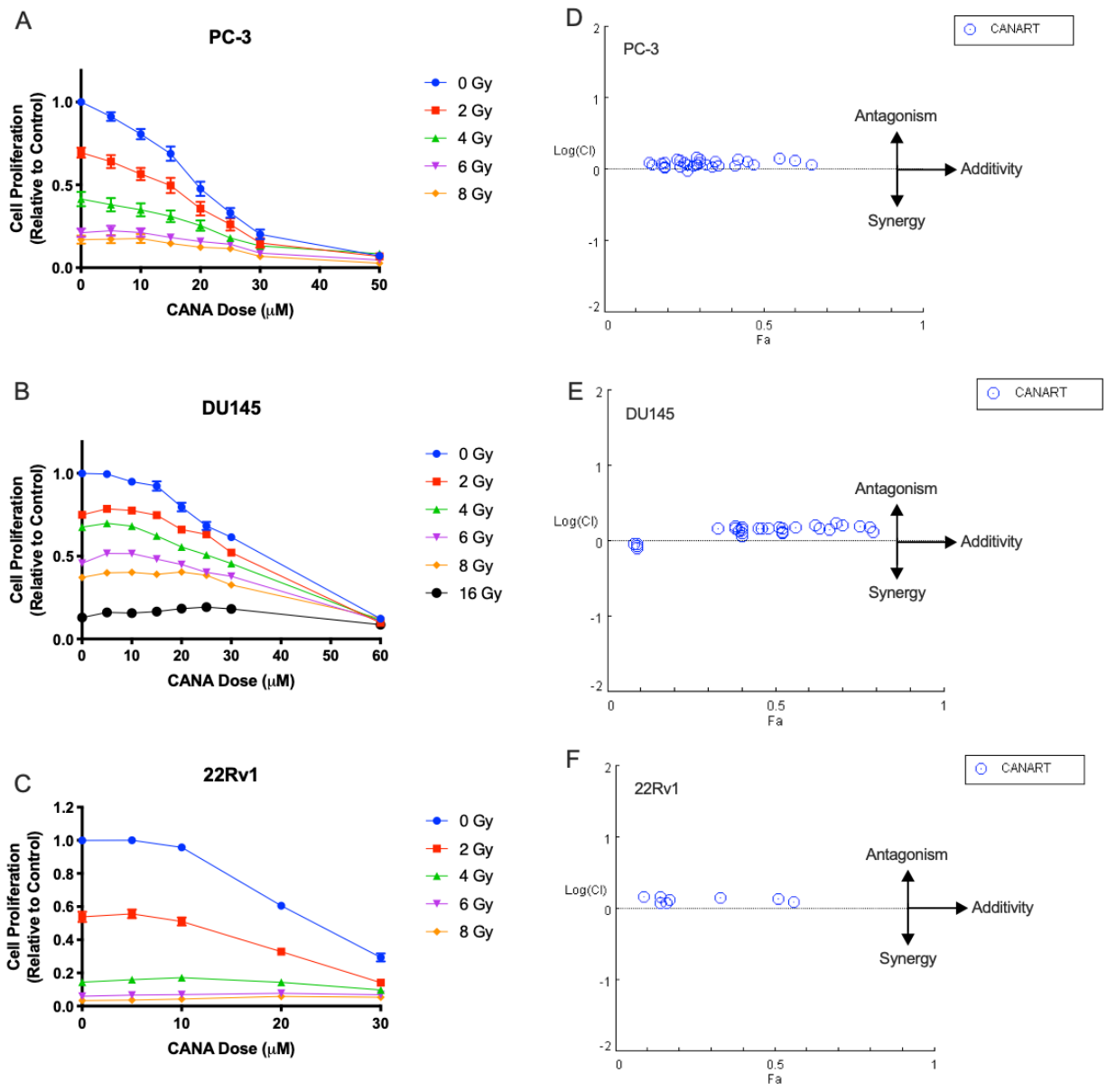

Figure 3.2: Canagliflozin inhibits the proliferation of prostate cancer cell lines alone and in combination with radiation. Proliferation assays were performed on three prostate cancer cell lines treated with Canagliflozin and radiation. Graphs **A-C** depict the effect of the combined treatment of Canagliflozin and radiation on the proliferation of prostate cancer cell lines. The results are expressed as the mean with the bars indicating the standard error mean (SEM). Three separate experiments were performed to obtain the results, n=3. A combination index analysis was performed on every cell line to better understand the interaction between Canagliflozin and radiation **(D-F)**. The chou-Talalay method for drug combination was used. Combination index plots use a logarithmic scale for the y-axis to depict the combination index while the fraction of cells affected (fa) is depicted on the x-axis. Log (CI)>0: antagonism, Log (CI)=0: additivity, Log (CI)<0: synergy.

3.3 Effect of the combined treatment of Canagliflozin and radiation on the ability of prostate cancer cell lines to form colonies

Figure 3.3 A-B, D-E shows the effect of Canagliflozin and radiation on the oncogenic capacity of PC-3 and DU154 cells. PC3 appear to be more sensitive to Canagliflozin treatment. The IC50 values for PC-3 cells were 16.82 μM, 18.83 μM, 16.48 μM for 0, 1 and 2 Gy respectively, while the IC50 values for DU145 cells were 15.86 μM, 18.69 μM and 19.81 μM for 0, 1 and 2 Gy respectively (Table 3.3). This demonstrates the relevance of this treatment since the dose required to obtain 50% inhibition of clonogenic survival is clinically achievable (Sha et al., 2011). Furthermore, the combination index analysis (Figure 3.3 C-F) validate the results obtained from proliferation assays indicating that Canagliflozin has an additive effect to radiation.

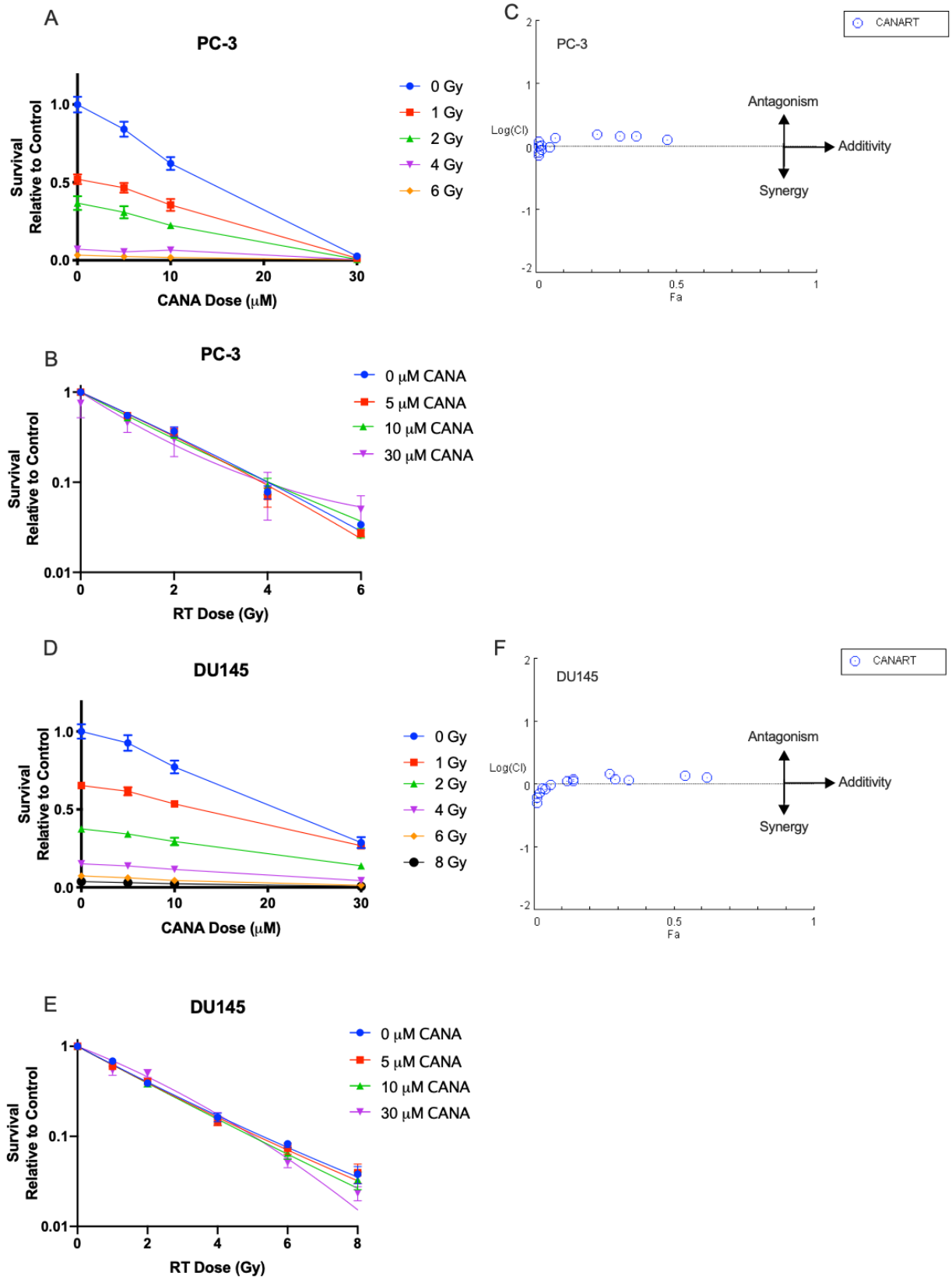
A
PC-3
Survival Relative to Control
1.0
0.5
0.0
0
10
20
30
CANA Dose (μM)
0 Gy
1 Gy
2 Gy
4 Gy
6 Gy
B
PC-3
Survival Relative to Control
1
0.1
0.01
0
2
4
6
RT Dose (Gy)
0 μM CANA
5 μM CANA
10 μM CANA
30 μM CANA
C
PC-3
CANART
Log(CI)
Antagonism
Additivity
Synergy
Fa
D
DU145
Survival Relative to Control
CANA Dose (μM)
0 Gy
1 Gy
2 Gy
4 Gy
6 Gy
8 Gy
E
DU145
Survival Relative to Control
RT Dose (Gy)
0 μM CANA
5 μM CANA
10 μM CANA
30 μM CANA
F
DU145
CANART
Log(CI)
Antagonism
Additivity
Synergy
Fa

Figure 3.3: Canagliflozin blocks the clonogenic survival of prostate cancer cell lines alone and in combination with radiation. Clonogenic survival assays were performed on two prostate cancer cell lines treated with Canagliflozin and radiation. Graphs **A-B,D-E** depict the effect of the combined treatment of Canagliflozin and radiation on clonogenic survival of prostate cancer cell lines. Results are plotted relative Canagliflozin (A, D) as well as relative RT doses (Log scale, B, E). The results are expressed as the mean with the bars indicating the standard error mean (SEM). Three separate experiments were performed to obtain the results, n=3. A combination index analysis was performed on every cell line to better understand the interaction between Canagliflozin and radiation **(C,F)**. The chou-Talalay method for drug combination was used. Combination index plots use a logarithmic scale for the y-axis to depict the combination index while the fraction of cells affected (fa) is depicted on the x-axis. Log (CI)>0: antagonism, Log (CI)=0: additivity, Log (CI)<0: synergy.

Table 3.3: The half-maximal inhibitory concentration (IC50) of Canagliflozin on the clonogenic survival of prostate cancer cell lines.

Cell Line	Radiation Dose (Gy)	IC50 (uM)
PC-3	0	16.92
	1	18.83
	2	16.48
	4	24.03
DU145	0	18.69
	1	19.81
	2	19.41
	4	19.24

3.4 Effect of the combined treatment of Canagliflozin and radiation on the proliferation and colony formation ability of regular and radioresistant prostate cancer cell lines.

Radiation resistance is a challenging feature of PCa, which, as discussed above, leads to a need for RT dose escalation in PCa clinical RT and an increase in the side effects associated with this treatment. Since the majority of prostate tumor cells do not die immediately and radio-resistance can develop even during the course of clinical RT, which takes up to 2 months to complete, it is important to investigate whether Canagliflozin could enhance RT-induced cell kill

in radio-resistant PCa cell lines. For that, proliferation and clonogenic assays were performed with irradiation resistant (IRR) DU145 (developed as described in Section 2.2) and parental DU145. As shown in figure 3.4 A,C, DU145-IRR showed significant radio-resistance at 2 Gy in the proliferation assays while they showed significant radio-resistance at 2, 4 and 6 Gy in the clonogenic assays. Furthermore, Figure 3.4 B, D shows a comparison between the effect of Canagliflozin alone on the DU145-IRR and parental DU145. Interestingly, in proliferation assays (Figure 3.4 B), DU145-IRR cells showed improved sensitivity to Canagliflozin with an IC50 value of 37.08 uM (Table 3.4). Importantly, this was verified and was indeed more significant in clonogenic survival assays where the IC50 value of 15.38 uM (Table 3.5) demonstrates the activity of the drug well within its therapeutic range (5-15 uM) (Devineni et al., 2013b). This signifies that Canagliflozin might be able to offer the advantage of addressing radio-resistance when tumour cells develop this condition in response to radiation. On the other hand, the responsiveness to Canagliflozin and radiation were also compared in parental 22Rv1 cell lines and 22Rv1-IRR cell lines. In proliferation assays, 22Rv1-IRR cell lines showed noticeable radio-resistance at all radiation doses (2-8 Gy) (Figure 3.4E). However, when 22Rv1-IRR cells were compared to parental 22Rv1 in terms of their responsiveness to Canagliflozin, the radio-resistant 22Rv1-IRR showed reduced sensitivity to Canagliflozin especially at the higher doses.

Further experiments were performed with the radio-resistant cell lines in order to examine the combined effect of Canagliflozin and radiation and compare the sensitivity to parental cell lines. DU145-IRR showed slightly higher sensitivity to Canagliflozin at 0 Gy compared to parental DU145 in proliferation as well as clonogenic assays (Figure 3.5A-B). In proliferation assays the IC50 values for DU145-IRR were 37.08 μM, 47. 39 μM and 33.47 μM

for 0,2 and 4 Gy respectively while they were 40.82 μM, 42.50 μM and 47.13 μM for parental DU145 cells (Table 3.4). In regard to clonogenic assays, the IC50 for DU145-IRR were 15.38 μM, 20.79 μM and 22.11 μM for 0,2 and 4 Gy respectively while they were 18.69 μM, 19.41 μM and 19.24 μM for parental DU145 cells (Figure 3.5). On the other hand, when 22Rv1-IRR cells were compared to parental 22Rv1, the former showed lower sensitivity to Canagliflozin (Figure 3.5 C) in proliferation assays which is demonstrated by the IC50 values (Table 3.6). In regard to the parental cell line, the IC50 values were 21.18 μM, 26.36 μM and 23.36 μM for 0, 2 and 4 Gy respectively while 22Rv1-IRR had higher IC50 values of 29.44 μM, 30.87 μM and 27.78 μM for 0,2 and 4 Gy respectively (Table 3.6). The combination index analysis (Figure 3.5D-F) showed an additive effect of Canagliflozin when combined with radiation. We have not been able to pursue clonogenic assays with 22Rv1 cells, as these cells do not grow in colonies.

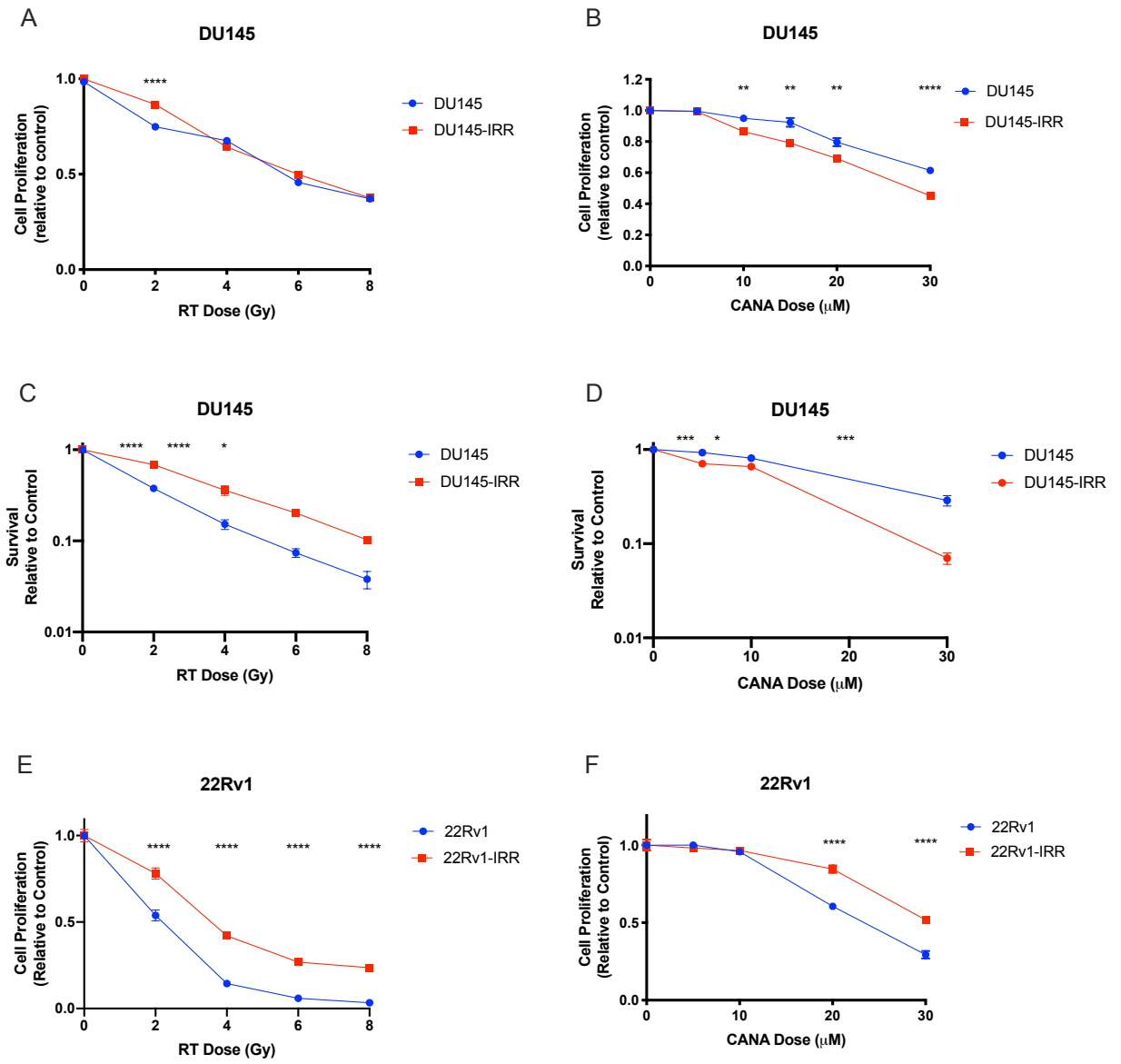

Figure 3.4: The response of radio-resistant prostate cancer cell lines to Canagliflozin and radiation. The effect of Canagliflozin and radiation alone was examined on the proliferation of parental DU145 and 22Rv1 and radio-resistant DU145 (DU145-IRR) and 22Rv1 (22Rv1-IRR) cell lines. In addition, the effect of Canagliflozin and radiation was examined on the clonogenic survival of parental DU145 and DU145-IRR. **A)** In proliferation assays, the effect of radiation was compared between DU145-IRR and the parental DU145 cell line. **B)** In proliferation assays, the effect of Canagliflozin was compared between DU145-IRR and the parental DU145 cell line. **C)** In clonogenic assays the effect of radiation was compared between DU145-IRR and the parental DU145 cell line (Log scale). **D)** In clonogenic assays, the effect of Canagliflozin was compared between DU145-IRR and the parental DU145 cell line (Log scale). **E)** In proliferation assays, the effect of radiation was compared between 22Rv1-IRR and the parental 22Rv1 cell

line. **F)** In proliferation assays, the effect of Canagliflozin was compared between 22Rv1-IRR and the parental 22Rv1 cell line. The results are expressed as the mean with the bars indicating the standard error mean (SEM). Three separate experiments were performed to obtain the results, n=3. A Two-Way analysis of variance (ANOVA) was performed to determine significance between the responsiveness of parental versus radio-resistant cell lines at every treatment dose. A Bonferroni *post hoc* test was performed to determine which groups are significantly different from each other where * = $p<0.05$, ** = $p<0.01$, *** = $p<0.001$ and **** = $p<0.0001$ as calculated.

Table 3.4: The half-maximal inhibitory concentration (IC50) of Canagliflozin on the proliferation of parental and irradiation resistant DU145 cell lines.

Radiation Dose (Gy)	DU145-IRR IC50 (uM)	DU145 IC50 (uM)
0	37.08	40.85
2	47.39	42.50
4	33.47	47.13

Table 3.5: The half-maximal inhibitory concentration (IC50) of Canagliflozin on the clonogenic survival of parental and irradiation resistant DU145 cell lines.

Radiation Dose (Gy)	DU145-IRR IC50 (uM)	DU145 IC50 (uM)
0	15.38	18.69
2	20.79	19.41
4	22.11	19.24

Table 3.6: The half-maximal inhibitory concentration (IC50) of Canagliflozin on the proliferation of parental and irradiation resistant 22Rv1 cell lines.

Radiation Dose (Gy)	22Rv1-IRR IC50 (uM)	22Rv1 IC50 (uM)
0	29.44	21.18
2	30.87	26.36
4	27.78	23.36

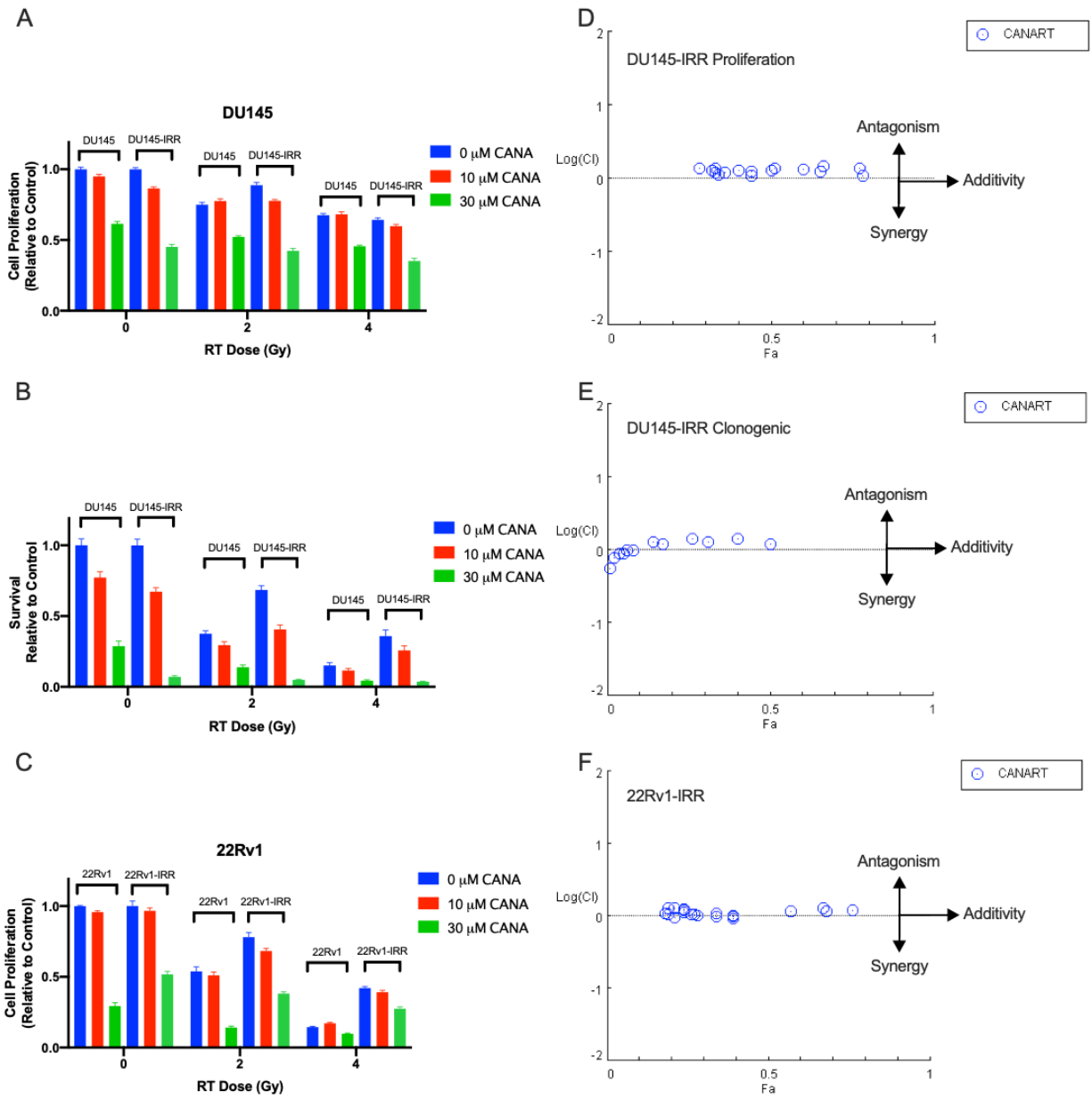

Figure 3.5: Canagliflozin inhibits the proliferation and blocks clonogenic survival of radio-resistant prostate cancer cell lines. Proliferation and clonogenic survival assays were performed on radio-resistant prostate cancer cell lines **A)** Proliferation assay of DU145 and DU145-IRR treated with Canagliflozin and radiation. **B)** Clonogenic assay of DU145 and DU145-IRR treated with Canagliflozin and radiation. **C)** Proliferation assay of 22Rv1 and 22Rv1-IRR treated with Canagliflozin and radiation. The results are expressed as the mean with the bars indicating the standard error mean (SEM). Three separate experiments were performed to obtain the results, n=3. Radiation doses of 6 and 8 Gy were also analyzed. Data is subjected to combination index analysis. **D-F)** A combination index analysis was performed on DU145-IRR in proliferation assays, DU14-IRR in clonogenic assays and on 22Rv1-IRR in proliferation

assays. The chou-Talalay method for drug combination was used. Combination index plots use a logarithmic scale for the y-axis to depict the combination index while the fraction of cells affected (fa) is depicted on the x-axis. Log (CI)>0: antagonism, Log (CI)=0: additivity, Log (CI)<0: synergy.

3.5 Canagliflozin regulates key molecular events supporting growth and survival within 4-8 hours

In order to understand the time frame at which Canagliflozin starts to mediate key metabolic events in the cell leading to anti-proliferative action, PC-3 cells were treated with $30\ uM$ Canagliflozin for different periods of time (1-24 hours). Lysates were then analyzed with immunoblotting. Three markers were used to explore the effect of Canagliflozin on cell cycle regulation, DNA replication and protein synthesis and survival through the mTO R pathway. Figure 3.7 A highlights the potent effect of Canagliflozin and the robust effect it had on the cells approximately 4-8 hours post treatment. Canagliflozin mediated an increase in the cellular protein levels of a key tumour suppressor protein, $p27^{Kip1}$ (CDKN1B) and was also able to effectively abolish the phosphorylation of histone H3 an established marker for DNA replication. In addition, phosphorylation levels of p70S6K were reduced. This was used as an mTOR pathway marker that is activated downstream of mTORC1. Inhibiting the mTOR pathway will ultimately lead to suppression of mRNA translation and protein synthesis. The quantification of the western blot results (Figure 3.7 B-D) shows significant difference in the levels of H3 and p70S6K phosphorylation and the levels of $p27^{Kip1}$ 8 hours after treatment. This suggests that Canagliflozin requires at least 4-8 hours to mediate its antiproliferative effects.

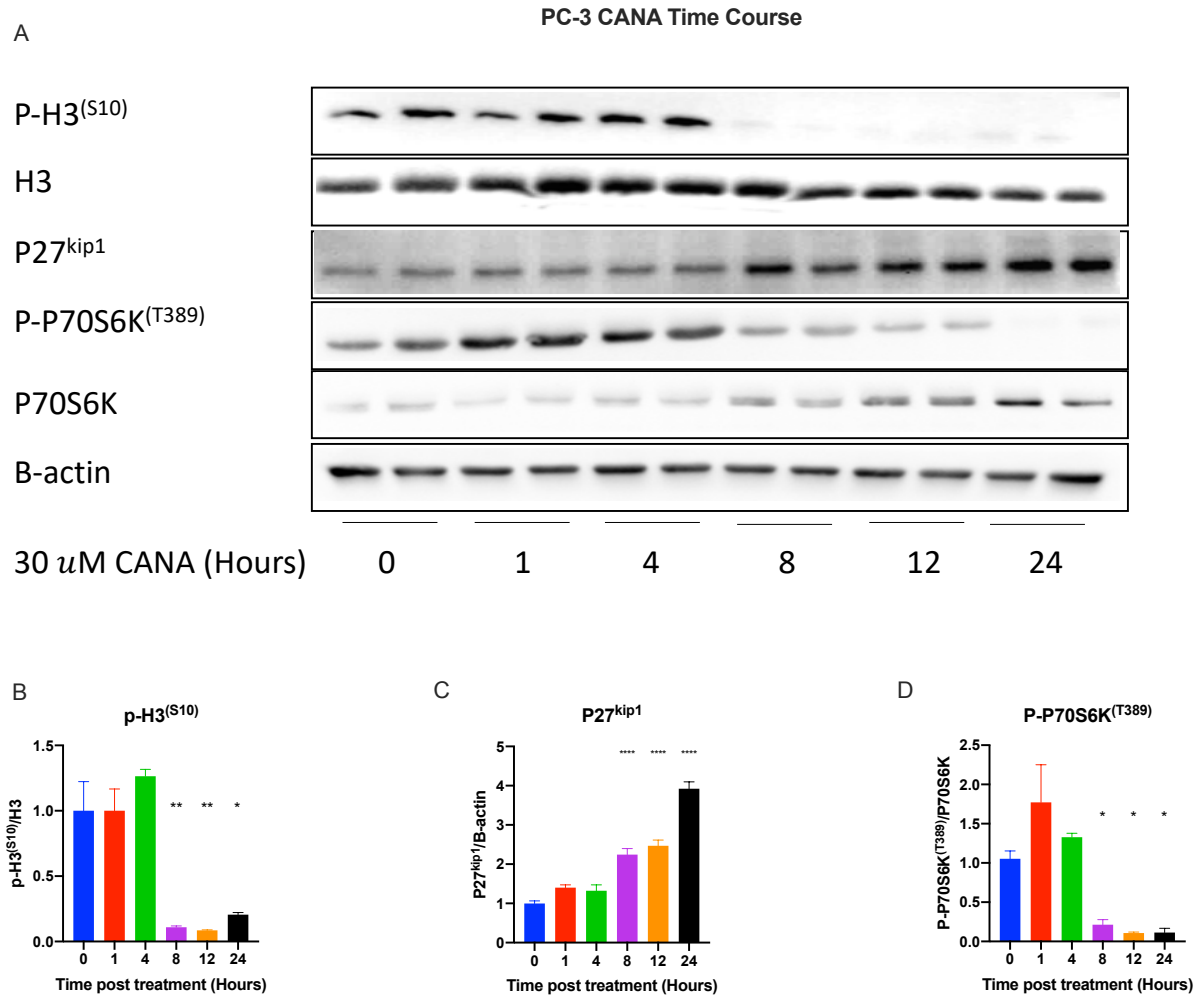

Figure 3.7: Canagliflozin blocks mitosis, cell cycle and the mTOR pathway within 4-8 hours. A western blot of a time course of PC-3 cells treated with 30 uM Canagliflozin treated for different periods of time. **A)** Immunoblotting of several markers for mitosis, cell cycle and the mTOR pathway. **B-D)** Quantification and densitometry of the markers tested above. Two separate experiments with 2 replicates each were performed to obtain the results, n=2. Densitometry was preformed using the software ImageJ. Protein levels were normalized to the control, B-actin and the results of the phosphorylated proteins are expressed as a fraction of the total levels. The results are expressed as the mean with the bars indicating the standard error mean (SEM). A One-Way analysis of variance (ANOVA) was performed to determine significance between different treatment groups. A Bonferroni *post hoc* test was performed to determine which groups are significantly different from the control group where * = $p<0.05$, ** = $p<0.01$, *** = $p<0.001$ and **** = $p<0.0001$ as calculated.

3.5 Effective suppression of the Akt-mTORC1 pathway and HIF-1$\boldsymbol{\alpha}$ in control and irradiated prostate cancer cells.

To further improve our understanding of the interaction of Canagliflozin and radiation and their antiproliferative effects, we performed western blots of lysates of PC-3 cells treated with different concentrations of Canagliflozin ($0 - 30\ uM$) and different doses of radiation (2-8 Gy) for 48 hours. We aimed to examine the lasting effects of Canagliflozin and RT on signaling events which likely determines the effects of these treatments on the proliferation and clonogenic survival of those cells. We examined the AMPK- mTOR-HIF-1α axis in depth. Earlier studies showed that Canagliflozin inhibits mitochondrial complex I (Villani et al., 2016) leading to AMPK activation. As a result of this inhibition, ATP levels in the cell are decreased compared to ADP and AMP levels. This in turn activates AMPK which influences numerus pathways in order to conserve energy for the cell. We also investigated HIF-1α which functions downstream of the mTOR pathway as a transcription factor that regulates multiple genes involved in metabolism, survival and tumour cell metastasis (Al Tameemi et al., 2019). HIF-1α is recognized as key cellular response to hypoxia, supports cell survival and proliferation of cancer cells in the hypoxic tumour microenvironment but also during normoxia as it mediates growth factor and mTOR signals (Cimmino et al., 2019).

Figure 3.8 A shows the effect of Canagliflozin and radiation on the mTOR pathway. As expected, untreated cells, incubated with standard growth media containing 10% FBS, showed significant basal phosphorylation of the Akt-mTOR pathway. Radiation showed a tendency to increase Akt phosphorylation levels 48 hours after treatment, but this was not statistically significant (Figure 3.8 B-C). However, Canagliflozin was able to significantly reduce the levels of phosphorylated Akt^{S473}, a site that contributes to the activation of Akt but is phosphorylated

by mTORC2. Importantly, RAPTOR^{S792} phosphorylation, a site specifically regulated by AMPK that leads to inhibition of mTORC1, was increased by 30 μM Canagliflozin. Although significant difference was only observed with cells treated with 30 μM Canagliflozin and 2 Gy of radiation (Figure 3.8 D), this increase is consistent with the increase in the phosphorylation levels of AMPKα. Increased phosphorylation of RAPTOR leads to its dissociation from the mTORC1 which in turn reduce the phosphorylation levels of its downstream targets namely p70S6K, S6K and 4E-BP1. In general, Canagliflozin leads to inhibition of the mTOR pathway that was statistically significant at the 30 μM dose. mTOR phosphorylation levels were significantly decreased with 30 μM in control and irradiated cells (Figure 3.8 E) which is consistent with a significant reduction of p70S6K and S6 phosphorylation (Figure 3.8 F,H). Reduction in the phosphorylation levels of 4E-BP1 (Figure 3.8 G) was also detected. Moreover, as a result of the mTOR pathway suppression, there is a significant reduction in the levels of HIF-1α (Figure3.8 I). Overall, our results suggest that Canagliflozin is able to suppress the mTOR pathway and its downstream targets likely through two mechanisms. The first one involves the suppression of Akt and the second one involves the activation of AMPK and the phosphorylation of RAPTOR.

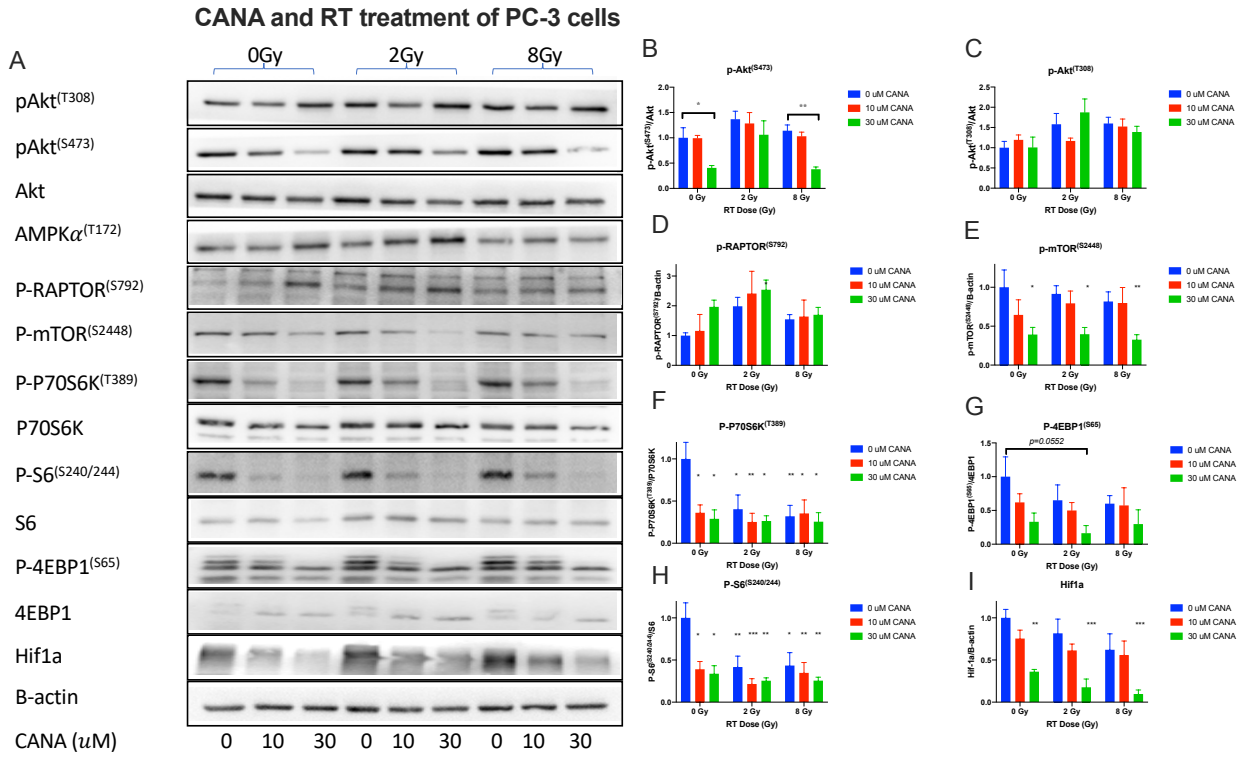

Figure 3.8: Canagliflozin blocks the mTOR pathway in control and irradiated cells. A western blot of PC-3 cells treated with Canagliflozin and/or radiation for 48 hours. **A)** Immunoblotting of several markers of the mTOR pathway. **B-I)** Quantification and densitometry of the markers tested above. Three separate experiments with two replicates each were performed to obtain the results, n=3. Densitometry was preformed using the software ImageJ. Protein levels were normalized to the control, B-actin, and the results of the phosphorylated proteins are expressed as a fraction of the total levels except for p-RAPTOR which is expressed as a fraction of B-actin. The results are expressed as the mean with the bars indicating the standard error mean (SEM). A Two-Way analysis of variance (ANOVA) was performed to determine significance between treatments groups and the control Group or other treatment groups. A Bonferroni *post hoc* test was performed to determine which groups are significantly different from the control group or from other treatment groups where * = $p<0.05$, ** = $p<0.01$, *** = $p<0.001$ and **** = $p<0.0001$ as calculated.

3.6 Suppression of DNA replication in control and irradiated prostate cancer cells

Investigation of H3 phosphorylation was used as a marker of the effect of Canagliflozin DNA replication (Figure 3.9 A). H3 phosphorylation was significantly decreased in cells treated with Canagliflozin alone or in combination with RT. This has led us to investigate potential upstream kinases of H3, p38 MAPK and ERK1/2. The phosphorylation levels of the two kinases showed trends for reduction with Canagliflozin treatment compared to untreated cells or cells treated with RT alone. However, this was not significant when density of the bands of phosphorylated form was normalized to total levels of these enzymes (Figure 3.9 C-D). It is possible that a meaningful decrease in the active/phosphorylated form of these enzymes does take place in intact cells.

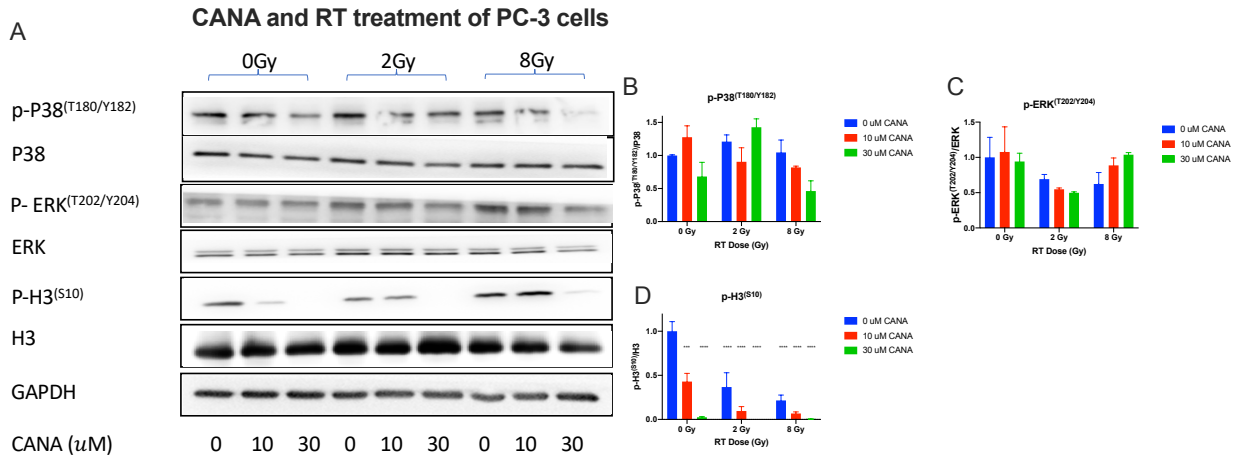

Figure 3.9: Canagliflozin blocks cell cycle and mitosis. A western blot of PC-3 cells treated with Canagliflozin and/or radiation for 48 hours. **A)** Immunoblotting of markers of DNA replication and MAPK pathway. **B-D)** Quantification and densitometry of the markers tested above. Three separate experiments were performed with 2 replicates each to obtain the results, n=3. Densitometry was preformed using the software ImageJ. Protein levels were normalized to the control, B-actin and the results of the phosphorylated proteins are expressed as a fraction of the total levels. The results are expressed as the mean with the bars indicating the standard error mean (SEM). A Two-Way analysis of variance (ANOVA) was performed to determine significance between treatments groups and the control Group or other treatment groups. A Bonferroni *post hoc* test was performed to determine which groups are significantly different

from the control group or from other treatment groups where * = $p<0.05$, ** = $p<0.01$, *** = $p<0.001$ and **** = $p<0.0001$ as calculated.

3.7 Canagliflozin inhibit tumour growth in vivo

To understand the implications of Canagliflozin *in vivo* a PC-3 xenograft model was studied. Balb/c nude mice (6-8 animals per group) were assigned to a control group that was fed a normal chow diet and did not receive radiation or one of three different treatment groups. The first treatment group (CANA treatment) was fed a CANA diet with a concentration of 416.7 ppm. This drug concentration was determined after taking into account the proportion of provided diet ultimately consumed by animals and drug bioavailability with the aim to achieve an estimated final daily concentration of 50 mg/Kg. The second treatment group (radiation treatment) received single dose of radiation (5 Gy), 5 days after the tumour reached 50 mm^3, and the third treatment group (combined treatment) was fed a CANA diet and received a single dose of radiation (5 Gy). All groups were drinking sterile water (*ad libitum*) throughout the experiment. Food intake was consistent across different treatments groups of the study while water intake was different (Figure 3.10 B-C). As expected, mice treated with Canagliflozin drank significantly more water compared to the control group consistent with the effect Canagliflozin exerts on the kidney. Furthermore, tumour growth was monitored, using a caliper, for 60 days after the beginning of the treatment. Figure 3.10 A shows the effect of Canagliflozin on tumour growth of treated mice compared to control mice where mice treated with Canagliflozin alone, radiation alone or a combination of both treatments grew tumours slower compared to the control group. This explains the difference in *ex vivo* tumour masses and volumes. Although there was an evident reduction in the size and mass of tumours in all treatment groups, significant difference was only observed in the groups treated with Canagliflozin alone or a combination of

Canagliflozin and radiation (Figure 3.10 E-F). It is also worth noting that the mass of mice in all groups were similar at endpoint signifying that Canagliflozin did not induce significant changes in the mass of mice receiving the drug (Figure 3.10 D).

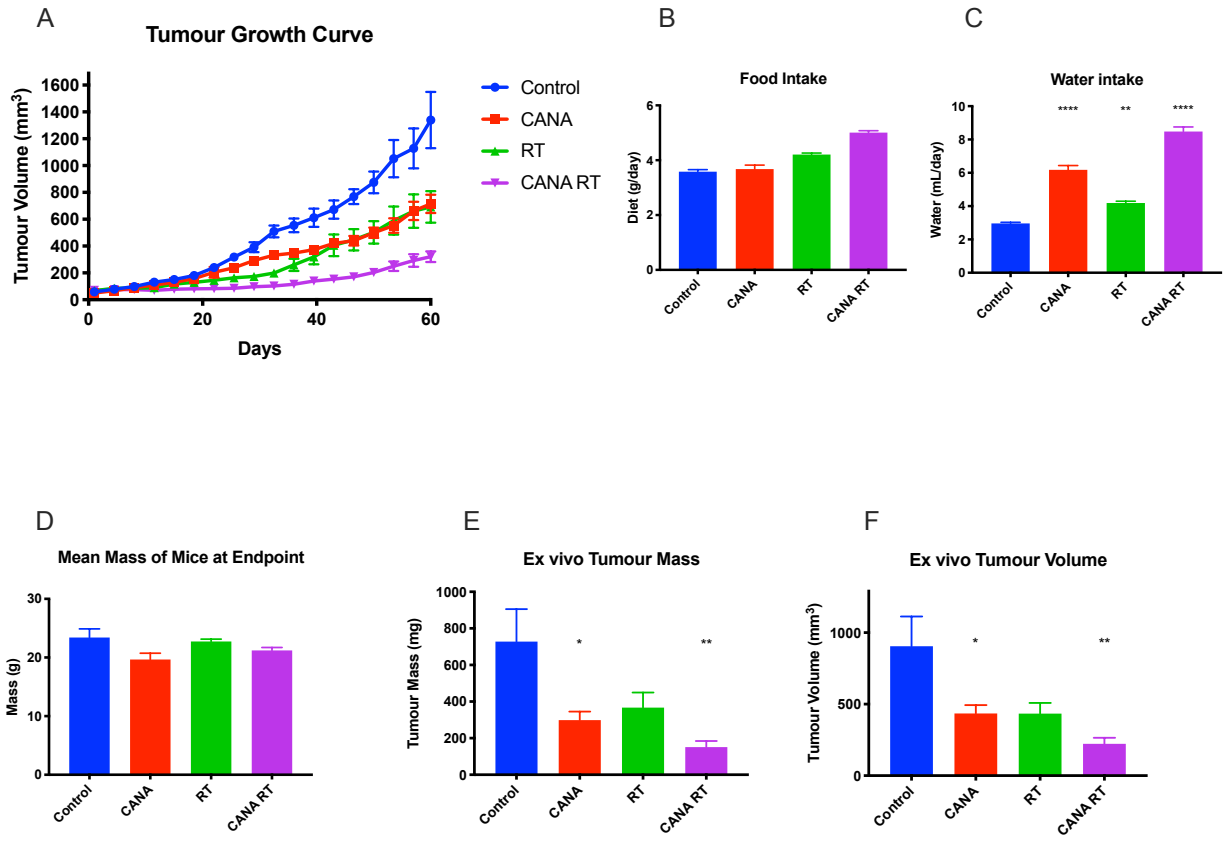

Figure 3.10: Canagliflozin slows down tumour growth *in vivo.* PC-3 grafted animals (6-8 animals per group) were treated with Canagliflozin and radiation while tumour growth was monitored. **A)** Tumour growth curve for different treatment groups. **B-C)** Food and water intake per treatment group respectively. **D)** Mass of mice at endpoint. **E-F)** Ex vivo tumour mass and volume respectively of mice in each treatment group. The results are expressed as the mean with the bars indicating the standard error mean (SEM). A One-Way analysis of variance (ANOVA) was performed to determine significance between treatments groups and the control group. A Bonferroni *post hoc* test was performed to determine which groups are significantly different from the control group where * = $p<0.05$, ** = $p<0.01$ as calculated.

CHAPTER IV - DISSCUSSION

DISSCUSSION

Radio-resistance remains a challenge for many cancers including prostate cancer. The aim of this study was to examine the therapeutic benefits of Canagliflozin when combined with radiation to treat prostate cancer. This work was planned based on our previous observations that Canagliflozin is able to inhibit proliferation and clonogenic survival at clinically achievable doses (5-15 μM) (Devineni et al., 2013a; Villani et al., 2016). In this study we observed that clinically achievable doses of Canagliflozin

1- Inhibited proliferation, clonogenic survival and tumour growth alone and in combination with radiation in an additive manner in most cases,
2- Blocked the mTORC1 pathway leading to downregulation of effectors such as HIF-1α,
3- May induce its antiproliferative effects through:
    a. $P27^{kip1}$ induction and cell cycle arrest
    b. Suppression of DNA replication, evident by blockade of H3 phosphorylation

5.1 Efficacy of canagliflozin on prostate cancer cell lines with different mutation profiles

The initial experiments aimed to test the responsiveness of PCa cell lines to radiation and Canagliflozin. The PCa cell lines used here carry different mutations and are representative of different stages of cancer progression. For instance, PC-3 and DU145 cells show androgen-independent growth while 22Rv1 cells are androgen responsive cell lines. It is also important to highlight that two of the cell lines represent a metastatic disease namely PC-3 and DU145 while 22Rv1 cells are not a metastatic cell line. Establishing the sensitivities of different cell lines to Canagliflozin alone or in combination with radiation was essential in order to begin identifying

disease characteristics with sensitivity to Canagliflozin to help focus our *in vivo* studies to the most promising PCa models. Our results suggest that PC-3 cells are the most responsive to Canagliflozin. This cell line is representative of a castration resistant, bone metastatic disease lacking p53 and PTEN activity.

5.2 Canagliflozin inhibits prostate cancer growth alone and in combination with radiation

We report that Canagliflozin is able to inhibit the proliferation of PCa cell lines alone and when combined with radiation. Proliferation assays performed in this study were slightly different than traditional proliferation assays where cells are treated for approximately 72 hours. In order to better understand the effect of our treatments on the proliferation of cells, cells were seeded at a lower density and were incubated for a longer period of time compared to the traditional proliferation assays (48 hours). This allows the cell to undergo multiple cycles of mitosis and permits us to assess more reliably the effects of treatments on all steps of cellular growth including DNA replication, mitosis, growth of cellular biomass and proliferation. Furthermore, clonogenic survival assays were used to determine tumorigenic potential following specific treatments. Results from proliferation and clonogenic survival assays were subjected to combination index analysis with the Chou-Talalay method to better interpret the interaction between Canagliflozin and radiation treatments. Overall, our results suggest an additive relationship between Canagliflozin and radiation treatments. Although these results did not confirm our initial hypothesis of potential radio-sensitization of PCa by Canagliflozin, nevertheless, they clearly illustrate a significant potential for Canagliflozin to offer clinically relevant activity. Canagliflozin could still be combined with radiation therapy in order to enhance the response of PCa to radiation. Furthermore, an analysis of the half maximal

inhibitory concentrations (IC50) shows that Canagliflozin, as a single agent, is able to inhibit the proliferation and clonogenic survival of most PCa cell lines at clinically achievable doses ($\leq 30\mu M$).

5.3 Response of radio-resistant cell lines to Canagliflozin

It is important to note that DU145-IRR and 22Rv1-IRR cells were obtained by irradiating parental DU145 and 22Rv1 with 2 Gy per day for multiple days to generate cells with resistance to conventionally fractionated radiotherapy. Although in proliferation assays, we observed radio-resistance of DU145-IRR cells only at 2 Gy, resistance to higher radiation doses was observed in clonogenic assays. Our results suggest that there is a significant difference between the sensitivity of radio-resistant cells to Canagliflozin compared to the parental cells. However, these results are particularly interesting for two reasons, i) they indicated that indeed Canagliflozin may offer an additional advantage of increased activity against some radio-resistant PCa and ii) Canagliflozin's capacity to exert sensitizing activity depends likely on a molecular profile that is not universally present in all cells that acquire radio-resistance. DU145-IRR cells showed higher sensitivity to Canagliflozin in both proliferation and clonogenic assays while 22Rv1-IRR cells showed less sensitivity to Canagliflozin in proliferation assays. Further analysis of these cell lines is required in order to better understand the molecular etiology of this difference. Although radio-resistant cells did not show consistently improved sensitivity to Canagliflozin, combination index analysis showed additivity between Canagliflozin and radiation for both the radio-resistant cell lines. This indicates that, overall, addition of Canagliflozin to radiotherapy would likely be beneficial in most PCa tumours, albeit to a different degree. It is possible that PCa cells surviving radiotherapy treatment may have differential dependence on oxidative phosphorylation and

sensitivity to mitochondria blockade by canagliflozin. Nevertheless, canagliflozin could have beneficial anti-tumor efficacy when used alone or in combination with RT in many prostate tumor cells.

5.4 Canagliflozin mediates key metabolic effects within 4-8 hours

An original time-course experiment was performed with PC-3 cells in order to determine how long it takes Canagliflozin to regulate cellular and molecular events within the cell and how long those effects last. $P27^{Kip1}$ is a cyclin dependent kinase (CDK) inhibitor which causes cell cycle arrest in the G1/S phase. This is achieved through binding and inactivating CDK 2 or CDK 4. $P27^{Kip1}$ levels are increased in quiescent cells and cells undergoing apoptosis, while its expression decreases during tumour development and progression and when cells are stimulated with mitogens (Lloyd et al., 1999). $P27^{kip1}$ was used in order to understand the potential impact of Canagliflozin on cell cycle checkpoint regulators. An increased in the levels of $p27^{kip1}$ suggests that Canagliflozin likely causes G1/S cell cycle arrest in treated cells (Figure 3.7). In addition, H3 was used as a marker for mitosis. H3 phosphorylation is a DNA replication and mitosis marker. H3 is highly modified post-translationally through acetylation and phosphorylation. These modifications are essential for the chromatin fiber de-condensation, which allows the DNA to be ready for replication during mitosis (Hans & Dimitrov, 2001). H3 phosphorylation levels of cells treated with Canagliflozin for 8 hours or more significantly lower than basal phosphorylation levels. This may provide evidence that Canagliflozin is able to suppress chromatin de-condensation and DNA replication. Similarly, the phosphorylation of p70S6K was assessed in order to determine whether Canagliflozin is able to inhibit the mTOR pathway. p70S6K phosphorylation is essential for the phosphorylation and activation of the ribosomal protein S6. Overall, our results (figure 3.7) suggest that Canagliflozin can indeed

influence the key pathways of DNA replication and protein biosynthesis within 4-8 hours after treatment.

5.5 Canagliflozin downregulates the mTOR pathway alone and in combination with radiation

We further investigated the mTOR pathways in order to examine whether Canagliflozin is able to suppress pathways regulating cellular growth and protein synthesis in combination with radiation, functions that are vital for tumour cell growth and survival. We examined Akt and AMPK as they are key upstream stimulatory and inhibitory regulators of mTOR, respectively. figure 3.8 results illustrate that Canagliflozin blocks the activation of key effectors of the mTOR pathway in both control and irradiated cells.

Akt regulation

Akt is regulated by the upstream kinase PDK1, through phosphorylation of residue T308, and also by a downstream positive feedback regulation with phosphorylation of residue S473 by mTORC2 (Mundi et al., 2016). Akt is found upregulated in a number of cancers including prostate cancer due to mutations to PTEN, a negative regulator of the Akt-mTOR pathway, as well as various growth factors resulting in activated receptor tyrosine kinases (RTKs) (Mundi et al., 2016). Our results suggest a decrease in the phosphorylation levels at S473 specifically, a site phosphorylated mainly by mTORC2 (Mundi et al., 2016). mTORC2 consists of several subunits including mLST8, Tti/Tel2, and DEPTOR. However, it contains the rapamycin insensitive companion of mTOR (RICTOR) as well as mSin1, which are not present in mTORC1 (L. C. Kim et al., 2017; Saxton & Sabatini, 2017b). mTORC2 is activated when the inhibitory unit mSin1 is relieved by binding to PIP3 upon stimulation with growth factors (Saxton & Sabatini, 2017b). It is also worth noting that Akt is activated by radiation (H. F. Li et al., 2009). DNA

damage and ATM activation has been associated with increased levels of Akt S473 phosphorylation however, the mechanism is not fully understood (Ditch & Paull, 2012; Liao & Hung, 2010). In addition, DNA-dependent protein kinase (DNA-PK) has also been associated with Akt phosphorylation at S473 (Bayascas & Alessi, 2005; Karen Tsui et al., 19601 B.C.E.; Stronach et al., 2011). Our results show that Canagliflozin blocked Akt phosphorylation on S473 but not on T308, which could have contributed further to the inhibition of the mTOR pathway. Further studies could focus on analyzing the modulation of ATM and DNA-PK activities by Canagliflozin, as contributors to reduced Akt S473 phosphorylation. However, in early results we did not detect modification of ATM phosphorylation by Canagliflozin in either control or irradiated cells (results not shown) The reduction in the phosphorylation levels of Akt, in response to Canagliflozin, could help counteract the effects of PTEN mutation which typically leads to constant stimulation of cell growth.

Modulation of mTOR by AMPK

Earlier we observed that Canagliflozin activates AMPK, an event observed also in the current experiments with phosphorylation of RAPTOR S792 which is a specific site of phosphorylation by AMPK (Gwinn et al., 2008b). This observation points specifically to the contribution of AMPK activation in regulating the mTOR pathway. Inhibition of Akt and activation of AMPK offer likely a combined effect to suppress activity of mTOR and its downstream effectors.

Regulation of mTOR effectors

Canagliflozin inhibited mTORC1 effectors namely p70S6K, S6 and 4E-BP1 which are crucial for protein translation and synthesis. The quantification results in Figure 3.8 B-H indicate the fraction of phosphorylated protein compared to the total protein concentration. This might undermine the effect of Canagliflozin since the phosphorylated form of the protein carries out the function. Another approach to present the data is to normalize immunoblotting results of the phosphorylated protein levels to a housekeeping protein such as B-actin or GAPDH. This may represent the effect of Canagliflozin more accurately.

Downregulation of HIF-1α

Furthermore, HIF-1α levels were also lowered significantly in cells treated with Canagliflozin. HIF-1α is a transcription factor involved in many processes leading to cell survival and tumour progression in hypoxic as well as normoxic environment. Reduction in the levels of HIF-1α will lead to impaired glucose metabolism, inability of cells to survive and grow which leads to decreased metastatic potential (Z. ji Liu et al., 2015; Ochiai et al., 2011). HIF-1α regulates the transcription of several genes resulting in the increase of glucose uptake. This increases aerobic glycolysis and promotes the Warburg effect. In addition, HIF-1α mediates EMT and metastasis and is also involved in angiogenesis by regulating VEGF (Krock et al., 2011; C. Li et al., 2019). The impact of downregulation of HIF-*1*α in PCa cells in response to Canagliflozin can be highly significant in determining the growth suppressive and anti-cancer properties of this drug. In addition, RNAseq analysis performed by our lab on A549 a non-small cell lung cancer (NSCLC) cells treated with Canagliflozin indicated major suppression of HIF-*1*α-dependent genes involved in metabolism, survival and metastasis. Analysis of the gene

expression profile on PCa cells in response to Canagliflozin with RNAseq is being planned for the near future.

5.6 Modulation of mitogen activated protein pathways (MAPKs) as a mechanism to histone regulation

The inhibitory effect of Canagliflozin on H3 phosphorylation were truly impressive in both irradiated and unirradiated cells. Canagliflozin amplifies the effect of radiation and completely abolishes the levels of phosphorylated H3 (figure 3.9). This led us to explore upstream regulators of H3 phosphorylation, namely p38 MAPK and ERK1/2, as an initial exploration of histone regulating pathways modulated by Canagliflozin. We examined the levels of phosphorylation of the p38 MAPK and Erk1/2 which illustrate their activation. Our results showed visible trends for suppression of p38 MAPK and Erk1/2 phosphorylation by canagliflozin. However, when normalized to total levels of the enzymes, changes in phosphorylation levels did not appear significant. It is possible that relative MAPK phosphorylation levels do not represent well changes in kinase activity of these enzymes that may take place in response to Canagliflozin. This can be examined further by analyzing also other substrates of MAPK kinase activity. Additionally, it is possible that MAPKs may not be the main regulators of H3 phosphorylation and activity in this setting and other kinases that might be implicated in the basal phosphorylation of H3 in PCa such as PIM1 and Aurora B kinase (Le et al., 2013; Zippo et al., 2007).

5.7 Canagliflozin attenuates tumour growth in PC-3 Xenografts

Lastly, in order to establish the effect of Canagliflozin and radiation *in vivo* a mouse xenograft model was pursued. PC-3 cells were used since they exhibited the highest sensitivity to Canagliflozin in our *in vitro* studies. The tumour growth curve (Figure 3.10) shows noticeable reduction in the volume of tumours of mice treated with Canagliflozin, radiation or a combined treatment. According to this graph, the tumours of irradiated mice (radiation group) were growing initially slower than the tumours of mice treated with Canagliflozin. However, after a few weeks (Day 40), it is evident that irradiated tumours began recovering from the irradiation effect and started growing relatively faster, as an early sign of radiation resistance. This likely indicates the ability of cells to repair DNA damage caused by radiation and resumption of DNA replication and growth. On the other hand, since the Canagliflozin treatment lasted for the whole duration of the experiment (60 days), the growth of tumours was consistently suppressed compared to the control group. Importantly, Canagliflozin hindered the ability of cells to recover from the initial effect of radiation in the group treated with both Canagliflozin and radiation. This indicates the promise of utilizing Canagliflozin in combination with radiation in order to prolong the anti-tumour efficacy of radiation. Overall Canagliflozin was well tolerated in treated animals. Canagliflozin treated mice drank more water, appeared healthy and did not show significant weight loss while they showed reduced tumour growth when Canagliflozin was used alone or in combination with radiation.

Mice were euthanized 60 days post treatment and tumours were collected for further analysis through immunohistochemistry and western blotting. Studies being planned for the near future will pursue detailed analysis of collected tumours with immunoblotting,

immunohistochemistry and qPCR techniques to determine whether *in vitro* observations of the modulation of molecular pathways by Canagliflozin can be verified *in vivo.*

Limitations and Future Directions

This study had its own limitations and challenges. It represents an early analysis of Canagliflozin in combination with radiation that was performed in a period of about 14 months. The study was significantly affected by the COVID-19 pandemic, which forced us to discontinue experimental work during its peak activity in early 2020 when a large number of experiments were planned. The interruption of work for about 5 months did not allow me complete a large number of planned experiments including analysis of gene expression effects in tissue culture with qPCR, metabolic analysis with oxygen consumption rates in response to treatments with Seahorse assays, performance of xenograft work with additional PCa models and immunohistochemistry analysis of tumour specimens. Additional concerns and limitations in the methodology include:

1- Limited analysis of baseline and after treatment gene expression profiles of wild type and radio-resistant cells
2- Limited investigation of effects of Canagliflozin on cellular pathways other than mTOR and cell lines other than PC-3 cells and lack of investigation of the specific role of driver mutations such as p53 and PTEN in the responsiveness of Canagliflozin
3- Limited investigation of the metabolic effects of Canagliflozin in untreated and irradiated cells
4- Need for investigation of the *in vivo* effects of the drug in models other than PC-3 cells

Developing radio-resistant cell lines is a very useful tool to examine the effect of Canagliflozin in combination with radiation. Understanding the levels of gene expression as well as the mutations present in those cell lines is essential to validate our results. For instance, two radio-resistant cell lines were examined in this project, DU145-IRR and 22Rv1-IRR. The former showed enhanced sensitivity to Canagliflozin compared to the parental cell line while the latter showed reduced sensitivity to Canagliflozin compared to the parental cell line. In addition, PC-3 cells represent a metastatic, androgen-insensitive model with deletions of PTEN and Tp53. Understanding the molecular profile of PCa and comparison to their response to Canagliflozin can help us dissect the detailed mechanism of action of this drug.

There are also limitations to our *in vivo* model. Although Canagliflozin demonstrated, in vivo, the effect expected based on the *in vitro* studies, the Canagliflozin dose received by each mouse was not accurately measured. This is because the mice received Canagliflozin in their diet and not by oral gavage. Furthermore, since immune-compromised balb/c nude mice were used in this xenograft model, it does not allow us to examine the effects of Canagliflozin on the immune system. A TRAMP syngeneic model might be useful in order to better understand the effect of Canagliflozin and radiation on the immune response, while work with PDX models could provide additional evidence for potential efficacy of Canagliflozin in clinical settings.

In order to further our understanding of the pathways regulated by Canagliflozin and radiation, a RT-PCR analysis is needed to examine the effect of the treatments on gene expression as well as the time period at which Canagliflozin exhibits changes in gene expression. Further, targeting specific genes such as p53, PTEN or HIF-1α with a knock down approach could help determine the role of these genes in the mechanism of Canagliflozin action. To do so,

proliferation experiments with small interfering RNA (siRNA) of target proteins will allow us to test their implications at mediating the effect of Canagliflozin.

The fact that PC-3 cell lines are the most sensitive to Canagliflozin may indeed relate to p53 or PTEN status in these cells. Loss of p53 has been implicated in radiation resistance (J. M. Lee & Bernstein, 1993). Studies suggested that metabolic stress induces a p53-dependent checkpoint in cancer cells (Jones et al., 2005). Jones and colleagues reported that metformin selectively inhibits p53 deficient tumour growth. Metformin as well as AICAR, an AMPK activator selectively increased apoptosis of the $p53^{-/-}$ colon cancer cell lines HCT116 *in vivo* (Buzzai et al., 2007). This raises the question whether the presence or absence of p53 plays a major role in mediating the effects of Canagliflozin or not. To answer this question, a model of p53 positive and p53 negative LNCaP cells is being developed in order to determine the effect of Canagliflozin in cells expressing WT p53 and with p53 knockout cells. Finally, oxygen consumption rate (seahorse) assays would be important to show the effect of Canagliflozin on oxygen consumption rate and ATP synthesis. In preliminary results from seahorse assays we observed a major suppression of oxidative phosphorylation by Canagliflozin (results not shown).

Conclusion

The original hypothesis of this work was that Canagliflozin sensitizes prostate cancer cells to radiation. After performing several *in vivo* and *in vitro* experiments, we cannot conclude that Canagliflozin is in fact a radio-sensitizer. Based on the combination index analysis performed using the data from proliferation and clonogenic assays, one can argue that Canagliflozin, at clinically achievable and safe doses, has significant anti-tumor activity in PCa as a single agent but it can also function as an effective adjunct to radiation which makes it clinically relevant. Radiation therapy, especially at high doses, is linked to multiple side effects. Canagliflozin may be able to reduce the side effect profile and improve the therapeutic ratio of radiotherapy in PCa patients. Although Canagliflozin might not sensitize cells to radiation, we continue to believe that it remains clinically relevant for the treatment of prostate cancer and it should be investigated next in early phase clinical trials in combination with radiotherapy.

References

Adhyam, M., & Kumar Gupta, A. (2012). A Review on the Clinical Utility of PSA in Cancer Prostate. *Indian Journal of Surgical Oncology*, *3*(2), 120–129. https://doi.org/10.1007/s13193-012-0142-6

Age standardized (World) incidence rates, prostate, all ages. (2018). https://doi.org/10.6

Al Tameemi, W., Dale, T. P., Al-Jumaily, R. M. K., & Forsyth, N. R. (2019). Hypoxia-Modified Cancer Cell Metabolism. *Frontiers in Cell and Developmental Biology*, *7*, 4. https://doi.org/10.3389/fcell.2019.00004

Alberti, C. (2014). Prostate cancer: Radioresistance molecular target-related markers and foreseeable modalities of radiosensitization. *European Review for Medical and Pharmacological Sciences*, *18*(16), 2275–2282.

Alizadeh, M., & Alizadeh, S. (2014). Survey of clinical and pathological characteristics and outcomes of patients with prostate cancer. *Global Journal of Health Science*, *6*(7), 49–57. https://doi.org/10.5539/gjhs.v6n7p49

Ameer, F., Scandiuzzi, L., Hasnain, S., Kalbacher, H., & Zaidi, N. (2014). De novo lipogenesis in health and disease. *Metabolism*, *63*(7), 895–902. https://doi.org/10.1016/j.metabol.2014.04.003

Artimo, P., Jonnalagedda, M., Arnold, K., Baratin, D., Csardi, G., De Castro, E., Duvaud, S., Flegel, V., Fortier, A., Gasteiger, E., Grosdidier, A., Hernandez, C., Ioannidis, V., Kuznetsov, D., Liechti, R., Moretti, S., Mostaguir, K., Redaschi, N., Rossier, G., … Stockinger, H. (2012). ExPASy: SIB bioinformatics resource portal | Nucleic Acids Research | Oxford Academic. *Nucleic Acids Research*, *40*(1), w597-2603. https://academic.oup.com/nar/article/40/W1/W597/1073688

Aschenbach, W. G., Hirshman, M. F., Fujii, N., Sakamoto, K., Howlett, K. F., & Goodyear, L. J. (2002). Effect of AICAR treatment on glycogen metabolism in skeletal muscle. *Diabetes*, *51*(3), 567–573. https://doi.org/10.2337/diabetes.51.3.567

Barretina, J., Caponigro, G., Stransky, N., Venkatesan, K., Margolin, A. A., Kim, S., Wilson, C. J., Lehár, J., Kryukov, G. V., Sonkin, D., Reddy, A., Liu, M., Murray, L., Berger, M. F., Monahan, J. E., Morais, P., Meltzer, J., Korejwa, A., Jané-Valbuena, J., … Garraway, L. A. (2012). The Cancer Cell Line Encyclopedia enables predictive modelling of anticancer drug sensitivity. *Nature*, *483*(7391), 603–607. https://doi.org/10.1038/nature11003

Baskar, R., Lee, K. A., Yeo, R., Yeoh, K.-W., Baskar, R., & Phil, M. (2012). Cancer and Radiation Therapy: Current Advances and Future Directions. *Int. J. Med. Sci*, *9*(3), 193–199. https://doi.org/10.7150/ijms.3635

Bayascas, J. R., & Alessi, D. R. (2005). Regulation of Akt/PKB Ser473 phosphorylation. In *Molecular Cell* (Vol. 18, Issue 2, pp. 143–145). Cell Press. https://doi.org/10.1016/j.molcel.2005.03.020

Bonora, M., Patergnani, S., Rimessi, A., de Marchi, E., Suski, J. M., Bononi, A., Giorgi, C., Marchi, S., Missiroli, S., Poletti, F., Wieckowski, M. R., & Pinton, P. (2012). ATP synthesis and storage. In *Purinergic Signalling* (Vol. 8, Issue 3, pp. 343–357). Springer. https://doi.org/10.1007/s11302-012-9305-8

Brand, D. H., Tree, A. C., Ostler, P., van der Voet, H., Loblaw, A., Chu, W., Ford, D., Tolan, S., Jain, S., Martin, A., Staffurth, J., Camilleri, P., Kancherla, K., Frew, J., Chan, A., Dayes, I. S., Henderson, D., Brown, S., Cruickshank, C., … Oommen, N. (2019). Intensity-modulated fractionated radiotherapy versus stereotactic body radiotherapy for prostate cancer (PACE-B): acute toxicity findings from an international, randomised, open-label,

phase 3, non-inferiority trial. *The Lancet Oncology*, *20*(11), 1531–1543. https://doi.org/10.1016/S1470-2045(19)30569-8

Buzzai, M., Jones, R. G., Amaravadi, R. K., Lum, J. J., DeBerardinis, R. J., Zhao, F., Viollet, B., & Thompson, C. B. (2007). Systemic treatment with the antidiabetic drug metformin selectively impairs p53-deficient tumor cell growth. *Cancer Research*, *67*(14), 6745–6752. https://doi.org/10.1158/0008-5472.CAN-06-4447

Chen, N., & Zhou, Q. (2016). The evolving gleason grading system. In *Chinese Journal of Cancer Research* (Vol. 28, Issue 1, pp. 58–64). AME Publishing Company. https://doi.org/10.3978/j.issn.1000-9604.2016.02.04

Cheng, L., Montironi, R., Bostwick, D. G., Lopez-Beltran, A., Berney, D. M., G, B. D., & M, B. D. (2012). Staging of prostate cancer. *Histopathology*, *60*(1), 87–117. https://doi.org/10.1111/j.1365-2559.2011.04025.x

Chou, T. C. (2010). Drug combination studies and their synergy quantification using the chou-talalay method. In *Cancer Research* (Vol. 70, Issue 2, pp. 440–446). American Association for Cancer Research. https://doi.org/10.1158/0008-5472.CAN-09-1947

Cihan, Y. (2018). The role and importance of SBRT in prostate cancer. In *International Braz J Urol* (Vol. 44, Issue 6, pp. 1272–1274). Brazilian Society of Urology. https://doi.org/10.1590/S1677-5538.IBJU.2018.0484

Cimmino, F., Avitabile, M., Lasorsa, V. A., Montella, A., Pezone, L., Cantalupo, S., Visconte, F., Corrias, M. V., Iolascon, A., & Capasso, M. (2019). HIF-1 transcription activity: HIF1A driven response in normoxia and in hypoxia. *BMC Medical Genetics*, *20*(1), 1–15. https://doi.org/10.1186/s12881-019-0767-1

Clinton, T. N., Woldu, S. L., & Raj, G. V. (2017). Degarelix versus luteinizing hormone-

releasing hormone agonists for the treatment of prostate cancer. *Expert Opinion on Pharmacotherapy*, *18*(8), 825–832. https://doi.org/10.1080/14656566.2017.1328056

Cooney, K. A. (2017). Inherited Predisposition to Prostate Cancer: From Gene Discovery to Clinical Impact. *Transactions of the American Clinical and Climatological Association*, *128*, 14–23. http://www.ncbi.nlm.nih.gov/pubmed/28790484

Cunningham, D., & You, Z. (2015). In vitro and in vivo model systems used in prostate cancer research. *Journal of Biological Methods*, *2*(1), 17. https://doi.org/10.14440/jbm.2015.63

D'Amico, A. V., Whittington, R., Bruce Malkowicz, S., Schultz, D., Blank, K., Broderick, G. A., Tomaszewski, J. E., Renshaw, A. A., Kaplan, I., Beard, C. J., & Wein, A. (1998). Biochemical outcome after radical prostatectomy, external beam radiation therapy, or interstitial radiation therapy for clinically localized prostate cancer. *Journal of the American Medical Association*, *280*(11), 969–974. https://doi.org/10.1001/jama.280.11.969

Dal Pra, A., & Souhami, L. (2016). Prostate cancer radiation therapy: A physician's perspective. *Physica Medica*, *32*(3), 438–445. https://doi.org/10.1016/j.ejmp.2016.02.012

Dashty, M. (2013). A quick look at biochemistry: Carbohydrate metabolism. In *Clinical Biochemistry* (Vol. 46, Issue 15, pp. 1339–1352). Elsevier. https://doi.org/10.1016/j.clinbiochem.2013.04.027

Dearnaley, D., Syndikus, I., Mossop, H., Khoo, V., Birtle, A., Bloomfield, D., Graham, J., Kirkbride, P., Logue, J., Malik, Z., Money-Kyrle, J., O'Sullivan, J. M., Panades, M., Parker, C., Patterson, H., Scrase, C., Staffurth, J., Stockdale, A., Tremlett, J., … Hall, E. (2016). Conventional versus hypofractionated high-dose intensity-modulated radiotherapy for prostate cancer: 5-year outcomes of the randomised, non-inferiority, phase 3 CHHiP trial. *The Lancet Oncology*, *17*(8), 1047–1060. https://doi.org/10.1016/S1470-2045(16)30102-4

Del Vecchio, V., Palma, G., Barbieri, A., Falco, M., Luciano, A., De Biase, D., Perdona, S., Facchini, G., & Arra, C. (2016). Mouse Models in Prostate Cancer Translational Research: From Xenograft to PDX. *BioMed Research International*. https://www.hindawi.com/journals/bmri/2016/9750795/

Desideri, I., Detti, B., Bonomo, P., Greto, D., Paiar, F., Simontacchi, G., Meattini, I., Scoccianti, S., Masoni, T., Cibatti, C., Turkaj, A., Serni, S., Minervini, A., Gacci, M., Carini, M., & Livi, L. (2014). Hypofractionation in Prostate Cancer: Radiobiological Basis and Clinical Appliance. *Biomed Research International*, *2014*. https://www.hindawi.com/journals/bmri/2014/781340/

Devineni, D., Curtin, C. R., Polidori, D., Gutierrez, M. J., Murphy, J., Rusch, S., & Rothenberg, P. L. (2013a). Pharmacokinetics and Pharmacodynamics of Canagliflozin, a Sodium Glucose Co-Transporter 2 Inhibitor, in Subjects With Type 2 Diabetes Mellitus. *The Journal of Clinical Pharmacology*, *53*(6), 601–610. https://doi.org/10.1002/jcph.88

Devineni, D., Curtin, C. R., Polidori, D., Gutierrez, M. J., Murphy, J., Rusch, S., & Rothenberg, P. L. (2013b). Pharmacokinetics and Pharmacodynamics of Canagliflozin, a Sodium Glucose Co-Transporter 2 Inhibitor, in Subjects With Type 2 Diabetes Mellitus. *The Journal of Clinical Pharmacology*, *53*(6), 601–610. https://doi.org/10.1002/jcph.88

Ditch, S., & Paull, T. T. (2012). The ATM protein kinase and cellular redox signaling: Beyond the DNA damage response. In *Trends in Biochemical Sciences* (Vol. 37, Issue 1, pp. 15–22). NIH Public Access. https://doi.org/10.1016/j.tibs.2011.10.002

Dong, J.-T. (2006). Prevalent Mutations in Prostate Cancer. *Journal of Cellular Biochemistry*, *97*, 433–447. https://doi.org/10.1002/jcb.20696

Dumitrescu, R., Mehedintu, C., Briceag, I., Purcărea, V. L., & Hudita, D. (2015). Metformin-

clinical pharmacology in PCOs. *Journal of Medicine and Life*, *8*(2), 187–192.

Eberlé, D., Hegarty, B., Bossard, P., Ferré, P., & Foufelle, F. (2004). SREBP transcription factors: master regulators of lipid homeostasis. *Biochimie*, *86*(2004), 839–848. https://doi.org/10.1016/j.biochi.2004.09.018

Edmondson, D. G., Davie, J. K., Zhou, J., Mirnikjoo, B., Tatchell, K., & Dent, S. Y. R. (2002). Site-specific loss of acetylation upon phosphorylation of histone H3. *Journal of Biological Chemistry*, *277*(33), 29496–29502. https://doi.org/10.1074/jbc.M200651200

Egevad, L., Delahunt, B., Srigley, J. R., & Samaratunga, H. (2016). International Society of Urological Pathology (ISUP) grading of prostate cancer-An ISUP consensus on contemporary grading. *Apmis*, *124*(6), 433–435. https://doi.org/10.1111/apm.12533

Eidelman, E., Twum-Ampofo, J., Ansari, J., & Siddiqui, M. M. (2017). The metabolic phenotype of prostate cancer. In *Frontiers in Oncology* (Vol. 7, Issue JUN). Frontiers Media S.A. https://doi.org/10.3389/fonc.2017.00131

Elgavish, A., Wood, P. A., Pinkert, C. A., Eltoum, I.-E., Cartee, T., Wilbanks, J., Mentor-Marcel, R., Tian, L., & Scroggins, S. E. (2004). Transgenic MouseWith Human Mutant p53 Expression in the Prostate Epithelium. *The Prostate*, *61*(1), 26–34. https://doi.org/10.1002/pros.20071

Elmore, S. (2007). Apoptosis: A Review of Programmed Cell Death. In *Toxicologic Pathology* (Vol. 35, Issue 4, pp. 495–516). NIH Public Access. https://doi.org/10.1080/01926230701320337

Faubert, B., Boily, G., Izreig, S., Griss, T., Samborska, B., Dong, Z., Dupuy, F., Chambers, C., Fuerth, B. J., Viollet, B., Mamer, O. A., Avizonis, D., Deberardinis, R. J., Siegel, P. M., & Jones, R. G. (2013). AMPK is a negative regulator of the warburg effect and suppresses

tumor growth in vivo. *Cell Metabolism*, *17*(1), 113–124. https://doi.org/10.1016/j.cmet.2012.12.001

Feng, Q., & He, B. (2019). Androgen Receptor Signaling in the Development of Castration-Resistant Prostate Cancer. In *Frontiers in Oncology* (Vol. 9, p. 858). Frontiers Media S.A. https://doi.org/10.3389/fonc.2019.00858

Ferraril, S., & Thomas2, G. (1994). S6 Phosphorylation and the p70s6k/p85s6k. In *Critical Reviews in Biochemistry and Molecular Biology* (Vol. 29, Issue 6).

Finkelstein, J., Eckersberger, E., Sadri, H., Taneja, S. S., Lepor, H., & Djavan, B. (2010). Open Versus Laparoscopic Versus Robot-Assisted Laparoscopic Prostatectomy: The European and US Experience. *Reviews in Urology*, *12*(1), 35–43. http://www.ncbi.nlm.nih.gov/pubmed/20428292

Fitzgerald, L. M., Raspin, K., Marthick, J. R., Field, M. A., Malley, R. C., Thomson, R. J., Blackburn, N. B., Banks, A., Charlesworth, J. C., Donovan, S., & Dickinson, J. L. (2017). Impact of the G84E variant on HOXB13 gene and protein expression in formalin-fixed, paraffin-embedded prostate tumours. *Scientific Reports*, *7*(1), 17778. https://doi.org/10.1038/s41598-017-18217-w

Foster, B. A., Gingrich, J. R., Kwon, E. D., Madias, C., Greenberg@, N. M., & Kidneyand Electrolyte, L. (1997). Characterization of Prostatic Epithelial Cell Lines Derived from Transgenic Adenocarcinoma of the Mouse Prostate (TRAMP) Model1. In *CANCER* (Vol. 57).

Franciosi, M., Lucisano, G., Lapice, E., Strippoli, G. F. M., Pellegrini, F., & Nicolucci, A. (2013). Metformin Therapy and Risk of Cancer in Patients with Type 2 Diabetes: Systematic Review. *PLoS ONE*, *8*(8). https://doi.org/10.1371/journal.pone.0071583

Freeman, A. K., & Morrison, D. K. (2011). 14-3-3 Proteins: Diverse functions in cell proliferation and cancer progression. In *Seminars in Cell and Developmental Biology* (Vol. 22, Issue 7, pp. 681–687). Elsevier Ltd. https://doi.org/10.1016/j.semcdb.2011.08.009

Fryer, L. G. D., Foufelle, F., Barnes, K., Baldwin, S. A., Woods, A., & Carling, D. (2002). Characterization of the role of the AMP-activated protein kinase in the stimulation of glucose transport in skeletal muscle cells. In *Biochem. J* (Vol. 363). https://portlandpress.com/biochemj/article-pdf/363/1/167/708378/bj3630167.pdf

Fullerton, M. D., Galic, S., Marcinko, K., Sikkema, S., Pulinilkunnil, T., Chen, Z. P., O'Neill, H. M., Ford, R. J., Palanivel, R., O'Brien, M., Hardie, D. G., MacAulay, S. L., Schertzer, J. D., Dyck, J. R. B., Van Denderen, B. J., Kemp, B. E., & Steinberg, G. R. (2013). Single phosphorylation sites in Acc1 and Acc2 regulate lipid homeostasis and the insulin-sensitizing effects of metformin. *Nature Medicine*, *19*(12), 1649–1654. https://doi.org/10.1038/nm.3372

Ghiam, A. F., Taeb, S., Huang, X., Huang, V., Ray, J., Scarcello, S., Hoey, C., Jahangiri, S., Fokas, E., Loblaw, A., Bristow, R. G., Vesprini, D., Boutros, P., & Liu, S. K. (2017). Long non-coding RNA urothelial carcinoma associated 1 (UCA1) mediates radiation response in prostate cancer. *Oncotarget*, *8*(3), 4668–4689. https://doi.org/10.18632/oncotarget.13576

Gilkes, D. M., Semenza, G. L., & Wirtz, D. (2014). Hypoxia and the extracellular matrix: Drivers of tumour metastasis. In *Nature Reviews Cancer* (Vol. 14, Issue 6, pp. 430–439). Nature Publishing Group. https://doi.org/10.1038/nrc3726

Glick, D., Barth, S., & Macleod, K. F. (2010). Autophagy: Cellular and molecular mechanisms. In *Journal of Pathology* (Vol. 221, Issue 1, pp. 3–12). NIH Public Access. https://doi.org/10.1002/path.2697

Green, S. M., Mostaghel, E. A., & Nelson, P. S. (2012). Androgen action and metabolism in prostate cancer. *Molecular and Cellular Endocrinology*, *360*(2012), 3–13. https://doi.org/10.1016/j.mce.2011.09.046

Gwinn, D. M., Shackelford, D. B., Egan, D. F., Mihaylova, M. M., Mery, A., Vasquez, D. S., Turk, B. E., & Shaw, R. J. (2008a). AMPK Phosphorylation of Raptor Mediates a Metabolic Checkpoint. *Molecular Cell*, *30*(2), 214–226. https://doi.org/10.1016/j.molcel.2008.03.003

Gwinn, D. M., Shackelford, D. B., Egan, D. F., Mihaylova, M. M., Mery, A., Vasquez, D. S., Turk, B. E., & Shaw, R. J. (2008b). AMPK Phosphorylation of Raptor Mediates a Metabolic Checkpoint. *Molecular Cell*, *30*(2), 214–226. https://doi.org/10.1016/j.molcel.2008.03.003

Hans, F., & Dimitrov, S. (2001). Histone H3 phosphorylation and cell division. In *Oncogene* (Vol. 20, Issue 24 REV. ISS. 3, pp. 3021–3027). Nature Publishing Group. https://doi.org/10.1038/sj.onc.1204326

Harvey, C. J., Pilcher, J., Richenberg, J., Patel, U., & Frauscher, F. (2012). Applications of transrectal ultrasound in prostate cancer. *British Journal of Radiology*, *85*(SPEC. ISSUE 1), S3. https://doi.org/10.1259/bjr/56357549

He, H., Ke, R., Lin, H., Ying, Y., Liu, D., & Luo, Z. (2015). Metformin, an old drug, brings a new era to cancer therapy. In *Cancer Journal (United States)* (Vol. 21, Issue 2, pp. 70–74). Lippincott Williams and Wilkins. https://doi.org/10.1097/PPO.0000000000000103

Healy, S., Khan, P., He, S., & Davie, J. R. (2012). Histone H3 phosphorylation, immediate-early gene expression, and the nucleosomal response: a historical perspective [1] This article is part of Special Issue entitled Asilomar Chromatin and has undergone the Journal's usual peer

review process. *Biochemistry and Cell Biology*, *90*(1), 39–54. https://doi.org/10.1139/o11-092

Home, P. D., Kahn, S. E., Jones, N. P., Noronha, D., Beck-Nielsen, H., & Viberti, G. (2010). Experience of malignancies with oral glucose-lowering drugs in the randomised controlled ADOPT (A Diabetes Outcome Progression Trial) and RECORD (Rosiglitazone Evaluated for Cardiovascular Outcomes and Regulation of Glycaemia in Diabetes) clinical trials. *Diabetologia*, *53*(9), 1838–1845. https://doi.org/10.1007/s00125-010-1804-y

Hong, S., Zhao, B., Lombard, D. B., Fingar, D. C., & Inoki, K. (2014). Cross-talk between sirtuin and mammalian target of rapamycin complex 1 (mTORC1) signaling in the regulation of S6 kinase 1 (S6K1) phosphorylation. *Journal of Biological Chemistry*, *289*(19), 13132–13141. https://doi.org/10.1074/jbc.M113.520734

Houten, S. M., & Wanders, R. J. A. (2010). A general introduction to the biochemistry of mitochondrial fatty acid β-oxidation. In *Journal of Inherited Metabolic Disease* (Vol. 33, Issue 5, pp. 469–477). Springer. https://doi.org/10.1007/s10545-010-9061-2

Huggins, C. (1941). STUDIES ON PROSTATIC CANCER. *Archives of Surgery*, *43*(2), 209. https://doi.org/10.1001/archsurg.1941.01210140043004

Hughes Hallett, J. E., Luo, X., & Capaldi, A. P. (2015). Snf1/AMPK promotes the formation of Kog1/raptor-bodies to increase the activation threshold of TORC1 in budding yeast. *ELife*, *4*(OCTOBER2015). https://doi.org/10.7554/eLife.09181

Humphrey, P. A. (2004). Gleason grading and prognostic factors in carcinoma of the prostate. In *Modern Pathology* (Vol. 17, Issue 3, pp. 292–306). Nature Publishing Group. https://doi.org/10.1038/modpathol.3800054

Hung, M. H., Chen, Y. L., Chen, L. J., Chu, P. Y., Hsieh, F. S., Tsai, M. H., Shih, C. T., Chao, T.

I., Huang, C. Y., & Chen, K. F. (2019). Canagliflozin inhibits growth of hepatocellular carcinoma via blocking glucose-influx-induced β-catenin activation. *Cell Death and Disease*, *10*(6), 1–15. https://doi.org/10.1038/s41419-019-1646-6

Inoki, K., Zhu, T., & Guan, K. L. (2003). TSC2 Mediates Cellular Energy Response to Control Cell Growth and Survival. *Cell*, *115*(5), 577–590. https://doi.org/10.1016/S0092-8674(03)00929-2

Jakher, H., Chang, T. I., Tan, M., & Mahaffey, K. W. (2019). Canagliflozin review – Safety and efficacy profile in patients with T2DM. In *Diabetes, Metabolic Syndrome and Obesity: Targets and Therapy* (Vol. 12, pp. 209–215). Dove Medical Press Ltd. https://doi.org/10.2147/DMSO.S184437

Jeon, S. M. (2016). Regulation and function of AMPK in physiology and diseases. In *Experimental & molecular medicine* (Vol. 48, Issue 7, p. e245). Korean Society for Biochemistry and Molecular Biology. https://doi.org/10.1038/emm.2016.81

Jones, R. G., Plas, D. R., Kubek, S., Buzzai, M., Mu, J., Xu, Y., Birnbaum, M. J., & Thompson, C. B. (2005). AMP-activated protein kinase induces a p53-dependent metabolic checkpoint. *Molecular Cell*, *18*(3), 283–293. https://doi.org/10.1016/j.molcel.2005.03.027

Jung, C., Kim, R. S., Zhang, H. J., Lee, S. J., & Jeng, M. H. (2004). HOXB13 induces growth suppression of prostate cancer cells as a repressor of hormone-activated androgen receptor signaling. *Cancer Research*, *64*(24), 9185–9192. https://doi.org/10.1158/0008-5472.CAN-04-1330

Karen Tsui, Amar Gajjar, Chenghong Li, Deokumar Srivastava, Alberto Broniscer, Cynthia Wetmore, Larry E. Kun, Thomas E. Merchant, David W. Ellison, Brent A. Orr, Frederick A. Boop, Paul Klimo, Jordan Ross, Leslie L. Robison, & Gregory T. Armstrong. (19601

B.C.E.). Subsequent neoplasms in survivors of childhood central nervous system tumors: risk after modern multimodal therapy. *Neuro-Oncology*, *17*(3), 448–456. https://doi.org/10.1093/NEUONC

Kasznicki, J., Sliwinska, A., & Drzewoski, J. (2014a). Metformin in cancer prevention and therapy. In *Annals of Translational Medicine* (Vol. 2, Issue 6, p. 57). AME Publishing Company. https://doi.org/10.3978/j.issn.2305-5839.2014.06.01

Kasznicki, J., Sliwinska, A., & Drzewoski, J. (2014b). Metformin in cancer prevention and therapy. In *Annals of Translational Medicine* (Vol. 2, Issue 6). AME Publishing Company. https://doi.org/10.3978/j.issn.2305-5839.2014.06.01

Kim, J. H., Park, J. M., Yea, K., Kim, H. W., Suh, P. G., & Ryu, S. H. (2010). Phospholipase D1 mediates AMP-activated protein kinase signaling for glucose uptake. *PLoS ONE*, *5*(3). https://doi.org/10.1371/journal.pone.0009600

Kim, L. C., Cook, R. S., & Chen, J. (2017). MTORC1 and mTORC2 in cancer and the tumor microenvironment. In *Oncogene* (Vol. 36, Issue 16, pp. 2191–2201). Nature Publishing Group. https://doi.org/10.1038/onc.2016.363

Kinsella, N., Helleman, J., Bruinsma, S., Carlsson, S., Cahill, D., Brown, C., & Van Hemelrijck, M. (2018). Active surveillance for prostate cancer: A systematic review of contemporary worldwide practices. In *Translational Andrology and Urology* (Vol. 7, Issue 1, pp. 83–97). AME Publishing Company. https://doi.org/10.21037/tau.2017.12.24

Krock, B. L., Skuli, N., & Simon, M. C. (2011). Hypoxia-Induced Angiogenesis: Good and Evil. *Genes and Cancer*, *2*(12), 1117–1133. https://doi.org/10.1177/1947601911423654

Kurth-Kraczek, E. J., Hirshman, M. F., Goodyear, L. J., & Wi, W. W. (1999). 5 AMP-Activated Protein Kinase Activation Causes GLUT4 Translocation in Skeletal Muscle. In *DIABETES*

(Vol. 48).

Lausch, A., Lamey, M., & Zeng, G. G. (2017). Automated prediction of dosimetric eligibility for hypofractionated prostate radiotherapy. *Journal of Applied Clinical Medical Physics*, *18*(6), 137–141. https://doi.org/10.1002/acm2.12198

Le, L. T. T., Vu, H. L., Nguyen, C. H., & Molla, A. (2013). Basal aurora kinase B activity is sufficient for histone H3 phosphorylation in prophase. *Biology Open*, *2*(4), 379–386. https://doi.org/10.1242/bio.20133079

LeBlanc, A. G., Demers, A., & Shaw, A. (2019). Recent trends in prostate cancer in Canada. *Health Reports*, *30*(4), 12–17. https://doi.org/10.25318/82-003-x201900400002-eng

Lee, J., & Kim, S. S. (2009). The function of p27KIP1 during tumor development. In *Experimental and Molecular Medicine* (Vol. 41, Issue 11, pp. 765–771). Nature Publishing Group. https://doi.org/10.3858/emm.2009.41.11.102

Lee, J. M., & Bernstein, A. (1993). p53 Mutations Increase Resistance to Ionizing Radiation. In *Source: Proceedings of the National Academy of Sciences of the United States of America* (Vol. 90, Issue 12).

Leitzmann, M. F., & Rohrmann, S. (2012). Clinical Epidemiology Risk factors for the onset of prostatic cancer: age, location, and behavioral correlates. *Clinical Epidemiology*, 4–5. https://doi.org/10.2147/CLEP.S16747

Lepor, H. (2005). A review of surgical techniques for radical prostatectomy. *Reviews in Urology*, *7 Suppl 2*(Suppl 2), S11-7. http://www.ncbi.nlm.nih.gov/pubmed/16985892

Li, C., Wang, Q., Shen, S., Wei, X., & Li, G. (2019). HIF-1α/VEGF signaling-mediated epithelial–mesenchymal transition and angiogenesis is critically involved in anti-metastasis effect of luteolin in melanoma cells. *Phytotherapy Research*, *33*(3), 798–807.

https://doi.org/10.1002/ptr.6273

Li, H. F., Kim, J. S., & Waldman, T. (2009). Radiation-induced Akt activation modulates radioresistance in human glioblastoma cells. *Radiation Oncology*, *4*, 43. https://doi.org/10.1186/1748-717X-4-43

Liao, Y., & Hung, M. C. (2010). Physiological regulation of Akt activity and stability. In *American Journal of Translational Research* (Vol. 2, Issue 1, pp. 19–42). e-Century Publishing Corporation. www.ajtr.org/AJTR910005

Liberti, M. V., & Locasale, J. W. (2016). The Warburg Effect: How Does it Benefit Cancer Cells? In *Trends in Biochemical Sciences* (Vol. 41, Issue 3, pp. 211–218). Elsevier Ltd. https://doi.org/10.1016/j.tibs.2015.12.001

Lin, F., Marcelo, K. L., Rajapakshe, K., Coarfa, C., Dean, A., Wilganowski, N., Robinson, H., Sevick, E., Bissig, K. D., Goldie, L. C., Means, A. R., & York, B. (2015). The CaMKK2/CaMKIV relay is an essential regulator of hepatic cancer. *Hepatology*, *62*(2), 505–520. https://doi.org/10.1002/hep.27832

Liu, P. F., Hu, Y. C., Kang, B. H., Tseng, Y. K., Wu, P. C., Liang, C. C., Hou, Y. Y., Fu, T. Y., Liou, H. H., Hsieh, I. C., Ger, L. P., & Shu, C. W. (2017). Expression levels of cleaved caspase-3 and caspase-3 in tumorigenesis and prognosis of oral tongue squamous cell carcinoma. *PLoS ONE*, *12*(7). https://doi.org/10.1371/journal.pone.0180620

Liu, W., Shen, S. M., Zhao, X. Y., & Chen Dr., G. Q. (2012). Targeted genes and interacting proteins of hypoxia inducible factor-1. In *International Journal of Biochemistry and Molecular Biology* (Vol. 3, Issue 2, pp. 165–178). e-Century Publishing Corporation. www.ijbmb.org

Liu, Y., Lai, Y. C., Hill, E. V., Tyteca, D., Carpentier, S., Ingvaldsen, A., Vertommen, D.,

Lantier, L., Foretz, M., Dequiedt, F., Courtoy, P. J., Erneux, C., Viollet, B., Shepherd, P. R., Tavare, J. M., Jensen, J., & Rider, M. H. (2013). Phosphatidylinositol 3-phosphate 5-kinase (PIKfyve) is an AMPK target participating in contraction-stimulated glucose uptake in skeletal muscle. *Biochemical Journal*, *455*(2), 195–206. https://doi.org/10.1042/BJ20130644

Liu, Z. ji, Semenza, G. L., & Zhang, H. feng. (2015). Hypoxia-inducible factor 1 and breast cancer metastasis. In *Journal of Zhejiang University: Science B* (Vol. 16, Issue 1, pp. 32–43). Zhejiang University Press. https://doi.org/10.1631/jzus.B1400221

Lloyd, R. V., Erickson, L. A., Jin, L., Kulig, E., Qian, X., Cheville, J. C., & Scheithauer, B. W. (1999). p27(kip1): A multifunctional cyclin-dependent kinase inhibitor with prognostic significance in human cancers. In *American Journal of Pathology* (Vol. 154, Issue 2, pp. 313–323). American Society for Investigative Pathology Inc. https://doi.org/10.1016/S0002-9440(10)65277-7

Loh, K., Tam, S., Murray-Segal, L., Huynh, K., Meikle, P. J., Scott, J. W., van Denderen, B., Chen, Z., Steel, R., LeBlond, N. D., Burkovsky, L. A., O'Dwyer, C., Nunes, J. R. C., Steinberg, G. R., Fullerton, M. D., Galic, S., & Kemp, B. E. (2019). Inhibition of Adenosine Monophosphate-Activated Protein Kinase-3-Hydroxy-3-Methylglutaryl Coenzyme A Reductase Signaling Leads to Hypercholesterolemia and Promotes Hepatic Steatosis and Insulin Resistance. *Hepatology Communications*, *3*(1), 84–98. https://doi.org/10.1002/hep4.1279

Lohiya, V., Aragon-Ching, J. B., & Sonpavde, G. (2016). Role of Chemotherapy and Mechanisms of Resistance to Chemotherapy in Metastatic Castration-Resistant Prostate Cancer. In *Clinical Medicine Insights: Oncology* (Vol. 10s1, Issue Suppl 1, pp. 57–66).

SAGE Publications Ltd. https://doi.org/10.4137/CMO.S34535

Lum, J. J., Bui, T., Gruber, M., Gordan, J. D., DeBerardinis, R. J., Covello, K. L., Simon, M. C., & Thompson, C. B. (2007). The transcription factor HIF-1 plays a critical role in the growth factor-dependent regulation of both aerobic and anaerobic glycolysis. *Genes and Development*, *21*(9), 1037–1049. https://doi.org/10.1101/gad.1529107

Maier, P., Hartmann, L., Wenz, F., & Herskind, C. (2016). Cellular pathways in response to ionizing radiation and their targetability for tumor radiosensitization. In *International Journal of Molecular Sciences* (Vol. 17, Issue 1). MDPI AG. https://doi.org/10.3390/ijms17010102

Masoud, G. N., & Li, W. (2015). HIF-1α pathway: Role, regulation and intervention for cancer therapy. In *Acta Pharmaceutica Sinica B* (Vol. 5, Issue 5, pp. 378–389). Chinese Academy of Medical Sciences. https://doi.org/10.1016/j.apsb.2015.05.007

McQuade, R. M., Stojanovska, V., Abalo, R., Bornstein, J. C., & Nurgali, K. (2016). Chemotherapy-induced constipation and diarrhea: Pathophysiology, current and emerging treatments. In *Frontiers in Pharmacology* (Vol. 7, Issue NOV, p. 414). Frontiers Media S.A. https://doi.org/10.3389/fphar.2016.00414

Michaelson, M. D., Cotter, S. E., Gargollo, P. C., Zietman, A. L., Dahl, D. M., & Smith, M. R. (2008). Management of Complications of Prostate Cancer Treatment. *CA: A Cancer Journal for Clinicians*, *58*(4), 196–213. https://doi.org/10.3322/ca.2008.0002

Mihaylova, M. M., Vasquez, D. S., Ravnskjaer, K., Denechaud, P. D., Yu, R. T., Alvarez, J. G., Downes, M., Evans, R. M., Montminy, M., & Shaw, R. J. (2011). Class IIa histone deacetylases are hormone-activated regulators of FOXO and mammalian glucose homeostasis. *Cell*, *145*(4), 607–621. https://doi.org/10.1016/j.cell.2011.03.043

Mohler, J. L., Antonarakis, E. S., Armstrong, A. J., D'Amico, A. V., Davis, B. J., Dorff, T., Eastham, J. A., Enke, C. A., Farrington, T. A., Higano, C. S., Horwitz, E. M., Hurwitz, M., Ippolito, J. E., Kane, C. J., Kuettel, M. R., Lang, J. M., McKenney, J., Netto, G., Penson, D. F., … Freedman-Cass, D. A. (2019). Prostate cancer, version 2.2019. *JNCCN Journal of the National Comprehensive Cancer Network*, *17*(5), 479–505. https://doi.org/10.6004/jnccn.2019.0023

Mor, A., & Philips, M. R. (2006). Compartmentalized Ras/MAPK signaling. In *Annual Review of Immunology* (Vol. 24, pp. 771–800). Annual Reviews. https://doi.org/10.1146/annurev.immunol.24.021605.090723

Morgan, S. C., Hoffman, K., Loblaw, D. A., Buyyounouski, M. K., Patton, C., Barocas, D., Bentzen, S., Chang, M., Efstathiou, J., Greany, P., Halvorsen, P., Koontz, B. F., Lawton, C., Leyrer, C. M., Lin, D., Ray, M., & Sandler, H. (2018). Hypofractionated Radiation Therapy for Localized Prostate Cancer: An ASTRO, ASCO, and AUA Evidence-Based Guideline. *Journal of Clinical Oncology*, *36*(34), 3411–3430. https://doi.org/10.1200/JCO.18.01097

Mundi, P. S., Sachdev, J., McCourt, C., & Kalinsky, K. (2016). AKT in cancer: new molecular insights and advances in drug development. In *British Journal of Clinical Pharmacology* (Vol. 82, Issue 4, pp. 943–956). Blackwell Publishing Ltd. https://doi.org/10.1111/bcp.13021

Nader, R., El Amm, J., & Aragon-Ching, J. (2018). Role of chemotherapy in prostate cancer. *Asian Journal of Andrology*, *20*(3), 221. https://doi.org/10.4103/aja.aja_40_17

Nasri, H., & Rafieian-Kopaei, M. (2014). Metformin: Current knowledge. In *Journal of Research in Medical Sciences* (Vol. 19, Issue 7, pp. 658–664). Isfahan University of Medical Sciences(IUMS). /pmc/articles/PMC4214027/?report=abstract

Navale, A. M., & Paranjape, A. N. (2016). Glucose transporters: physiological and pathological roles. In *Biophysical Reviews* (Vol. 8, Issue 1, pp. 5–9). Springer Verlag. https://doi.org/10.1007/s12551-015-0186-2

Neal, B., Perkovic, V., Mahaffey, K. W., de Zeeuw, D., Fulcher, G., Erondu, N., Shaw, W., Law, G., Desai, M., & Matthews, D. R. (2017). Canagliflozin and Cardiovascular and Renal Events in Type 2 Diabetes. *New England Journal of Medicine*, *377*(7), 644–657. https://doi.org/10.1056/NEJMoa1611925

Nguyen, P. L., Alibhai, S. M. H., Basaria, S., D'Amico, A. V., Kantoff, P. W., Keating, N. L., Penson, D. F., Rosario, D. J., Tombal, B., & Smith, M. R. (2015). Adverse effects of androgen deprivation therapy and strategies to mitigate them. In *European Urology* (Vol. 67, Issue 5, pp. 825–836). Elsevier. https://doi.org/10.1016/j.eururo.2014.07.010

Obinata, D., Takayama, K., Urano, T., Murata, T., Ikeda, K., Horie-Inoue, K., Ouchi, Y., Takahashi, S., & Inoue, S. (2012). ARFGAP3, an androgen target gene, promotes prostate cancer cell proliferation and migration. *International Journal of Cancer*, *130*(10), 2240–2248. https://doi.org/10.1002/ijc.26224

Ochiai, D., Goda, N., Hishiki, T., Kanai, M., Senoo-Matsuda, N., Soga, T., Johnson, R. S., Yoshimura, Y., & Suematsu, M. (2011). Disruption of HIF-1α in hepatocytes impairs glucose metabolism in diet-induced obesity mice. *Biochemical and Biophysical Research Communications*, *415*(3), 445–449. https://doi.org/10.1016/j.bbrc.2011.10.089

Oh, W. K., Hurwitz, M., D'Amico, A. V., Richie, J. P., & Kantoff, P. W. (2003). *Biology of Prostate Cancer*. BC Decker. https://www.ncbi.nlm.nih.gov/books/NBK13217/

Otto Warburg, B., Wind, F., & Negelein, N. (1927). THE METABOLISM OF TUMORS IN THE BODY. *Journal of General Physiology*, *8*(6), 519–530.

Park, M., Kim, M., Park, I., Kang, H., Yoo, H., Park, S., Rhee, C., Hong, S., & Lee, S. (2002). PTEN Suppresses Hyaluronic Acid-induced Matrix Metalloproteinase-9 Expression in U87MG Glioblastoma Cells through Focal Adhesion Kinase Dephosphorylation. *Cancer Research*, *62*(21), 6318–6322. https://www.ncbi.nlm.nih.gov/pmc/articles/PMC4081099/

Patel, A. R., & Klein, E. A. (2009). Risk factors for prostate cancer. In *Nature Clinical Practice Urology* (Vol. 6, Issue 2, pp. 87–95). MedReviews, LLC. https://doi.org/10.1038/ncpuro1290

Patel, S., Parliament, M., Kostaras, X., Hagen, N., Olivotto, I. A., Nordal, R., & Aronyk, K. (2014). Recommendations for the referral of patients for proton-beam therapy, an Alberta Health Services report: A model for Canada? *Current Oncology*, *21*(5), 251–262. https://doi.org/10.3747/co.21.2207

Perlmutter, M. A., & Lepor, H. (2007). Androgen deprivation therapy in the treatment of advanced prostate cancer. *Reviews in Urology*, *9 Suppl 1*(Suppl 1), S3-8. http://www.ncbi.nlm.nih.gov/pubmed/17387371

Pilie, P., Giri, V., & Cooney, K. (2016). HOXB13 and other high penetrant genes for prostate cancer. *Asian Journal of Andrology*, *18*(4), 530–532. https://doi.org/10.4103/1008-682X.175785

Podhorecka, M., Skladanowski, A., & Bozko, P. (2010). H2AX Phosphorylation: Its Role in DNA Damage Response and Cancer Therapy. *Journal of Nucleic Acids*, *2010*, 2010. https://www.hindawi.com/journals/jna/2010/920161/

Polotti, C. F., Kim, C. J., Chuchvara, N., Polotti, A. B., Singer, E. A., & Elsamra, S. (2017). Androgen deprivation therapy for the treatment of prostate cancer: a focus on pharmacokinetics. *Expert Opinion on Drug Metabolism & Toxicology*, *13*(12), 1265–1273.

https://doi.org/10.1080/17425255.2017.1405934

Porta, C., Paglino, C., & Mosca, A. (2014). Targeting PI3K/Akt/mTOR signaling in cancer. In *Frontiers in Oncology: Vol. 4 APR*. Frontiers Research Foundation. https://doi.org/10.3389/fonc.2014.00064

Prasanna Kumar, K., Ghosh, S., Canovatchel, W., Garodia, N., & Rajashekar, S. (2017). A review of clinical efficacy and safety of canagliflozin 300 mg in the management of patients with type 2 diabetes mellitus. *Indian Journal of Endocrinology and Metabolism*, *21*(1), 196–209. https://doi.org/10.4103/2230-8210.196016

Prostate cancer statistics - Canadian Cancer Society. (n.d.). Retrieved July 25, 2020, from https://www.cancer.ca/en/cancer-information/cancer-type/prostate/statistics/?region=on

Qin, X., Jiang, B., & Zhang, Y. (2016). 4E-BP1, a multifactor regulated multifunctional protein. In *Cell Cycle* (Vol. 15, Issue 6, pp. 781–786). Taylor and Francis Inc. https://doi.org/10.1080/15384101.2016.1151581

Rena, G., Hardie, D. G., & Pearson, E. R. (2017). The mechanisms of action of metformin. In *Diabetologia* (Vol. 60, Issue 9, pp. 1577–1585). Springer Verlag. https://doi.org/10.1007/s00125-017-4342-z

Roddam, A. W., Duffy, M. J., Hamdy, F. C., Ward, A. M., Patnick, J., Price, C. P., Rimmer, J., Sturgeon, C., White, P., & Allen, N. E. (2005). Use of prostate-specific antigen (PSA) isoforms for the detection of prostate cancer in men with a PSA level of 2-10 ng/ml: Systematic review and meta-analysis. In *European Urology* (Vol. 48, Issue 3, pp. 386–399). Elsevier. https://doi.org/10.1016/j.eururo.2005.04.015

Rodrigues, G., Warde, P., Pickles, T., Crook, J., Brundage, M., Souhami, L., & Lukka, H. (2012). Pre-treatment risk stratification of prostate cancer patients: A critical review. In

Journal of the Canadian Urological Association (Vol. 6, Issue 2, pp. 121–127). Canadian Medical Association. https://doi.org/10.5489/cuaj.11085

Rouillard, A., Gundersen, G., Fernandez, N., Wang, Z., Monteiro, C., McDermott, M., & Ma'ayan, A. (2016). *harmonizome: a collection of processed datasets gathered to serve and mine knowledge about genes and proteins | Database | Oxford Academic*. https://academic.oup.com/database/article/doi/10.1093/database/baw100/2630482

Roy, S. (2019). Administration of Once-daily Canagliflozin to a Non-diabetic Patient in Addition to Standard Aerobic Exercise: A Case Report. *Cureus*, *11*(4). https://doi.org/10.7759/cureus.4352

Sarnoski-Brocavich, S., & Hilas, O. (2013). Canagliflozin (Invokana), a novel oral agent for type-2 diabetes. In *P and T* (Vol. 38, Issue 11, p. 656). MediMedia, USA.

Saxton, R. A., & Sabatini, D. M. (2017a). mTOR Signaling in Growth, Metabolism, and Disease. In *Cell* (Vol. 168, Issue 6, pp. 960–976). Cell Press. https://doi.org/10.1016/j.cell.2017.02.004

Saxton, R. A., & Sabatini, D. M. (2017b). mTOR Signaling in Growth, Metabolism, and Disease. In *Cell* (Vol. 168, Issue 6, pp. 960–976). Cell Press. https://doi.org/10.1016/j.cell.2017.02.004

Schröder, F., Crawford, E. D., Axcrona, K., Payne, H., & Keane, T. E. (2012). Androgen deprivation therapy: past, present and future. *BJU International*, *109*(SUPPL. 6), 1–12. https://doi.org/10.1111/j.1464-410X.2012.11215.x

Sciacovelli, M., Gaude, E., Hilvo, M., & Frezza, C. (2014). The Metabolic Alterations of Cancer Cells. *Methods in Enzymology*, *542*, 1–23. https://doi.org/10.1016/B978-0-12-416618-9.00001-7

Sha, S., Devineni, D., Ghosh, A., Polidori, D., Chien, S., Wexler, D., Shalayda, K., Demarest, K., & Rothenberg, P. (2011). Canagliflozin, a novel inhibitor of sodium glucose co-transporter 2, dose dependently reduces calculated renal threshold for glucose excretion and increases urinary glucose excretion in healthy subjects. *Diabetes, Obesity and Metabolism*, *13*(7), 669–672. https://doi.org/10.1111/j.1463-1326.2011.01406.x

Shackelford, D. B., & Shaw, R. J. (2009). The LKB1-AMPK pathway: Metabolism and growth control in tumour suppression. In *Nature Reviews Cancer* (Vol. 9, Issue 8, pp. 563–575). NIH Public Access. https://doi.org/10.1038/nrc2676

Skowronek, J. (2013). Brachytherapy in the therapy of prostate cancer - An interesting choice. In *Wspolczesna Onkologia* (Vol. 17, Issue 5, pp. 407–412). Termedia Publishing. https://doi.org/10.5114/wo.2013.38557

Skowronek, J. (2017). Current status of brachytherapy in cancer treatment – short overview. *Journal of Contemporary Brachytherapy*, *9*(6), 581–589. https://doi.org/10.5114/jcb.2017.72607

Smith, L., Cancer Society, C., John, S., Ryan Woods, L., Brenner, D., Bryan, S., Louzado, C., Shaw, A., Turner, D., Manitoba, C., Hannah Weir, M. K., Demers, A., Ellison, L., & Dixon, M. (2019). *Canadian Cancer Statistics*. Canadian Cancer Society. https://www.cancer.ca/~/media/cancer.ca/CW/cancer information/cancer 101/Canadian cancer statistics/Canadian-Cancer-Statistics-2019-EN.pdf?la=en

Sooriakumaran, P., Nyberg, T., Akre, O., Haendler, L., Heus, I., Olsson, M., Carlsson, S., Roobol, M. J., Steineck, G., & Wiklund, P. (2014). Comparative effectiveness of radical prostatectomy and radiotherapy in prostate cancer: Observational study of mortality outcomes. *BMJ (Online)*, *348*. https://doi.org/10.1136/bmj.g1502

Spinelli, J. B., & Haigis, M. C. (2018). The multifaceted contributions of mitochondria to cellular metabolism. In *Nature Cell Biology* (Vol. 20, Issue 7, pp. 745–754). Nature Publishing Group. https://doi.org/10.1038/s41556-018-0124-1

Sramokoski, M., Pretlow, T., Giaconia, J., Pretlow, T., Schwartz, S., Sy, M.-S., Marengo, S., Rhim, Johng; Zhang, D., & Jacobberger, J. (1999). A NEW HUMAN PROSTATE CARCINOMA CELL LINE, 22Rvl. In *In Vitro Cell. Dev. Biol.-Animal* (Vol. 35).

Steinberg, G. R., & Carling, D. (2019). AMP-activated protein kinase: the current landscape for drug development. In *Nature Reviews Drug Discovery* (Vol. 18, Issue 7, pp. 527–551). Nature Research. https://doi.org/10.1038/s41573-019-0019-2

Stronach, E. A., Chen, M., Maginn, E. N., Agarwal, R., Mills, G. B., Wasan, H., & Gabra, H. (2011). DNA-PK mediates AKT activation and apoptosis inhibition in clinically acquired platinum resistance. *Neoplasia*, *13*(11), 1069–1080. https://doi.org/10.1593/neo.111032

Suissa, S., & Azoulay, L. (2012). Metformin and the risk of cancer: Time-related biases in observational studies. In *Diabetes Care* (Vol. 35, Issue 12, pp. 2665–2673). American Diabetes Association. https://doi.org/10.2337/dc12-0788

Syntichaki, P., & Tavernarakis, N. (2002). Death by necrosis: Uncontrollable catastrophe, or is there order behind the chaos? *EMBO Reports*, *3*(7), 604. https://doi.org/10.1093/EMBO-REPORTS/KVF138

Takayama, K.-I., & Inoue, S. (2013). Transcriptional network of androgen receptor in prostate cancer progression. *International Journal of Urology*, *20*(8), 756–768. https://doi.org/10.1111/iju.12146

Talley, J. T., & Mohiuddin, S. S. (2020). Biochemistry, Fatty Acid Oxidation. *StatPearls*.

Tan, M. E., Li, J., Xu, H. E., Melcher, K., & Yong, E. L. (2015). Androgen receptor: Structure,

role in prostate cancer and drug discovery. In *Acta Pharmacologica Sinica* (Vol. 36, Issue 1, pp. 3–23). Nature Publishing Group. https://doi.org/10.1038/aps.2014.18

Tate, J. G., Bamford, S., Jubb, H. C., Sondka, Z., Beare, D. M., Bindal, N., Boutselakis, H., Cole, C. G., Creatore, C., Dawson, E., Fish, P., Harsha, B., Hathaway, C., Jupe, S. C., Kok, C. Y., Noble, K., Ponting, L., Ramshaw, C. C., Rye, C. E., … Forbes, S. A. (2019). COSMIC: The Catalogue Of Somatic Mutations In Cancer. *Nucleic Acids Research*, *47*(D1), D941–D947. https://doi.org/10.1093/nar/gky1015

Taylor, A., & Powell, M. E. B. (2004). Intensity-modulated radiotherapy - What is it? *Cancer Imaging*, *4*(2), 68–73. https://doi.org/10.1102/1470-7330.2004.0003

Teslaa, T., & Teitell, M. A. (2014). Techniques to monitor glycolysis. In *Methods in Enzymology* (Vol. 542, pp. 91–114). Academic Press Inc. https://doi.org/10.1016/B978-0-12-416618-9.00005-4

Viglietto, G., Motti, M., & Fusco, A. (2002). Understanding p27kip1 Deregulation in Cancer. *Cell Cycle*, *1*(6), 394–300. https://journals-scholarsportal-info.libaccess.lib.mcmaster.ca/pdf/15384101/v01i0006/394_updicdom.xml

Villani, L. A., Smith, B. K., Marcinko, K., Ford, R. J., Broadfield, L. A., Green, A. E., Houde, V. P., Muti, P., Tsakiridis, T., & Steinberg, G. R. (2016). The diabetes medication Canagliflozin reduces cancer cell proliferation by inhibiting mitochondrial complex-I supported respiration. *Molecular Metabolism*, *5*(10), 1048–1056. https://doi.org/10.1016/j.molmet.2016.08.014

Wang, J. song, Wang, H. juan, & Qian, H. li. (2018). Biological effects of radiation on cancer cells. In *Military Medical Research* (Vol. 5, Issue 1). BioMed Central Ltd. https://doi.org/10.1186/s40779-018-0167-4

Wee, P., & Wang, Z. (2017). Epidermal growth factor receptor cell proliferation signaling pathways. In *Cancers* (Vol. 9, Issue 5, p. 52). MDPI AG. https://doi.org/10.3390/cancers9050052

Wroński, S. (2012). Radical perineal prostatectomy - the contemporary resurgence of a genuinely minimally invasive procedure: Procedure outline. comparison of the advantages, disadvantages, and outcomes of different surgical techniques of treating organ-confined prostate can. *Central European Journal of Urology*, *65*(4), 188–194. https://doi.org/10.5173/ceju.2012.04.art2

Wu, N., Zheng, B., Shaywitz, A., Dagon, Y., Tower, C., Bellinger, G., Shen, C.-H., Wen, J., Asara, J., Mcgraw, T. E., Kahn, B. B., & Cantley, L. C. (2013). Molecular Cell AMPK-Dependent Degradation of TXNIP upon Energy Stress Leads to Enhanced Glucose Uptake via GLUT1. *Molecular Cell*, *49*(6), 1167–1175. https://doi.org/10.1016/j.molcel.2013.01.035

Wu, X., Gong, S., Roy-Burman, P., Lee, P., & Culig, Z. (2013). Current mouse and cell models in prostate cancer research. In *Endocrine-Related Cancer* (Vol. 20, Issue 4). NIH Public Access. https://doi.org/10.1530/ERC-12-0285

Yuan, T. L., & Cantley, L. C. (2008). PI3K pathway alterations in cancer: Variations on a theme. In *Oncogene* (Vol. 27, Issue 41, pp. 5497–5510). NIH Public Access. https://doi.org/10.1038/onc.2008.245

Zadra, G., Photopoulos, C., & Loda, M. (2013). The fat side of prostate cancer. In *Biochimica et Biophysica Acta - Molecular and Cell Biology of Lipids* (Vol. 1831, Issue 10, pp. 1518–1532). Elsevier B.V. https://doi.org/10.1016/j.bbalip.2013.03.010

Zaidi, S., Gandhi, J., Joshi, G., Smith, N. L., & Khan, S. A. (2019). The anticancer potential of

metformin on prostate cancer. In *Prostate Cancer and Prostatic Diseases* (Vol. 22, Issue 3, pp. 351–361). Nature Publishing Group. https://doi.org/10.1038/s41391-018-0085-2

Zaorsky, N. G., Harrison, A. S., Trabulsi, E. J., Gomella, L. G., Showalter, T. N., Hurwitz, M. D., Dicker, A. P., & Den, R. B. (2013). Evolution of advanced technologies in prostate cancer radiotherapy. In *Nature Reviews Urology* (Vol. 10, Issue 10, pp. 565–579). Nature Publishing Group. https://doi.org/10.1038/nrurol.2013.185

Zaorsky, N. G., Ohri, N., Showalter, T. N., Dicker, A. P., & Den, R. B. (2013). Systematic review of hypofractionated radiation therapy for prostate cancer. In *Cancer Treatment Reviews* (Vol. 39, Issue 7, pp. 728–736). W.B. Saunders Ltd. https://doi.org/10.1016/j.ctrv.2013.01.008

Zippo, A., De Robertis, A., Serafini, R., & Oliviero, S. (2007). *PIM1-dependent phosphorylation of histone H3 at serine 10 is required for MYC-dependent transcriptional activation and oncogenic transformation*. *9*(8), 932–944. https://doi.org/10.1038/ncb1618